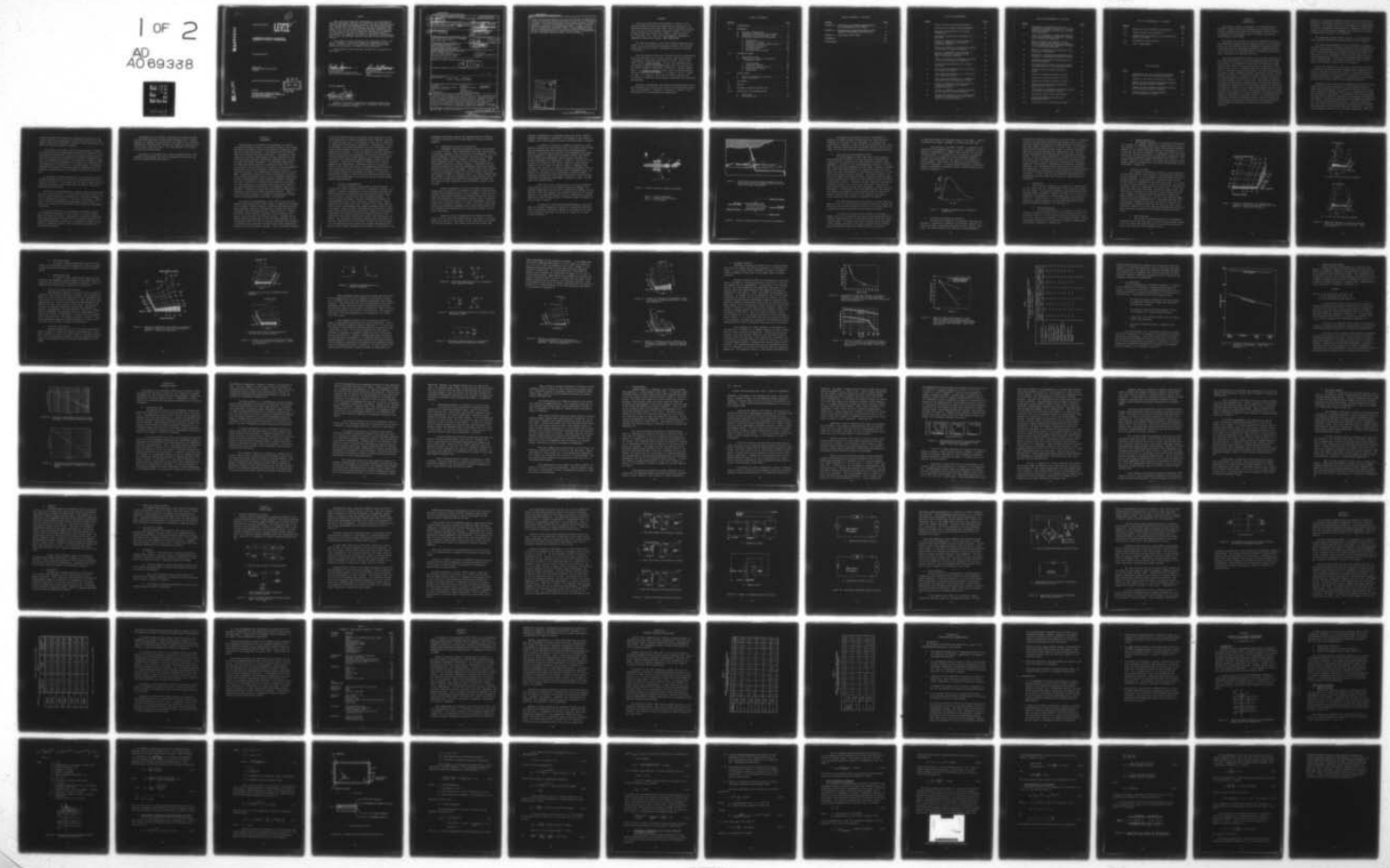
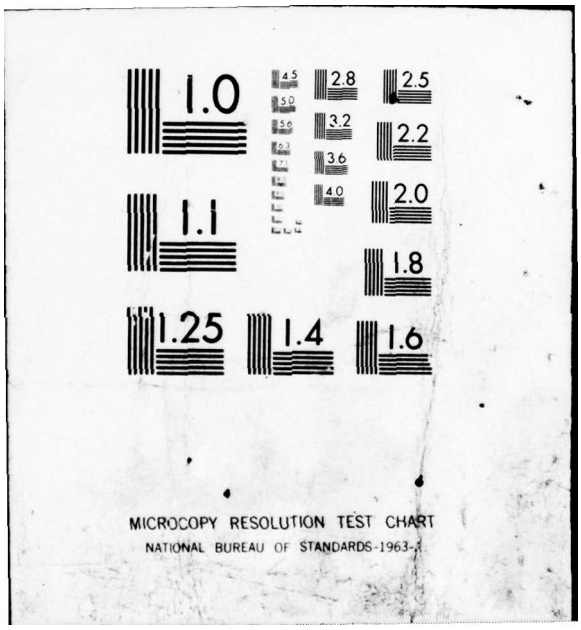
AD-A069 338 TECHNOLOGY/SCIENTIFIC SERVICES INC DAYTON OH F/G 1/3
ATMOSPHERIC ELECTRICITY HAZARD (AEH) ASSESSMENT OF AIRCRAFT TRA--ETC(U)
DEC 78 A V SERRANO F33601-78-D-0042
UNCLASSIFIED T/SSI-0140-01 AFFDL-TR-78-164 NL

1 OF 2
AD
A069338




1.0
1.1
1.25
1.4
1.6
1.8
2.0
2.2
2.5
2.8
3.2
3.6
4.0
4.5
5.0
5.6
MICROCOPY RESOLUTION TEST CHART
NATIONAL BUREAU OF STANDARDS-1963-A

AD A069338

DDC FILE COPY

Report AFFDL-TR-78-164

LEVEL II

ATMOSPHERIC ELECTRICITY HAZARD (AEH) ASSESSMENT OF AIRCRAFT TRANSPARENCIES

Vehicle Equipment Division

December 1978
TECHNICAL REPORT AFFDL-TR-78-164
Final Report

Approved for public release; distribution unlimited

DDC
RECEIVED
JUN 4 1979
A

Prepared for

AIR FORCE FLIGHT DYNAMICS LABORATORY
AIR FORCE WRIGHT AERONAUTICAL LABORATORIES
AIR FORCE SYSTEMS COMMAND
Wright-Patterson Air Force Base, Ohio 45433

NOTICE

When Government drawings, specifications, or other data are used for any purpose other than in connection with a definitely related Government procurement operation, the United States Government thereby incurs no responsibility nor any obligation whatsoever; and the fact that the Government may have formulated, furnished, or in any way supplied the said drawings, specifications, or other data, is not to be regarded by implication or otherwise as in any manner licensing the holder or any other person or corporation, or conveying any rights or permission to manufacture, use, or sell any patented invention that may in any way be related thereto.

This report has been reviewed by the Information Office (OI) and is released to the National Technical Information Service (NTIS). At NTIS it will be available for public release with distribution unlimited, including foreign nationals.

This technical report has been reviewed and is approved for publication.

TIMOTHY SEYMOUR
Project Monitor
Electromagnetic Hazards Group
Survivability/Vulnerability Branch

LARRY G. MOOSMAN, 2Lt, USAF
Project Monitor
Improved Windshield Protection
ADPO
Vehicle Equipment Division

FOR THE COMMANDER

AMBROSE B. NUTT, Director
Vehicle Equipment Division

Copies of this report should not be returned unless return is required by security considerations, contractual obligations, or notice on a specific document.

UNCLASSIFIED

SECURITY CLASSIFICATION OF THIS PAGE *(When Data Entered)*

REPORT DOCUMENTATION PAGE

READ INSTRUCTIONS BEFORE COMPLETING FORM

1. REPORT NUMBER: AFFDL-TR-78-164
2. GOVT ACCESSION NO.
3. RECIPIENT'S CATALOG NUMBER

4. TITLE *(and Subtitle)*: ATMOSPHERIC ELECTRICITY HAZARD (AEH) ASSESSMENT OF AIRCRAFT TRANSPARENCIES

5. TYPE OF REPORT & PERIOD COVERED: Final Report, 1 Jul - 30 Sep 78

6. PERFORMING ORG. REPORT NUMBER: T/SSI-0140-01

7. AUTHOR(s): Arturo V. Serrano

8. CONTRACT OR GRANT NUMBER(s): F33601-78-D-0042

9. PERFORMING ORGANIZATION NAME AND ADDRESS
Technology/Scientific Services Incorporated
3821 Colonel Glenn Highway
Dayton, OH 45431

10. PROGRAM ELEMENT, PROJECT, TASK AREA & WORK UNIT NUMBERS
2202, 03, 07

11. CONTROLLING OFFICE NAME AND ADDRESS
Electromagnetic Hazards Group (FESL)
Vehicle Equipment Division
Air Force Flight Dynamics Laboratory
Wright-Patterson AFB, OH 45433

12. REPORT DATE: December 1978

13. NUMBER OF PAGES: 174

14. MONITORING AGENCY NAME & ADDRESS *(if different from Controlling Office)*
Improved Windshield Protection ADPO (FEA)
Vehicle Equipment Division
Air Force Flight Dynamics Laboratory
Wright-Patterson AFB, OH 45433

15. SECURITY CLASS. *(of this report)*: Unclassified

15a. DECLASSIFICATION/DOWNGRADING SCHEDULE: N/A

16. DISTRIBUTION STATEMENT *(of this Report)*
Approved for public release; distribution unlimited.

17. DISTRIBUTION STATEMENT *(of the abstract entered in Block 20, if different from Report)*

63211F

18. SUPPLEMENTARY NOTES
Project Monitors: Timothy Seymour (AFFDL/FESL)
Lt Larry G. Moosman (AFFDL/FEA)

19. KEY WORDS *(Continue on reverse side if necessary and identify by block number)*

Analysis	Lightning	Vulnerability
Atmospheric Electricity Hazards	Precipitation Static	Windshields
Electrical Properties	Plastic	
EMP	Transparencies	
Flashblindness	Shielding Effectiveness	

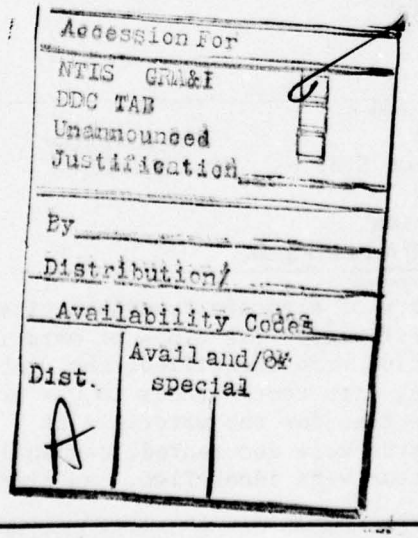
20. ABSTRACT *(Continue on reverse side if necessary and identify by block number)*
A literature survey relating to the survivability of aircraft transparencies and electrical circuits embedded within them was performed. The types of materials used in transparencies and their edge construction were identified, the electrical properties of interest were defined along with test methods in use or available, the availability of electrical properties for the materials of interest was determined, the physiological hazards were documented, and analytical methods for evaluation of transparency systems were identified. As a result

DD FORM 1 JAN 73 1473 EDITION OF 1 NOV 65 IS OBSOLETE

UNCLASSIFIED 411 202

SECURITY CLASSIFICATION OF THIS PAGE *(When Data Entered)*

of this study it was concluded that the electrical parameters of interest are affected by temperature, frequency and exposure and that data for the materials of interest are not generally available over the ranges of interest for these parameters. If was also concluded that insufficient information is currently available for evaluation of the physiological hazards. Finally, analytical models for evaluation of transparency systems in an electromagnetic environment were found available that could be used to analyze transparency designs. However, these methods need to be computerized and validated. Recommendations are made to eliminate existing data gaps by tests and analyses.



FOREWORD

This report describes work performed in support of the Improved Windshield Protection Program being conducted by the Windshield Program Office ADPO (FEW), Vehicle Equipment Division (FE), Air Force Flight Dynamics Laboratory (AFFDL), Air Force Wright Aeronautical Laboratories (AFWAL), Wright-Patterson Air Force Base, Ohio, under Job Order 22020307, "Windshield Atmospheric Electricity Hazards (AEH) Assessment."

The work was assigned to the Electromagnetic Hazards Group (FESL) of the Survivability/Vulnerability Branch (FES) and performed under Project 240223, "Atmospheric Electricity Hazards to Aircraft."

The work reported herein was performed jointly by Technology/Scientific Services, Inc. (T/SSI), Dayton, Ohio and Technology Incorporated, Instruments and Controls Division, Dayton, Ohio, under Contract F33601-78-D0042. The work was performed during the period 11 July to 30 September 1978, under the direction of Lt. Larry G. Moosman (AFFDL/FEW) and Vernon L. Mangold (AFFDL/FESL). Mr. Arturo V. Serrano (T/SSI) served as program manager, and was assisted by Jean Reazer, K. J. Maxwell, and L. C. Walko of T/SSI. Dr. Robert B. Finch was the project Engineer and Dr. William S. McCormick the principal investigator for Technology Incorporated.

During the program many individuals and organizations within the Government and Industry were contacted and contributed assistance and information. Although too numerous to mention, their contributions are acknowledged and appreciated.

TABLE OF CONTENTS

Section		Page
I	INTRODUCTION	1
II	BACKGROUND	5
	A. Aircraft Transparencies	6
	B. Atmospheric Electricity and Aircraft	7
	C. Lightning and Electromagnetic Pulse	11
	D. Electrical Properties of Materials	12
	1. Resistivity	13
	2. Dielectric Strength	14
	3. Dielectric Constant (Permittivity)	17
	4. Dielectric Loss Factor	17
	5. Flashover Strength	24
	6. Arc Resistance	28
	7. Shielding Effectiveness	30
III	LITERATURE SURVEY	33
	A. Transparency Data	33
	B. Physiological Effects of Lightning on Aircraft Crews	36
	1. Flashblindness	38
	2. Electrical Hazards	45
	3. Blast and Acoustic Effects	47
	4. Psychological Effects	47
	5. Conclusions	47
IV	SYSTEM SURVEY	49
	A. Aircraft Transparency Circuits	49
	B. Surge Protection	56
V	DATA MATRIX	61
VI	ANALYSIS	67
VII	LIGHTNING ACCIDENT/INCIDENT DATA	69
VIII	CONCLUSIONS AND RECOMMENDATIONS	73
	A. Conclusions	73
	B. Recommendations	74

TABLE OF CONTENTS - Concluded

Section	Page
APPENDIX A - ANALYSIS OF AN AIRCRAFT TRANSPARENCY IN AN ELECTROMAGNETIC ENVIRONMENT	77
APPENDIX B - APPLICATION OF ANALYTICAL MODEL TO TWO AIRCRAFT TRANSPARENCY CONFIGURATIONS	93
APPENDIX C - DATA MATRIX DATA SHEETS	103
REFERENCES	153
BIBLIOGRAPHY	159

LIST OF ILLUSTRATIONS

Figure		Page
1	Typical Aircraft Lightning Attachment	9
2	Illustration of Swept Stroke Phenomenon	10
3	Capacitor Representation of Aircraft Transparency	10
4	"Standard" Description of Lightning of EMP Pulse	12
5	Effects of Temperature and Frequency on Dielectric Strength on One Type of Dielectric Material	15
6	Effects of Exposure on Dielectric Strength on One Type of Dielectric Material	16
7	Effects of Temperature and Frequency on Relative Dielectric Constant on One Type of Dielectric Material	18
8	Effects of Exposure on Dielectric Constant on One Type of Dielectric Material	19
9	Electrical Representation of a Perfect Dielectric	20
10	Electrical Representation of a Dielectric with Conductive Losses	21
11	Electrical Representation of a Dielectric with Absorptive Losses	21
12	Electrical Representation of a Dielectric with Conductive and Absorptive Losses	21
13	Effects of Temperature and Frequency on Dissipation Factor on One Type of Dielectric Material	22
14	Effects of Exposure on Dissipation Factor on One Type of Dielectric Material	23
15	Effects of Exposure at 85°C, Humidity and Frequency on Dissipation Factor on One Type of Dielectric Material	23

LIST OF ILLUSTRATIONS - Continued

Figure		Page
16	Dependence of Flashover Strength on Dielectric Constant at 60 Hz, with 3/8-Inch Electrode Separation Distance and 1/8-Inch-Thick Separations	25
17	Effect of Frequency on Flashover Strength, with 3/8-Inch Electrode Separation Distance and 1/8-Inch-Thick Specimens	25
18	Effect of Short Time Exposure at 100% Relative Humidity for Various Dielectrics, with 3/8-Inch Electrode Separation Distance and 1/8-Inch-Thick Specimens	26
19	Effects of Temperature and Moisture on Arc Resistance of Polyester	29
20	Variations of Shielding Effectiveness with Frequency (10-Ohm/Square Conductive Glass) . .	31
21	Variation of Shielding Effectiveness with Surface Resistance	31
22	Time Required to Perceive an Acuity Target Following Exposure to an Adapting Flash	41
23	Typical Aircraft Windshield Heating System	49
24	Typical AC Windshield Heater Circuits	53
25	Typical DC Windshield Heater Circuits	54
26	Equivalent Windshield Heater Circuits	55
27	Simplified and Equivalent Windshield Heater Control Circuit	57
28	Installation of Lightning Protective Devices in Aircraft Transparency Circuits	59
29	Sample Data Matrix Data Summary Sheet	62
A-1	Stratified Medium Consisting of M Homogeneous Layers	77
A-2	Line Source over a Layered Half-Space	79

LIST OF ILLUSTRATIONS - Concluded

Figure		Page
A-3	Reference 29 Test Specimen Configuration . . .	82
A-4	Douglas P-Static Test Simulator	88
A-5	Transmission Line Analogy for the Stratified Medium of M Layers	90
B-1	Transparency Cross Sections	94
B-2	Case 1 Approximation	99

LIST OF TABLES

Table		Page
1	Comparison of AC, DC, and Impulse Flashover Strength of Various Dielectric Materials . . .	27
2	Summary of Data Matrix (Appendix C) Contents .	65
3	Summary of USAF Lightning Accidents/Incidents and Transparency Related Incidents	70
4	Summary of Navy Lightning Accidents/Incidents and Transparency Related Incidents	71
B-1	Lightning-Induced Voltages Measured in S-3A Electrical Circuits	101

SECTION I
INTRODUCTION

This report documents the results of an intensive effort directed at state-of-the-art assessment for the protection of aircraft transparencies against the atmospheric electric hazards of lightning and precipitation static (p-static) and nuclear electromagnetic pulse (NEMP).

This effort was initiated to provide a comprehensive look at the transparency industry and the state-of-the-art of transparency design for the protection against atmospheric electrical hazards. Of interest were the electrical properties of transparency materials, the electrical characteristics of transparency systems and their influence on the aircraft and crew.

The Improved Windshield Program Office has been concerned with the overall performance of aircraft windshields and their protection against all the hazards to which they are subjected. These hazards result from both the non-operating and operating environments and can result in windshield failures of degradation to the point of affecting mission effectiveness. Failures and degradation can result from environmental factors, operational factors, natural hazards, and combat. If windshield failure occurs during a critical mission phase the potential for loss of aircraft is enhanced with the attendant risk to flight crews. Much work has been done to improve the mechanical characteristics of windshield systems to withstand the environmental and operational stresses to which they are exposed. However, the all-weather requirements imposed on many of today's and future aircraft, particularly those with a military mission, have resulted in a higher incidence of windshield problems caused by atmospheric electricity hazards. The incorporation of electrical circuits and conductive films in aircraft windshields may increase the hazard and probability of failure and may also affect mission effectiveness by resulting in catastrophic failures.

Therefore, the Improved Windshield Program Office has undertaken a program for atmospheric electricity protection of aircraft transparencies. As a logical step in the development and demonstration of aircraft transparency designs against atmospheric electricity hazards, a state-of-the-art assessment was required for aircraft transparencies, materials and construction.

The assessment reported herein provides a baseline against which candidate materials and design criteria can be compared.

The program was conducted by first performing a literature survey of all available literature relating to the survivability of aircraft transparencies and the possible circuits imbedded within them. Because physiological hazards are present as a result of interaction of the atmospheric electricity environment with aircraft transparencies, the search also encompassed the identification of these hazards. The nature, sources and extent of this survey are discussed in Section III of the report.

Section IV discusses the results of a system survey performed to assess the hazard to aircraft transparencies, electrical circuits in them and other aircraft circuits. This survey resulted in the identification of circuit protection techniques that should minimize the hazard, or eliminate it, particularly if incorporated at the initial design stages of the transparency system.

Although the survey was not as encompassing as would have been liked, due to the time constraints, it was confirmed that the electrical characteristics of the specific materials used in aircraft transparency systems, particularly in windshields, were typically unknown or unpublished. The suspicion that this was indeed the case was the reason for performing the assessment described in this report. The data identified during the program are summarized in a data matrix presented in Section V. The matrix shows that there are large voids of information pertaining to the electrical characteristics of transparency materials, especially in the area of environmental effects on the electrical properties. Also, the

electrical properties, normally of engineering interest, do not include some of the properties that are more relevant in an atmospheric electricity environment. However, from an analytical viewpoint this does not present a problem.

In an effort to eliminate voids in the data matrix, analytical investigations were performed to determine the feasibility of extrapolating existing data, as well as to permit using the available data in analyzing the response of aircraft transparency systems to atmospheric electricity. The analysis was useful in identifying the electrical parameters of interest and in defining the test parameters for acquisition of the data needed. The analysis performed and resultant electrical property measurement and test parameter recommendations are contained in Section VI of the report.

To determine the hazard probability, the available aircraft accident/incident reports for the U.S. Air Force and Navy were reviewed and analyzed. It was found that for some aircraft types and missions the hazard is more severe than for others. Section VII summarized these findings.

Conclusions and recommendations resulting from the program are presented in Section VIII. It is felt that much work remains to be done to properly assess the vulnerability of aircraft transparencies to atmospheric electricity. The task is not simple. Accordingly, several recommendations are presented so that future efforts, it is hoped, will be performed in an orderly and cost-effective manner.

It is anticipated that investigators not normally familiar with atmospheric electricity and its impact on aircraft performance will read this report. Consequently, a brief but comprehensive background section (Section II) is included to acquaint the reader with atmospheric electricity, the hazard it creates via the aircraft transparency system, and the electrical properties of transparency materials.

An Appendix (A) is included to describe the analytical model that was found applicable to multilayer transparencies. A second Appendix (B) presents an application of the model to two different transparency configurations, one with two conductive layers and one with a single conductive layer. The final Appendix (C) presents the data matrix data sheets.

The report is concluded with a list of references and a comprehensive bibliography dealing with atmospheric electricity and aircraft transparencies and materials.

SECTION II
BACKGROUND

Traditionally, the selection or development of aircraft transparency materials used in windshields, canopies, and windows has been on the basis of optical and mechanical properties rather than on electrical properties. This has been the case because their basic function has been non-electric. Consequently, most research on aircraft transparencies has been directed at structural and impact strength, temperature characteristics, optical qualities and weather resistance. The increased capabilities of today's and future aircraft, particularly those with a military mission, have resulted in an increase in the electromagnetic hazard from the natural atmospheric electricity sources of lightning, p-static, and triboelectric charging, as well as from NEMP. Configuration changes to aircraft transparency construction involving transparent armor, electrical heating (anti-icing) systems, electromagnetic energy shielding, conductive coatings for static electricity and swept-stroke protection, and others have also resulted in an increased concern over their impact on aircraft-transparency vulnerability to atmospheric electricity and NEMP. In addition, recent years have shown the emergence of atmospheric electricity-related accidents/incidents. There is also a potential increase in incidence of physiological effects (shock and flashblindness) which bears investigation.

The aircraft transparencies of today and of the future are complex system designs that often consist of laminations including glass or plastic glazing materials, flexible interlayer materials, edge attachment materials, and adhesives; coatings for abrasion resistance, anti-fogging/anti-icing, radar reflection, radiation protection, solar (thermal) reflection, anti-reflection, anti-static, rain repellency, and heating circuits. Although the important electrical properties of the individual elements of the transparency system are known or readily obtainable using standard test methods, the electrical characteristics of the transparency system as a whole are largely unknown. Also, the normally measured

electrical characteristics are obtained under laboratory or standard temperature and pressure conditions using standard thicknesses, direct current (DC), or alternating current (AC) at commercial or communication/navigational frequencies. Unfortunately, as will be discussed, the electric properties of most transparency materials are particularly sensitive to variations in temperature, humidity and frequency. In the environment of aircraft operations these variations must be considered, particularly as pertains to the static electricity charge buildup on the transparency materials(s) and the lightning and NEMP atmospheric electricity environments. Aside from the physical considerations of costly damage to the transparency, lightning flashes in the range of vision of the flight crew create a flashblindness hazard that may prove catastrophic during all mission phases, especially critical mission phases such as takeoff and landing. In addition, a physiological hazard of electrical shock also exists during both air and ground operations, and could also affect critical mission phases catastrophically.

A. Aircraft Transparencies

The term "aircraft transparencies" covers optically transparent aircraft components such as windshields, canopies, and windows. Aircraft transparencies in early aircraft performed the simple functions of protecting the pilot from wind, bugs, engine oil, and steam or boiling water from overheated radiators. In today's flying environment, aircraft transparencies perform the more demanding roles of high visibility, pressurization, impact protection from birds, hail, rain, and anti-icing. Thus, whereas early aircraft transparencies were simple one-piece glass or plastic screens, today's aircraft transparencies are multilayer laminations including various glazing materials, adhesive and conductive interlayers, and various coatings for thermal protection, anti-reflection, anti-static electricity buildup, radar reflection, and others. The increasing all-weather capability and utilization of aircraft, particularly in the military, coupled with the incorporation of electrical circuits within the aircraft transparency for anti-icing and impact resistance, has resulted in an increase in the

atmospheric electricity hazard and lightning-related accidents/ incidents (see Section VII) for some types of military aircraft/ missions.

B. Atmospheric Electricity and Aircraft

Atmospheric electrical phenomena interact with aircraft in a number of ways. These interactions range from insignificant to annoying, hazardous, and occasionally to catastrophic. The most severe atmospheric electricity is that resulting from lightning discharges between clouds or between a cloud and ground. Often these discharges occur in the vicinity of flying aircraft and occasionally involve the aircraft directly. Associated with the lightning discharge are large electromagnetic fields that radiate radially from the lightning channel. These fields induce voltages in aircraft electrical systems that may reach severe levels and cause physical damage or functional upset. In those instances when the aircraft is struck by lightning the current flowing along and through the aircraft skin generates electromagnetic fields that also induce voltage transients in the electrical circuits of the aircraft.

Another atmospheric electrical phenomenon results from triboelectric charging of an aircraft as a result of friction with aerosols and particulate matter in the atmosphere. This charge is typically distributed throughout the exterior surfaces of the aircraft and dissipated to the atmosphere through corona and streamering at aircraft sharp edges or at static dischargers. When the triboelectric charging results in a level that causes uncontrolled corona and streamering, broadband static electricity results that may interfere with communication and navigation systems, and aircraft instruments.

Because aircraft transparencies are basically dielectrics, that is, non or poor conductors of electricity, an electric charge can build up on them that is higher than that on the metallic aircraft surfaces. This charge can reach such levels that

flashover (streamering) to conductive areas can result, electromagnetic interference is generated, local damage to the canopy is possible, and a shock hazard to flight and ground crews is created.

In efforts to eliminate or reduce the effects of triboelectric charging and static electricity, anti-static coatings have been developed and are used on some aircraft transparencies. However, in performing this function, the transparency may become more susceptible to swept-stroke attachment effects than before. In the swept-stroke phenomenon, where lightning attaches at a primary attachment zone (Reference 1, Figure 1), the motion of the aircraft with respect to the "fixed" lightning current channel causes the arc to "bend" as shown in Figure 2, exposing other aircraft areas that are not normally lightning attachment zones to attachment. One such area is the aircraft transparency area. Because of the proximity of the transparency, physical damage to conductive coatings and outer layer materials may result that may necessitate transparency replacement; flashover to other aircraft areas will probably occur.

Since some of the transparencies in use have conductive interlayers for anti-icing and impact resistance purposes, the physical damage may be in the form of dielectric breakdown, that is, puncture. When this happens, the lightning current can be directly applied to the conductive coating with the consequence of possible damage to it and the possibility of inducing voltage transients in other aircraft circuits.

In addition to the effects discussed above, we can consider an aircraft transparency (typically a windshield) which has both an anti-static conductive coating on one surface and an anti-icing conductive interlayer on another as a capacitor as illustrated in Figure 3.

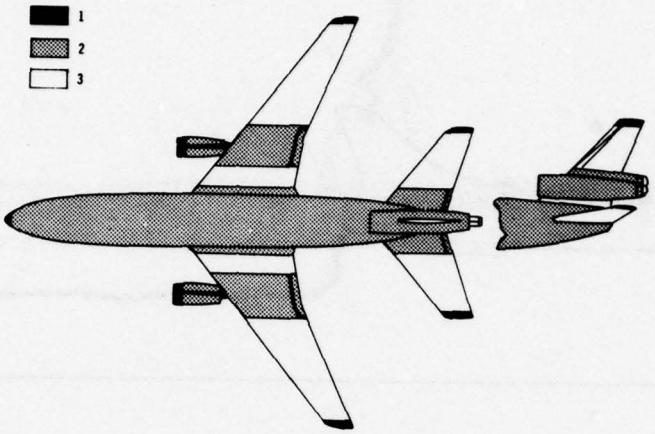


Figure 1. Typical Aircraft Lightning Attachment

Zone 1 - Primary Attachment
Zone 2 - Swept Stroke Attachment
Zone 3 - No Attachment

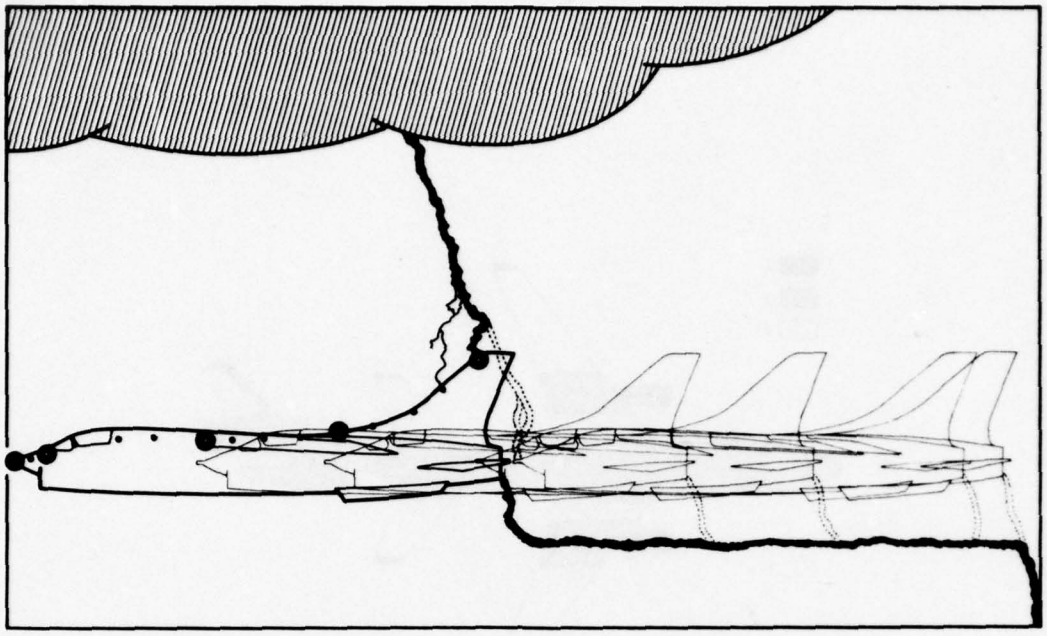


Figure 2. Illustration of Swept Stroke Phenomenon (Large Dots Denote Primary Attachments While Small Dots Denote Secondary Attachments)

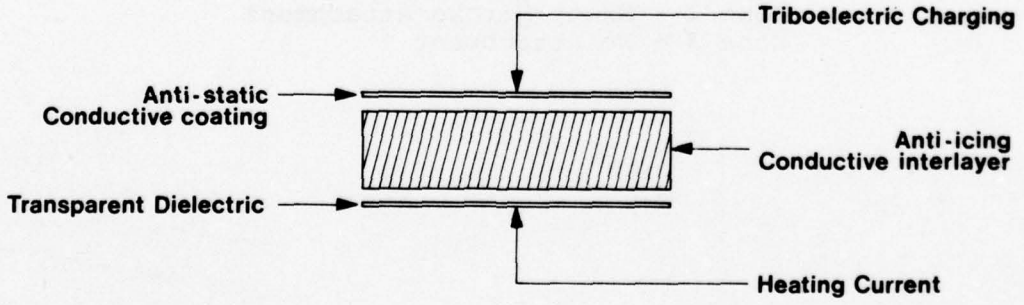


Figure 3. Capacitor Representation of Aircraft Transparency

In operation the heating circuit is susceptible to lightning (or NEMP)-induced voltages which may cause dielectric breakdown at the edges, as just discussed, in instances when triboelectric charging by itself would not be sufficient for breakdown. Heating currents through the damaged heating interlayer may result in "hot spots" and local damage of the transparent material.

C. Lightning and Electromagnetic Pulse

The electromagnetic pulse (EMP) from nuclear weapons, often referred to as NEMP, is an electromagnetic transient that results from the interaction of gamma radiation with the earth's atmosphere. In that it is an electromagnetic transient, it resembles the lightning electromagnetic pulse (LEMP). However, the NEMP have higher peak amplitudes and have shorter durations with much faster rise time (nanoseconds vs. microseconds) resulting in a substantially broader frequency spectrum. The higher frequency content of the NEMP allows smaller aircraft apertures (than for LEMP) to permit penetration of NEMP into the aircraft interior and couple to electrical circuits. Similarly, shorter lengths of unprotected electrical circuits (e.g. wires) can function as "antennas" and allow induced currents to flow which may damage, or cause upset to, components. The mechanisms that cause NEMP are such that significant NEMP may be present at large distances from the nuclear explosion, whereas LEMP is thought to be hazardous only when it occurs relatively near (within 1 kilometer) of a system.

The same characteristics that serve to contrast NEMP and LEMP give rise to the problem that effective protection against the one may not be effective against the other if it was not taken into consideration during the design of the protective scheme.

In terms of transient effects analysis the methods, or models, used are the same with the results being determined by the response characteristics of the circuit and the source term chosen (NEMP or LEMP). The source term in this context can be described as the mathematical model of the EMP in question and is normally some standard pulse shape with specified rise t_1 and decay

t_2 times that govern the frequency content of the model. Figure 4 illustrates the common "standard" or source term model used.

The severity of the NEMP, or LEMP, is governed by the selection of the parameters A_{max}, t_1 and t_2. Generally, in vulnerability assessments an "average" and a "severe" set of conditions are chosen. An "average" set of conditions is generally one that has a 50% probability of being exceeded, whereas a "severe" set of conditions is one that has a 1% probability of being exceeded. The criteria for LEMP are normally chosen as defined in Reference 2. An unclassified description of NEMP phenomena is contained in Reference 3 while a model of NEMP is contained in Reference 4.

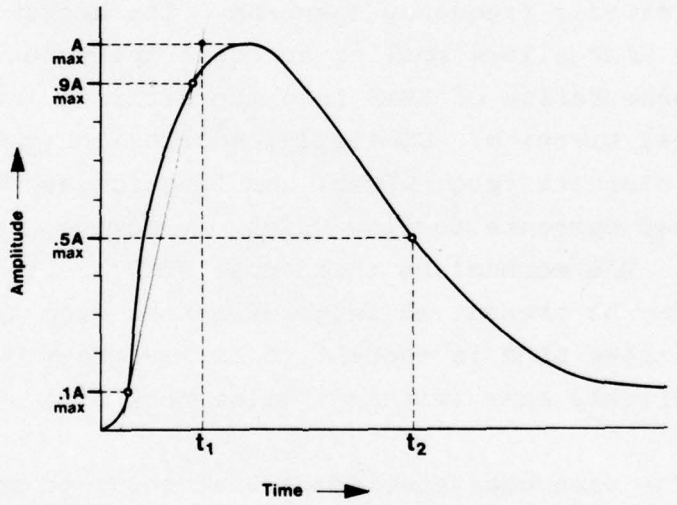


Figure 4. "Standard" Description of Lightning or EMP Pulse

D. Electrical Properties of Materials

The electrical properties of dielectric materials are, typically: resistivity, dielectric and flashover strength, dielectric constant, dielectric dissipation factor, and arc resistance. For those materials that function as electromagnetic

shields the shielding effectiveness is also of interest. Published values of the electrical properties are normally those resulting from test methods published by the American Society for Testing and Materials (ASTM) in coordination (in recent years) with the American National Standards Institute (ANSI), or methods approved by ASTM such as used by Underwriter's Laboratories (UL). The following paragraphs briefly describe each of the electrical properties. In the following discussions illustrations are included that depict the multi-dimensional nature of the electrical properties described. For most dielectric materials the electrical properties are frequency-, temperature- and humidity- (exposure) dependent. The illustrations were chosen mainly to demonstrate this dependency. The materials for which data were found available to illustrate these variations are used primarily as electrical insulators. As such, they are not necessarily representative of transparency material except that they may be edge construction candidates.

1. Resistivity

The electrical resistance of a material is usually given per unit length and unit cross-sectional area or per unit length and unit weight. For dielectric materials using ASTM methods where standard sample thicknesses (volumes) are used in all tests, the resistance is expressed as a volume resistivity or as a surface resistivity. In both cases, it is a DC measurement and the test method and related procedures, circuits and calculations are described by ASTM Test Method D-257 (Reference 5).

a. Volume Resistivity

The volume resistivity is a measure of ability of a dielectric material to resist the flow of an electric current. It is given by the ratio of the electrical potential gradient (parallel to the current in the material) to the current density. Volume resistivity of dielectrics is affected by changes in temperature and humidity (Reference 6, Chapter III).

b. Surface Resistivity

The surface resistivity is a measure of the ability of a surface of a dielectric material to resist the flow of electric current. It is given by the ratio of the potential gradient parallel to the current along the surface of the material to the current per unit width of surface. In combination with the volume resistivity, surface resistivity is often used to assess the purity of an insulating material during development and production. The surface resistivity of a material is particularly sensitive to frequency, humidity, contamination, and related environmental factors (Reference 6, Chapter IV).

2. Dielectric Strength

The dielectric strength of a material is that property of an insulating material which enables it to successfully withstand electric stresses. It is the highest electric strength that an insulating material can withstand for a specified period of time without electrical breakdown by any path in its bulk. It is given by the potential difference, in volts, divided by the test specimen thickness, usually in thousandths of an inch (mils). In previous years four basic tests were used: short-time, step-by-step, slow rate-of-rise, (generally an alternate to step-by-step) and long-time. However, in the most recent revisions of the ASTM Test Method, ASTM D-149 (Reference 7), only the first three are specified and are briefly described below. The method specifies commercial power frequencies which are typically 50 and 60 Hz, but measurements are generally made also at 1 KHz and 1 MHz, since dielectric strength is in most cases frequency-sensitive as well as being affected by temperature and humidity (reference Figures 5 and 6).

a. Short-Time Test

The voltage is increased from zero to breakdown at a uniform rate of 100, 500, 1000, or 3000 volts per second, depending on the total time specified and the voltage/time characteristics of the material, until breakdown occurs.

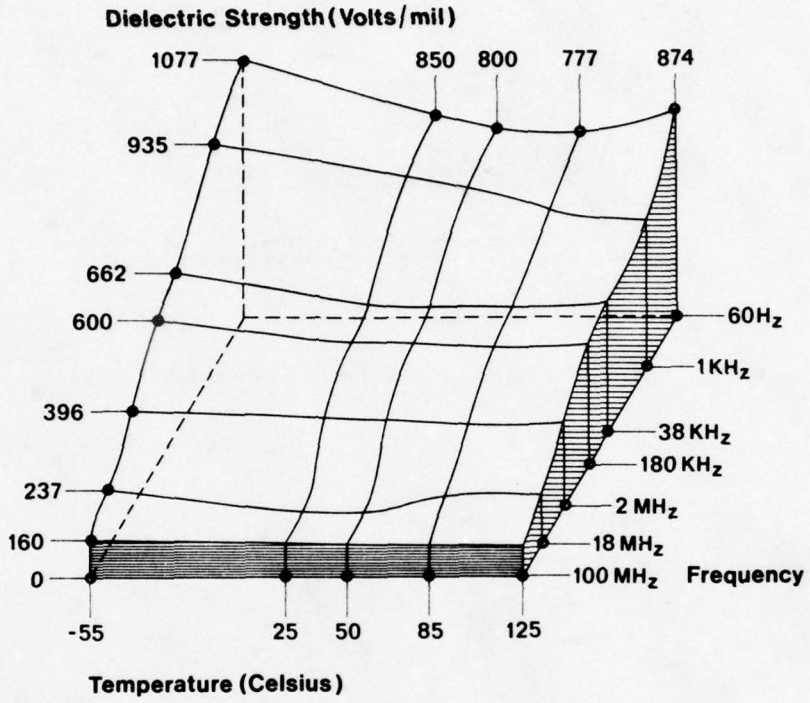
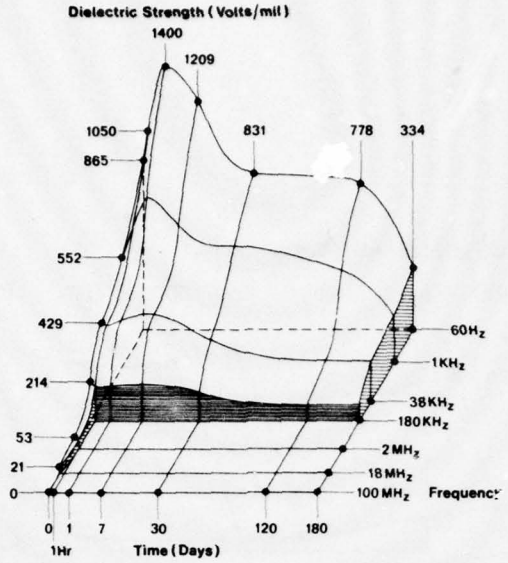
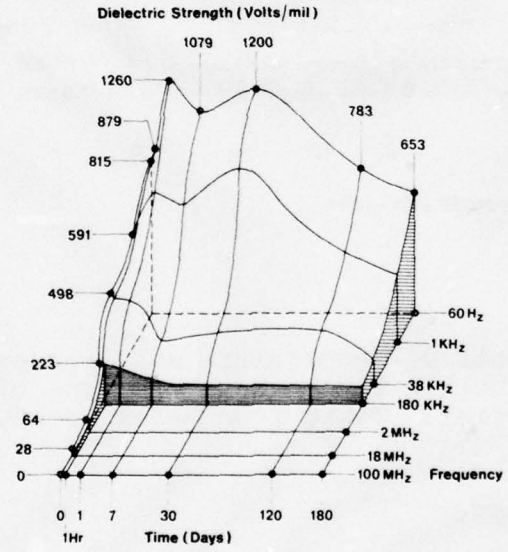


Figure 5. Effects of Temperature and Frequency on Dielectric Strength on One Type of Dielectric Material. Taken from Reference 6.



a. At 50°C and 100% Relative Humidity



b. At 25°C and 100% Relative Humidity

Figure 6. Effects of Exposure on Dielectric Strength of One Type of Dielectric Material. Taken from Reference 6.

b. Slow Rate-of-Rise

An initial voltage, approximately equal to fifty percent of the breakdown voltage obtained in the short-time test, is applied and then increased at a uniform rate until breakdown occurs.

c. Step-by-Step Test

An initial voltage, approximately equal to fifty percent of the breakdown voltage obtained in the short-time test, is applied and then increased as rapidly as possible in equal increments and maintained for a specified period of time.

3. Dielectric Constant (Permittivity)

The dielectric constant of a material that is normally specified is the relative dielectric constant. For practical purposes, it is the ratio of the capacitance of two electrodes separated solely by the dielectric material to their capacitance when separated by air. Ideally vacuum should be used instead of air; however, the error thus incurred is very small. The dielectric constant of a material generally increases with temperature, humidity, and exposure. For most materials, dielectric constant varies considerably with frequency and to a lesser extent with voltage as a result of polarization. Figures 7 and 8 illustrate some of these effects. The relative dielectric constant is typically measured at commercial power frequency (e.g. 60 Hz) and at 1 KHz and 1 MHz according to ASTM 150 (Reference 8).

4. Dielectric Loss Factor

A perfect dielectric can be electrically represented as shown in Figure 9. From basic physics it is known that in this purely capacitive circuit the current leads the applied voltage by 90°. In a real dielectric, however, there are conductive and/or absorptive losses which cause this phase relationship to be altered.

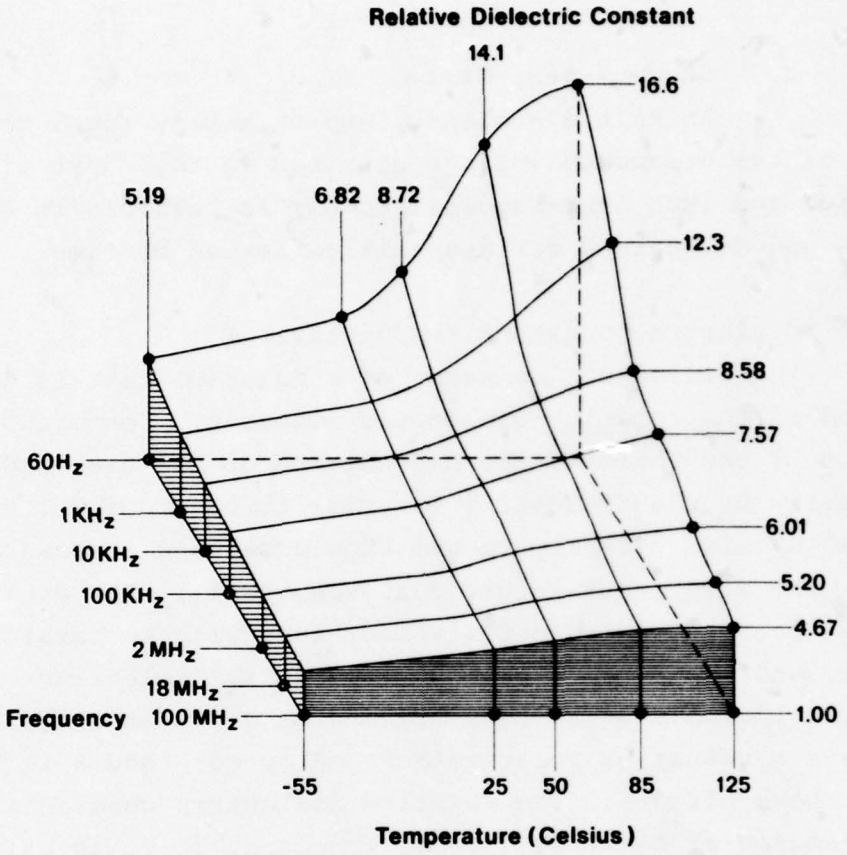
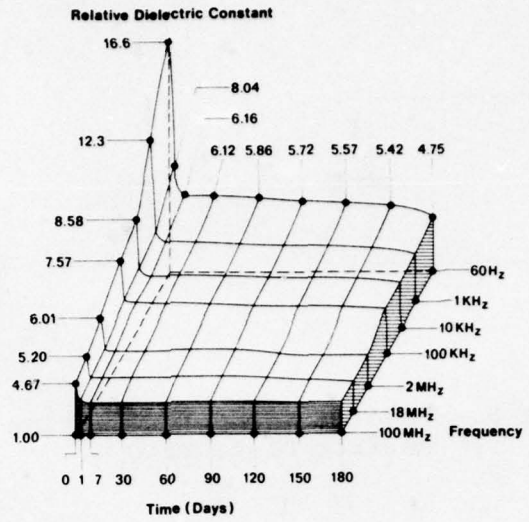
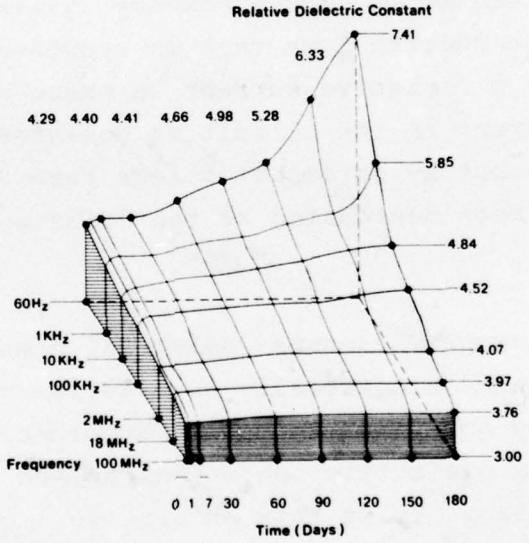


Figure 7. Effects of Temperature and Frequency on Relative Dielectric Constant on One Type of Dielectric Material. Taken from Reference 6.



a. Asbestos-Filled Diallyl Phthalate Molding Compound



b. Silica-Filled Epoxy Coating Compound at 25°C and 100% Relative Humdity

Figure 8. Effects of Exposure on Dielectric Constant on One Type of Dielectric Material. Taken from Reference 6.

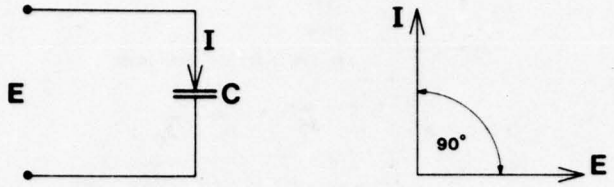


Figure 9. Electrical Representation of a Perfect Dielectric

When conductive losses (only) are present the usual electrical representation of such a dielectric is as shown in Figure 10. In essence this is the low frequency equivalent circuit (Reference 9). The conductive loss that is represented by the parallel resistance causes a resistive current in phase with the voltage. The resultant current in the circuit as depicted in Figure 10 still leads the voltage but by an amount δ less than 90°. The tangent of this angle δ has been designated as the "dissipation" or "dielectric" loss factor.

When absorptive losses (only) are present (Figure 11) these are represented electrically as a series resistance. This is the high frequency equivalent circuit (Reference 9). In this case the current in the dielectric leads the applied voltage by an angle δ less than 90° also. It is this absorptive loss that makes it incorrect to represent an imperfect dielectric as an R-C parallel circuit (Reference 10). However, although equivalent circuits do not explain physical phenomena, it is sometimes helpful to relate observed behavior to a circuit which exhibits such characteristics. In this context, a dielectric with conductive and absorptive losses could be represented as shown in Figure 12. In such a circuit the capacitance and resistance values are chosen to approximate the

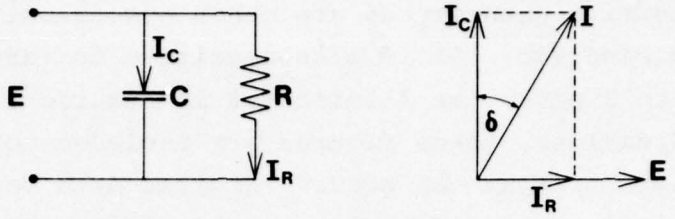


Figure 10. Electrical Representation of a Dielectric with Conductive Losses

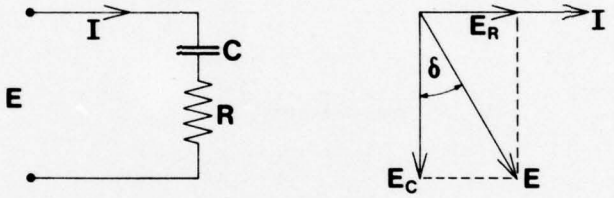


Figure 11. Electrical Representation of a Dielectric with Absorptive Losses

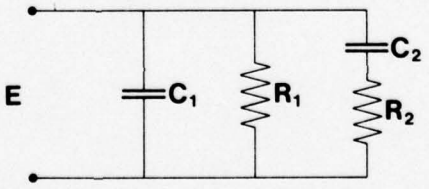


Figure 12. Electrical Representation of a Dielectric with Conductive and Absorptive Losses

actual performance of the dielectric material. It is evident from the circuit representations shown (i.e. the capacitive reactance, $X_C = (2\pi f C)^{-1}$) that the dielectric loss factor (tangent δ) is a frequency-sensitive quantity as are other electrical characteristics of a dielectric. It is also sensitive to variations in humidity and to exposure as illustrated in Figures 13, 14, and 15. As was stated earlier, these figures are included to illustrate the types of variations that can occur. Similar data for actual transparency materials was not found in the literature reviewed. Since the dissipation loss factor is closely associated with the dielectric constant it is usually measured at the same frequencies according to the methods in Reference 8.

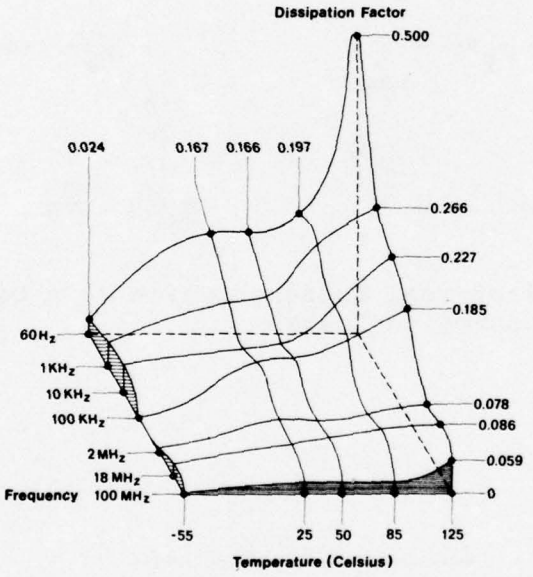


Figure 13. Effects of Temperature and Frequency on Dissipation Factor on One Type of Dielectric Material. Taken from Reference 6.

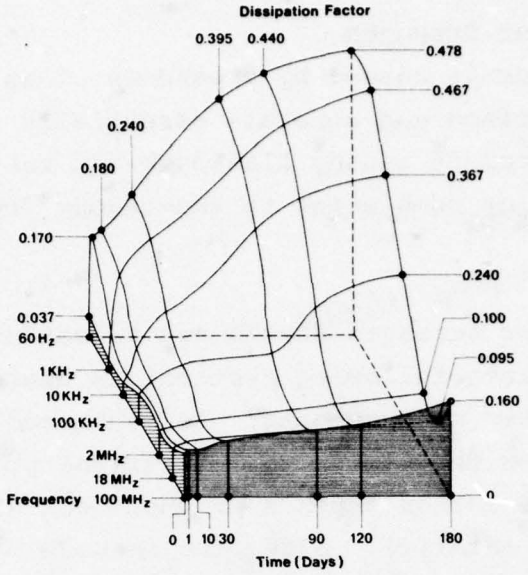


Figure 14. Effects of Exposure on Dissipation Factor on One Type of Dielectric Material. Taken from Reference 6.

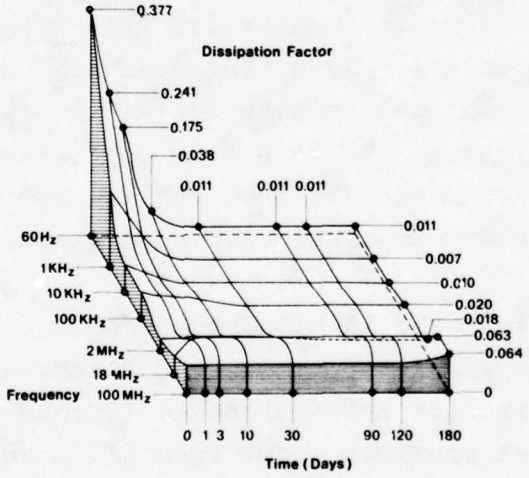


Figure 15. Effects of Exposure at 85°C, Humidity and Frequency on Dissipation Factor on One Type of Dielectric Material. Taken from Reference 6.

5. Flashover Strength

Flashover is caused by breakdown of an insulating material along its surface and consists essentially of a gaseous discharge. In an aircraft canopy flashover can result from swept-stroke attachment at some point to the canopy frame or support structure.

Flashover strength should not be confused with arc resistance (discussed in a following section) as there is no relationship between the two measurements. As mentioned in the following section, the former depends on the electrical properties of the material while the latter depends on the chemical and physical properties of the material. Also, the methods of measurement are different. In contrast to the arc resistance test in which spark discharges are created near the surface of the material, in the flashover strength tests the electrode voltage is increased until flashover between the electrodes occurs along the material surface. There appears to be a relationship between dielectric constant and flashover strength at a given input voltage frequency (Figure 16). Flashover strength appears to decrease with frequency (Figure 17) and exposure (Figure 18). Also, the flashover strength values differ between AC, DC, and impulse excitation of the electrodes as shown in Table 1. As is the case with the illustrations contained in this section, the materials included are not necessarily used in transparencies but may be considered edge construction candidates.

Since flashover is highly dependent on the geometry of the specimen it is difficult to compare flashover strength measurements on actual aircraft transparencies. Comparisons should only be made if the test specimen geometries and electrode configurations are know to be the same. Some investigators (Reference 11) have devised a "flashover distance" method of comparison that gives a relative measure useful in comparing two similar canopy configurations. The comparisons were made based on measurements made on the F-15 (Reference 12) and the F-16 canopies and their respective geometries. The flashover distance is the maximum circumferential

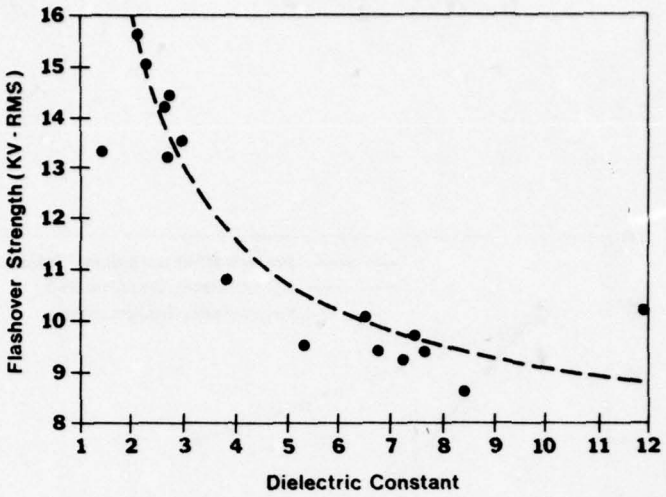


Figure 16. Dependence of Flashover Strength on Dielectric Constant at 60 Hz, with 3/8-Inch Electrode Separation Distance and 1/8-Inch-Thick Separations. Taken from Reference 6.

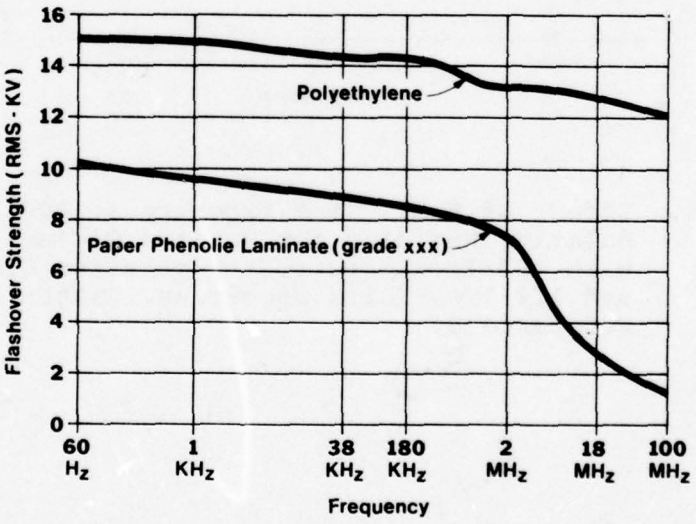


Figure 17. Effect of Frequency on Flashover Strength, with 3/8-Inch Electrode Separation Distance and 1/8-Inch-Thick Specimens. Taken from Reference 6.

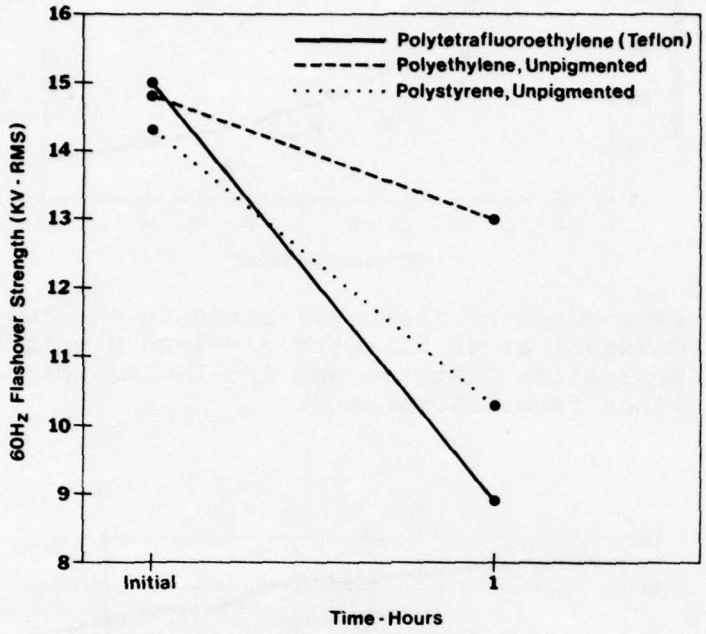


Figure 18. Effect of Short Time Exposure at 100% Relative Humidity for Various Dielectrics, with 3/8-Inch Electrode Separation Distance and 1/8-Inch-Thick Specimens. Taken from Reference 6.

TABLE 1

COMPARISON OF AC, DC, AND IMPULSE FLASHOVER STRENGTH
OF VARIOUS DIELECTRIC MATERIALS

(Taken from Reference 6)

Dielectric Material	Flashover Strength				
	A.C.	D.C.		Impulse	
	60 Hz Peak KV	Positive KV	Negative KV	Positive KV	Negative KV
Polytetrafluoroethylene (Teflon)	21.4	20.2	20.6	25.2	25.0
Polystyrene, Unpigmented	20.2	14.6	17.3	24.8	24.2
Polyethylene, Unpigmented	21.2	14.5	14.3	23.9	23.7
Asbestos-Fabric, Phenolic Molding Compound	13.3	14.4	14.5	13.5	13.8
Asbestos-Filled, Phenolic Molding Compound	12.2	11.7	11.7	12.8	13.4
Asbestos-Filled, Diallyl Phthalate Molding Compound	13.7	15.2	16.0	16.7	17.0
Glass Cloth, Silicon-Base Laminate	15.3	15.5	15.4	17.9	22.0
Glass Cloth, Melamine-Base Laminate	13.4	13.9	14.9	16.2	16.9
Glass Cloth, Epoxy-Base Laminate	13.4	14.2	15.9	16.3	17.7

distance measured along the surface of the canopy over which the current in a lightning strike must travel to reach the surrounding metallic fuselage. The shorter the flashover distance the higher the probability that flashover will occur and the lower the probability of puncture (dielectric breakdown) which is related to the dielectric strength of the material.

6. Arc Resistance

The arc resistance of a dielectric material is a measure of the resistance of its surface to breakdown under electrical stress. It is given by the time in seconds during which an arc of increasing severity is applied intermittently to the surface until failure occurs. Failure may be one of four general types:

a. The material becomes incandescent and hence capable of conducting current but regains its insulating qualities upon cooling.

b. The material bursts into flame (ignites) without the formation of a visible conducting path.

c. A thin wiry line (tracking) forms along the surface between the electrodes.

d. The surface carbonizes until a conductive path forms.

The arc resistance test is generally performed according to ASTM 495 (Reference 13) and depends on the chemical and physical properties of the material. This test and resulting data should not be confused with flashover tests and data which are related to the electrical properties of the material. Generally, the arc resistance of a dielectric decreases as a function of both temperature and humidity as illustrated in Figure 19.

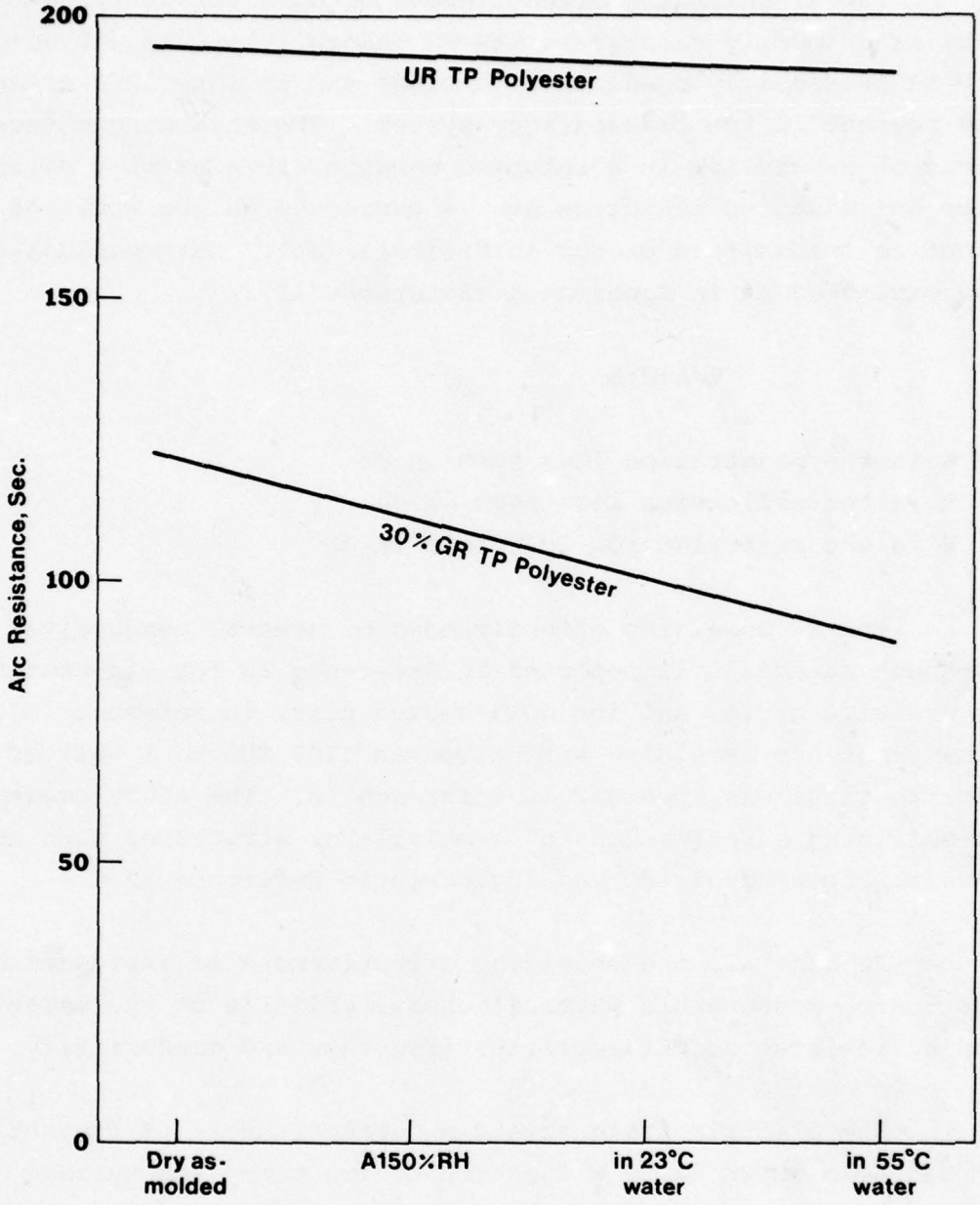


Figure 19. Effects of Temperature and Moisture on Arc Resistance of Polyester. Taken from Reference 14.

7. Shielding Effectiveness

The RF shielding effectiveness of an aircraft transparency is primarily related to its RF absorptivity and reflectivity as provided by conductive coatings and/or interlayers that may be present in the transparency system. The shielding effectiveness of a material is a relative measure of material's ability to keep out unwanted radiation and is expressed as the ratio of incident to transmitted energy in decibels (db). Mathematically it can be expressed as in Equation 1 (Reference 15):

$$S=A+R+B$$

where A is the penetration loss term in db
R is the reflection loss term in db
B is the re-reflection loss term in db

The RF shielding effectiveness of several conductive transparent materials is reported in Reference 16 for tin-coated glass and wire grids, and for gold-coated glass in Reference 17. The low frequency shielding effectiveness (100 KHz to 1 MHz) of conductive glass was reported in Reference 18. The electromagnetic shielding effectiveness of a multilayer structure, such as in an aircraft windshield, was addressed in Reference 19.

In general, the shielding effectiveness is expressed as a function of measureable physical characteristics of the material including resistance, permeability, frequency and conductivity.

The electric field shielding effectiveness of conductive films has been shown to be a function of frequency and surface resistance (References 17 and 18). Figures 20 and 21 illustrate these relationships for the frequency ranges nearest to those present in lightning and nuclear EMP environments. Selection of a conductive material must be based on the overall transparency requirement for light transmission, anti-static protection, shielding effectiveness, heating factors and other related factors.

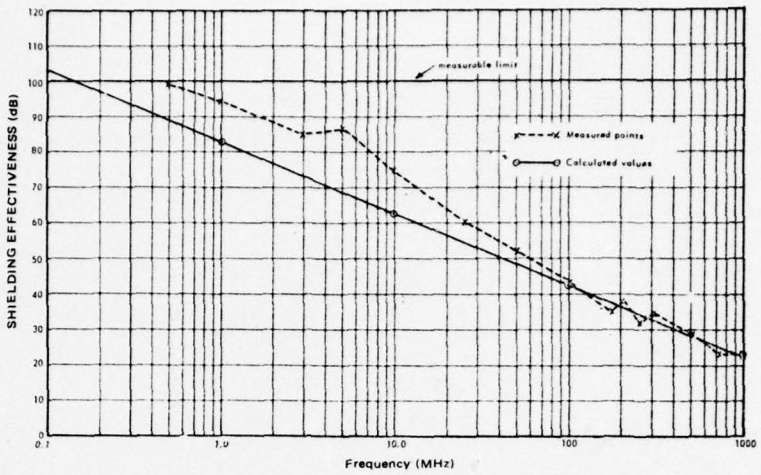


Figure 20. Variation of Shielding Effectiveness with Frequency (10-Ohm/Square Conductive Glass)

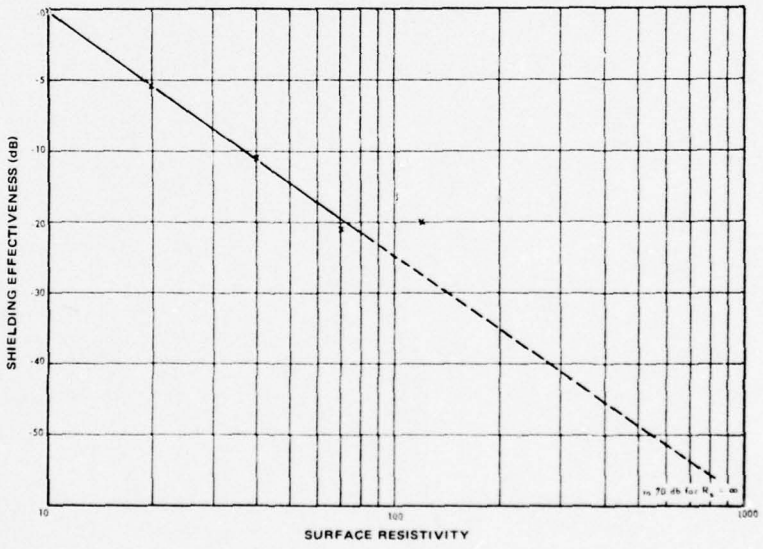


Figure 21. Variation of Shielding Effectiveness with Surface Resistance. Referenced to 10 Ohms/ Square.

SECTION III
LITERATURE SURVEY

The purpose of the literature survey was to identify, obtain and review the significant literature on the subject of aircraft transparencies, their interaction with the atmospheric electricity environment, and physiological effects. Consequently, several sources of information were employed as discussed in the following paragraphs.

A. Transparency Data

Information was sought on the transparency construction details for operational (e.g. F-4) and near-term (e.g. F-18) aircraft. The emphasis was placed on U.S. military and on commercial aircraft with a military application. Sources of information were aircraft technical manuals for maintenance and overhaul and engineering drawings. Work performed by the University of Dayton (Reference 20) and McDonnell Douglas Corporation (Reference 21) on windshield/canopy life cycle cost and failure analysis served as a foundation since both contained aircraft transparency construction details for a number of aircraft of interest.

Once the construction details and the materials used were identified, the transparency system and the transparency material manufacturers were contacted for engineering data, with emphasis on electrical characteristics. Also, trade publications on materials were researched for similar data on transparent materials that might be candidates for use in aircraft. Scientific journals and published books were also researched. In general it was found that the majority of the available electrical data was obtained according to ASTM test methods and published in abbreviated form as presented in Table II of Reference 22. This type of information, although covering a wide range of materials, seldom contained data at more than one temperature or humidity. The most comprehensive reference was Chapman and Frisco (Reference 6) which investigated, in considerable detail, the dielectric properties of materials and

the effects of temperature, humidity, frequency, and exposure on them. The work, however, is over twenty years old and does not include materials of particular interest. Other useful sources of information that did present some information on a variety of transparency materials were engineering handbooks on glass (Reference 23) and plastics (Reference 24).

Key word searches (e.g. lightning and aircraft transparencies) were performed at the Defense Documentation Center (DDC), using the Wright-Patterson Air Force Base terminal, to identify work performed or in progress under independent research programs or under DOD sponsorship pertaining to aircraft transparencies. It was found that most of the work in progress emphasized the mechanical and optical properties of aircraft transparency materials. However, attempts were in progress to develop design guidelines (Reference 16) and specifications (Reference 25) covering all aspects of aircraft transparency systems, particularly windshields.

To obtain information on work performed or being performed under other than DOD sponsorship or of DOD interest (Independent Research and Development), published searches by the National Technical Information Service (NTIS) dealing with lightning, surge and transient protection (Reference 26) and by the Smithsonian Science Information Exchange (SSIE) on thunderstorms and lightning (Reference 27) were obtained and reviewed. In addition, specialized key word searches as were performed at DDC were performed at both facilities.

Many technical reports were identified, acquired and reviewed. Many of these, although of related interest, did not contain quantitative data and are included in the bibliography. Some were found completely irrelevant and were excluded. A group of reports, especially those dealing with EMP, were classified and presented a problem in their acquisition during the time available. Review of the technical documents revealed that, even though some testing programs were being conducted or had been conducted using

aircraft transparencies or transparency replicas as test specimens, most of these were qualitative in nature. Tests have been conducted to investigate the probability of lightning attachment and damage resulting from static electricity and flashover. The most significant work of interest has been performed in recent years (References 28, 29, 30, and 31). In these sources it is evident that researchers are beginning to zero-in on the electrical characteristics of aircraft transparencies that are, or may be, of interest in an atmospheric electricity environment. However, this "enlightenment" has served to identify some of the limitations in commonly available data (i.e. electrical properties of transparency materials) and in the test methods currently in use (Reference 28). Some of these areas are addressed in subsequent sections of this report.

The literature sources used in the assessment that resulted from the literature survey are listed either in the list of references or bibliography presented at the end of this report.

The quantity and quality of electrical data readily available decreases significantly between the primary materials (i.e. glazing and conductive materials) and the secondary materials (i.e. protective coatings, adhesives, sealants, edge construction) of aircraft transparencies. Although some of the electrical properties for some of the materials used might be inferred from the generic material properties, enough differences exist in manufacturing processes and chemical compositions to lower, significantly, the degree of confidence in such inferences. Oftentimes the exact manufacturing processes and chemical compositions are not obtainable because of their proprietary nature.

The increasing concern over the electrical behavior of aircraft transparencies, the on-going programs to reduce their susceptibility to atmospheric electricity, and probable future design and qualification requirements will require that the results of this survey be maintained current by periodic updates and acquisition of the necessary electrical data for all transparency system

materials. However, the emphasis should not be to merely fill gaps. The important gaps, namely the permittivity and conductivity and their variation over the span of the operating and non-operating environmental ranges of aircraft and the LEMP and NEMP electromagnetic frequencies, specially at the extremes, are needed for analytical evaluations using the model described in a subsequent section.

B. Physiological Effects of Lightning on Aircraft Crews

A review of Air Force losses due to lightning strikes (Reference 32) shows that personnel report cases of electrical shock, balls-of-fire running down arms and legs, temporary dazing and flashblindness. An F-101B crashed when a lightning strike temporarily blinded the pilot during landing. An F-4 was destroyed during a low level flight; the pilot bailed out after an explosion threw him to the left side of the cockpit. In other F-4 lightning strike incidents crewmen have reported very mild parathesia, temporary blinding and pressures equal to the muzzle blast of a rifle at close range. In the case of helicopters, electric shock to the crew may be severe since little protection is provided.

A report summarizing lightning strike data from five commercial airlines for the period 1 June 1971 to 1 November 1974 gives a good indication of problems experienced by transport aircraft flight crews. There are 214 incidents reported, involving strikes to Boeing 707, 720, 727, 737, 747; McDonnell Douglas DC-8, DC-9, DC-10; and Lockheed L-188 (Electra) and L-1011 aircraft. In all these cases there were no occurrences of injuries to any flight crew members (Reference 33).

Minor problems reported included 16 instances of flashblindness, 6 cases of exposure to concussive/shock force, and one instance of momentary crew disorientation because of compass outages. There were no cases of electrical shock.

Other incidents reported separately by airlines included secondary currents induced in audio circuits that produced temporary, deafening crashes in earphones, momentary potentials which caused slight shocks and flash blindness persisting for several minutes (Reference 34).

The characteristics of lightning relative to physiological effects are summarized below. The literature survey and direct contacts with physiological effects researchers revealed a lack of information in the areas of luminous output and acoustic shock of lightning.

Most cloud-to-ground lightning flashes consist of faintly luminous leader passing from cloud-to-ground, followed by a brilliant return streamer from ground-to-cloud back along the path of the leader. Several more leader and return streamers often follow along the established conductive path. Most flashes consist of three separate strokes separated by a 40 millisecond time interval; however, time intervals of 10-150 milliseconds have been recorded. The usual flash lasts 0.25 seconds. Although there are variations between cloud-to-ground and cloud-to-cloud lightning, the conditions of cloud-to-ground lightning are generally accepted to be more severe and are consequently used as criteria for susceptibility, vulnerability and/or survivability assessments.

The most frequent peak current value is 20,000 amps, followed by a continuing current in the 40 to 300 amp range. Median rise times for first strokes are 1-3 microseconds but subsequent dart leaders are associated with rises of 0.3-1 microseconds. Data on aircraft strike characteristics indicate a peak rise rate of 5000 amperes/microsecond.

Peak temperatures in the channel are about 30,000°K, decaying to 15,000°K in 25-30 microseconds. Average pressure during the first 5 microseconds is about 8 atmospheres decreasing to ambient within 20 microseconds.

1. Flashblindness

Flashblindness is a temporary loss of vision resulting from exposure to a high intensity light flash. The greatest flashblindness threat to flight crews results from lightning attachment at the area forward of the cockpit and being "swept" to the windshield. The flash light adapts the retinal areas where primary or secondary light sources within the visual field are imaged by bleaching the photopigment of the visual receptors (rods and cones) of the retina and affecting the neural component. Vision is most severely affected when the afterimage is superimposed on the foveal and parfoveal regions of the retina. The fovea is a pit located in the center of a rod-free area centered on the retina that subtends an angle of about two degrees at the pupil. As the retinal photopigments are regenerated, the afterimage fades and the observer can again see visual detail. The elapsed time between exposures and return of vision is referred to as the recovery time (Reference 35).

The bulk of available knowledge on flashblindness is based on investigations involving the nuclear explosion flash. As such, data is presented in part as a function of the angle subtended at the eyeball by a circular source and the brightness of the source. This subtended angle can then be related to a specific set of conditions of source size (a function of the nuclear device yield) and distance. In contrast to this, the lightning flashblindness hazard results primarily from a lightning strike to the nose of an aircraft that may, or may not, be swept over the windshield. The source here is a long source of a length dependent on the viewing angle of the cockpit windshield/canopy, and a breadth depending on the size of the lightning channel current. To relate the lightning flashblindness hazard to that from a nuclear explosion it is necessary to define the former in the same terms as the latter.

Investigations performed by Flowers (Reference 36) revealed that the lightning channel cross-sectional area is approximately a linear function of the current of a spark discharge in

air. That is:

$$\text{Channel Cross-sectional Area } (cm^2) \approx \text{Current (kiloamperes)}$$

Therefore, for average (30 kiloamperes) and severe (200 kiloamperes) lightning strokes, the corresponding channel diameters, assuming a circular cross-section, are 6 and 16 centimeters, respectively. These values are useful approximations to the lightning channel width.

To define the length of the channel, the criteria for aircrew station vision requirements (Reference 37) determined that the pilot's vertical field of view must be between 21° (for fighter/attack aircraft) and 95° (for single-pilot helicopters). The practical application of this requirement was further investigated by calculating a mean windshield area for a number of operational aircraft windshields, including helicopter, fighter, cargo, and bomber aircraft. The result was an area of about 0.4 square meter which, assuming a square windshield area, give a vertical length of about 62 centimeters. A circular windshield shape would yield a similar dimension (equal to the diameter) of about 71 centimeters.

Using the values for channel width and length thus derived, the areas of the lightning channel sources for average and severe strokes are roughly 400 and 1000 square centimeters, respectively. To relate these values to nuclear source data we relate them to circular areas having diameters of about 22 and 36 centimeters, respectively. Assuming an average distance of 50 centimeters between the pilot's eye and the windshield and a swept stroke, the angle subtended by these equivalent sources would be about 12 and 20 degrees, respectively.

To estimate the source brightness we assume a lightning channel (cloud to ground) of five kilometer length and a potential difference between the beginning of the leader and ground of 30

megavolts. We assume a cloud-to-ground stroke because this is generally considered to be a "worst" case. Based on these assumptions and the current values for average and severe lightning strokes, the corresponding power dissipated values are 9×10^{11} and 6×10^{12} watts, respectively. If we assume the lightning channel to radiate as a black body source and a luminous efficiency of 520 lumens per watt, the visible energy for average and severe lightning strokes is about 5×10^{14} and 3×10^{15} lumens. These values correspond to illuminances of about 2×10^{12} and 4×10^{12} lumens per square meter, respectively. These values may be compared to the daylight illuminance on a horizontal surface (at sea level with the sun at the zenith, clear sky) of about 10^5 lumens/m^2 and the starlight illuminance (no moon) of 3×10^{-4} lumens/m^2. (Reference 38).

Admittedly, several assumptions were made in the preceding discussion. The numerical approximations serve two purposes. First, they will enable relating nuclear flashblindness data to lightning, and second, they point out that a flashblindness hazard exists even with the eyes adapted to broad daylight.

Several variables affect recovery time, including flash intensity and duration, the visual angle subtended by the flash field retinal location of the afterimage, pupil diameter, target luminance and the degree of pre-flash adaptation. The effects of multiple flashes and/or simultaneous flashes subtending separate or overlapping visual fields also should be considered.

Rates of recovery following exposure to high intensity flashes with durations of 33 and 165 microseconds and 9.8 milliseconds were measured for luminances up to 8.6 log milliLamberts (mL) (4×10^8 lumens/m^2) by J. H. Hill and G. T. Chisum in 1962 (Reference 39). A luminance of one milliLambert is approximately that level present at a twilight sky condition (10 lumens/m^2). Aircraft instrument lighting is adjustable between about 0.23 lumens/m^2 and about 11.25 lumens/m^2. The log milliLambert scale is used to linearize the plots and for data compression. Thus a display luminance of 0.5 log mL corresponds to 3.2 mL. Visual sensitivity

was determined by the resolution of gratings requiring acuities of 0.13 and 0.32 at display luminances of -2.50 to 2.25 log mL (3.2×10^{-3} to 1.8×10^{2} lumens/m^2). Recovery time decreased as display luminance increased. Recovery time increased with increases in acuity level at display luminances below 0.5 log mL (3.2 lumens/m^2) and with increases in either the luminance or the duration of the adapting flash. Flash duration was not found to be as critical as previously thought since a sixty-fold difference in duration for two flashes of equal total energy only doubled recovery times. Some graphs showing the recovery times obtained are shown in Figure 22. Adapting flash luminance, adapting flash duration and visual acuity level were held constant during each session and the display luminance was varied.

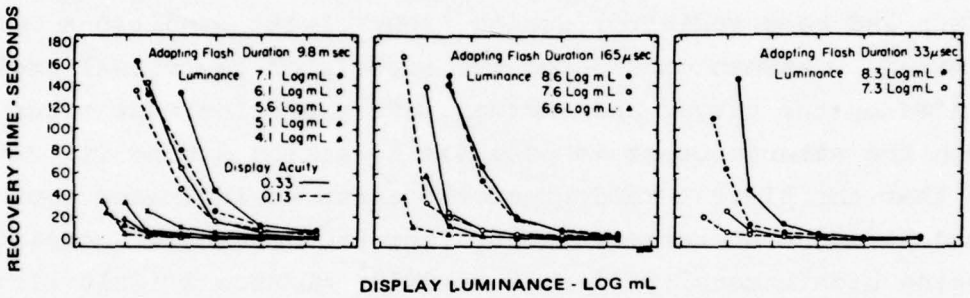


Figure 22. Time Required to Perceive an Acuity Target Following Exposure to an Adapting Flash (Note: 1 mL = 10^{-2} lumens/m^2)

In 1973, G. Chisum (Reference 40) measured the times required to detect a simple display following exposure to adapting flashes of different durations but equal integrated luminances. Results indicated no consistent variation in response times as a function of flash duration.

The effect of flash field size on flashblindness in an aircraft cockpit was measured by W. H. Cushman in 1971 (Reference 41). Flashblindness recovery times were determined for several aircraft instruments after volunteers were exposed to high intensity double pulse light flashes with flash fields subtending 1°, 3°, 5°, 10°, and 15° of visual angle. These subtended angle flash

fields are selected to be representative of nuclear bomb fireballs from either different yields at a given range or a given yield at various ranges. In either case, the fireball will subtend an angle at an observer's eyes corresponding to the apparent fireball diameter. Recovery time increased with the visual angle subtended by the flash field. Countermeasures such as looking around the afterimage and body movement reduced recovery times. Studies of cumulative flashblindness effects after multiple flash exposures were performed by Cushman in 1971 (Reference 35). Subjects seated in an aircraft flight simulator were exposed to a series of high intensity (10^8 mL or 10^6 lumens/m^2 duration (2 milliseconds) light flashes with intervals of 15, 45, 120, or 300 seconds between flashes. Recovery times for interpreting the air speed indicator and turn and bank indicator during night flying conditions were determined. Cushman considered the effects of the visual angle subtended by the target and whether interpretation must occur through the afterimage or is possible by seeing around it. It was found that the digital readout of the airspeed indicator could not be read at night at various times after each of three successively occurring high intensity flashes of $2x10^5$ mL/second ($2x10^3$ lumens/m^2/sec) with 12° flash field. The multiple flash hazard was not nearly as high for the turn and bank indicator, which could be read around a 12° afterimage. Target luminance effects on recovery time were also investigated by increasing the luminance of the airspeed indicator from 0.07 to 2.1 mL ($0.7x10^{-4}$ to $2.1x10^{-2}$ lumens/watt) immediately after the third flash. Mean recovery time decreased 82%. When thunderstorm lights providing 150 footcandles of supplementary instrument panel illumination were used, mean recovery time was decreased 94%.

In 1974, G. Chisum and P. Morway (Reference 42) measured the recovery times for detecting the orientation of a display following exposure to two flashes separated by intervals ranging from 2 to 90 seconds. Their results show that for a fixed flash duration, as would be the case for an air crewman wearing dynamic flashblindness protection equipment, exposure to two flashes is not associated with simple variations in response time.

Response times as a function of adapting flash area and retinal location were measured following exposure to high-intensity, short duration flashes in eighteen retinal locations (Reference 43). It was found that intraocular effects operate in flash-blindness, producing small but consistent increases in foveal response times following extrafoveal stimulation by an adapting flash.

The rate at which parafoveal vision is recovered is significant since parafoveal acuity is necessary to maintain safety in flight. The extent of the disruption of parafoveal sensitivity as a function of retinal location was studied by G. Chisum in 1971 (Reference 44). The times required for parafoveal detection of a simple display were measured following exposure to three adapting flash areas in nine locations. Both factors produced variations in recovery time, indicating that intraocular effects are involved in parafoveal flashblindness and that part of the intraocular effect can be attributed to retinal interaction.

The aircraft cockpit configuration influences the angle subtended by the flash field. Other variables are introduced by protective reactions such as the blink reflex, head and body movement, adjusting lighting levels, and by using sunglasses, goggles, eyepatches and light-activated closing devices. Recovery of visual function to the levels required for reading vital instruments was recorded without protection, with the use of a monocular eye patch and with the use of a 2% transmission gold-coated visor and supplementary instrument illumination (Reference 45). The eye patch was found to give superior performance for general night use whether it was raised immediately after the flash or transferred to the other eye. With the thunderstorm lights on, however, the visor gave an increase in average recovery time of 78% over the best eye patch recovery time.

Other research in protective devices has been done (References 46 and 47), but was applicable primarily to providing protection from nuclear explosions. Also nine papers on visual aids

and eye protection for the aviator were presented at the Aerospace Medical Panel Specialists' Meeting held in Denmark, 5-9 April 1976 (Reference 48).

Only one study of the effect of color on visual recognition was found (Reference 49). Visual perception of blue filtered light was significantly better than for white, red or orange-red filtered light when a glare was imposed. With increased use of digital readouts, investigations of the influence of color variations on instrument readability after exposure to lightning flashes might be of interest.

The common recommendation for dealing with possible vision loss during thunderstorm penetration is to turn up the lights in the cockpit. R. H Golde (Reference 50) reports that the intense light emission caused by a final current pulse in lightning strikes to the aircraft can cause temporary blinding to aircraft pilots but no quantitative data are given. In an analysis of the lightning susceptibility of a NASA T-38 aircraft (Reference 51) it is reported that 76.6% of all strikes to these aircraft are to the pitot boom at the nose, posing a threat of flashblindness from the lightning arc. In addition, USAF and USN lightning incident reports include many instances of flashblindness occurrences. Pitot booms are likely attachment points for lightning due to their forward position and needle-like geometry and this statistical relationship probably occurs for other aircraft configurations as well.

Since cockpit configurations and transparency designs vary from aircraft to aircraft, each aircraft design can produce variations in the factors affecting flashblindness, (i.e. visual angle subtended by the flash). Individual tests have been reported in the F-104G, B-52D, F-106B, F-4C, and C-131 but no known attempt has been made to correlate these results according to the effects of cockpit/transparency design.

2. Electrical Hazards

The degree of shock from an electrical incident is measured by the amount of current forced through the body and not the voltage applied (Reference 52). Voltage is important only because its level and the body resistance between the points of contact determine how much current flows. Since resistance varies from 1000 ohms in wet skin to over 500,000 ohms in dry skin, a dangerous voltage level cannot be predicted.

The threshold of sensation is around 0.003 amperes while currents of 0.01 amperes cause pain. Muscle contractions start at 0.02 amperes; severe shock occurs at about 0.03 amperes, and extreme breathing difficulty is experienced at over 0.06 amperes. Ventricular fibrillation occurs between 0.1 and 0.2 amperes and is considered lethal. Above this level the heart is forcibly clamped which prevents ventricular fibrillation and may not cause death if resuscitation efforts begin immediately. However, severe burns and unconsciousness will result.

In a metal aircraft struck by lightning the flight crew are shielded by the fuselage which forms a continuous, conductive shell (Faraday cage) of such low resistance that current usually does not flow long enough to cause serious problems from electrical shock. Serious electrical shock can, however, be caused if currents and voltages are conducted via control cables or wiring leading to the cockpit from control surfaces struck by lightning. The shock level may be sufficient to cause numbness of hands or feet, disorientation, confusion or unconsciousness (Reference 1).

There are some instances of minor shocks to flight crew members. Some slight shocks have occurred to F-4 crew members, probably through wiring to the cockpit switches (Reference 53). NASA T-38 pilots have reported annoying but not hazardous shocks from seat belt buckles; the cause of these shocks was studied by the U.S. Air Force and a final report is in preparation (Reference 51).

a. Canopies

Aircraft canopies are sometimes struck by lightning but the crew is protected from harm by the dielectric strength of the canopy and the conductive canopy frame. This concept is discussed in a paper on lightning protection for advanced fighter aircraft and it is recommended that high voltage tests be performed on an actual canopy during aircraft design, including mockups of the ejection seat and pilot's helmet, to insure that the canopy will not puncture during a direct strike. This work was followed by mathematical analysis of the hazard (Reference 54), preliminary tests in flat polycarbonate sheets and a simulated canopy, and finally tests in an actual fighter canopy with ejection seat. The results show that the canopy would not puncture as the result of a direct lightning strike. Tests were also conducted to determine the magnitude of corona streamering currents inside the canopy just before a strike occurs. A helmet, including grounded earphones and mike, was attached to the seat. It was concluded that corona levels were too small to be a hazard to personnel but no data were given.

Further study of medical aspects is recommended. The AFSC Design Handbook (Reference 1) reports that shock can be induced on flight crews under dielectric covers such as canopies by the electric fields during thunderstorms, a phenomenon which generally occurs without puncture of the dielectric covering.

b. Helicopters

Problems with lightning protection to helicopters are occurring more frequently as they begin operating in all-weather conditions. Shock hazards to the crew can be introduced if an ungrounded conductor is mounted in a transparency (or a non-conducting skin area) in such a way that it can lead a lightning strike or streamer into the enclosure (Reference 16). An example is the outside air temperature gauge. However, grounding the gauge to the air frame eliminates this hazard.

3. Blast and Acoustic Effects

Crew members sometimes mention blast effects, accompanied by high noise levels, which occur during lightning strikes. Physiologically, these incidents do not appear to be serious and no reports of investigations have been found in the lightning literature. Although no physiological data were found, the magnitudes of shock waves from lightning strike are significant and can be calculated (Reference 55) and should be evaluated for physical effects.

4. Psychological Effects

The only research that appears to deal directly with psychological effects to aircraft crews in the thunderstorm environment was performed by the Aerospace Medical Laboratory of Japan. This work was not available in time for this report. It would seem that this is an area deserving of further study since a thunderstorm environment is know for the fear it produces and could cause resulting interference with physiological functions.

5. Conclusions

a. There is a large volume of literature available on flashblindness effects. This work, which is concerned mainly with protection from nuclear explosions, should be applicable to lightning if the luminous output of lightning flashes is defined.

b. Corona streamering current measurements beneath aircraft canopies should be made to determine the potential for electric shock to crew members.

c. Blast and acoustical effects occurring during a lightning strike should be measured to determine if shock and noise levels could be a hazard to personnel.

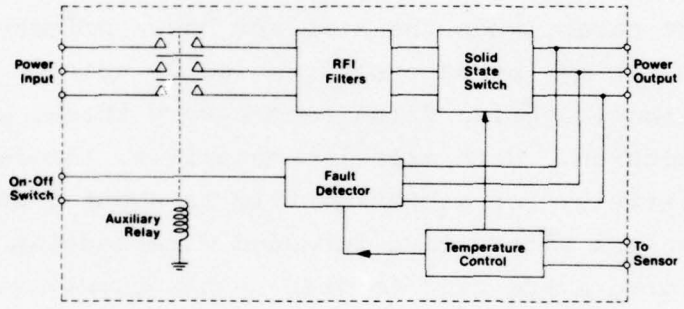
d. The effects of combined psychological effects due to lightning require further investigation.

SECTION IV

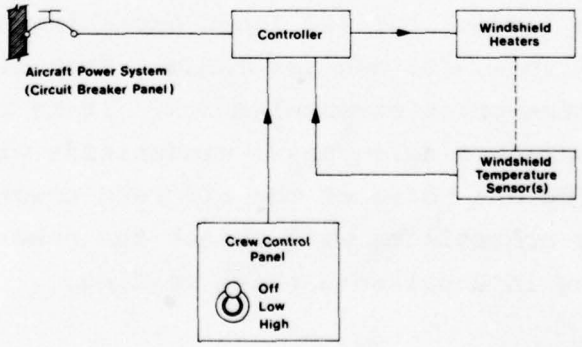
SYSTEM SURVEY

A. Aircraft Transparency Circuits

Circuits used for windshield or transparency heating for de-icing are basically AC or DC power circuits. Electrical resistance heating is one of the most common methods used to provide heat for anti-icing of aircraft windshields. The electrical power is converted to heat by applying a voltage to a conductive film or mesh of fine wires embedded within the transparency system. Circuit routing is usually from AC or DC power busses through relay contacts to the heating elements embedded within the transparency system. Figure 23 is a diagram of a typical windshield heating system.



a. Typical Block Diagram of Heating System



b. Block Diagram of Power Controller with Auxiliary Relay

Figure 23. Typical Aircraft Windshield Heating System. Taken from Reference 16.

The electrical power supply for windshield heating will normally be 400 Hz at a nominal 115/200 volts rms. From one reference source (Reference 56) the specifications on transparency systems used in a variety of aircraft produced the following statistics. Operating voltages for the heating systems range from 50 to 230VAC. Total power requirements vary from 174 to 4750 watts depending on the size of the transparency. The power density in relation to the area of the transparency can vary from 0.58 watts/in.^{2} to 4.9 watts/in.^{2}.

In special cases, when the heated area is very large, higher voltages may be required. Transformers or autotransformers are required to step up the voltage, become part of the windshield heating system and result in added weight and cost.

In other cases, when the aircraft has a primary DC electric power system, it may be necessary to use 28 volt DC supplies. For this low voltage, heating films become very thick, which reduces light transmission. With existing materials, the lowest practical surface resistivity for a heating film is about 3 ohms per square. Therefore, unless alternative imbedded wire heating systems or power transformers are used to step up the supply voltage, the DC systems are normally restricted to small areas of coverage.

Windshields must conform to the power requirements of MIL-STD-704A (Reference 57) for utilization equipment. This standard calls for three-phase loading for all loads exceeding 500 volt-amperes, and when practicable, for smaller loads. Each windshield must contain its own three-phase power elements. It is normally unacceptable to use separate single-phased windshields with each one connected to a different phase of the aircraft power supply because the temperature controllers will switch the power on at different times, resulting in unbalanced phase loading.

Windshield loads may be configured for wye or delta type connections in order to provide the most convenient phase voltage. The wye configuration provides 115 VAC to each heated section, while the delta connection applies 200 VAC.

A fixed power level for windshield heat is impractical because a power density that will prevent ice formation under the worst conditions of temperature and aircraft speed will result in severe overheating in less extreme conditions. A temperature control system is therefore employed that responds to signals from one or more temperature sensors embedded in the windshield. These sensors consist of a fine resistance wire formed into a grid and mounted in a thin transparent plastic sheet, with an area up to about one inch square located very close to the conductive coating or heating elements.

Power can be applied to the windshield by an on-off controller, or a controller with a stepped or continuously variable power output.

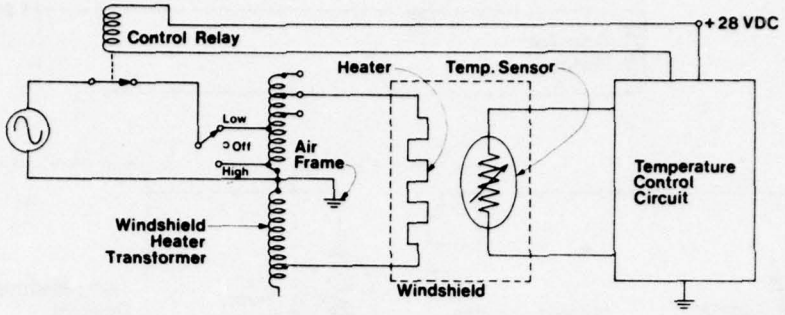
A study of a number of aircraft transparency de-icing circuits reveals that there are considerable variations between circuits from aircraft to aircraft and, in many cases, from window to window within the same aircraft.

As stated previously, the most common source of power for these heater circuits is 3Ø, 400 HZ, at 115 volts rms per phase. The most common heater element is a conductive film applied to one of the inner plys of the transparency during the manufacturing process. The film thickness is apparently difficult to control, resulting in deviations of up to ±10% from the desired resistance. To insure that the proper power is applied to the windshield heater, the aircraft heater circuits must have provisions to compensate for this 10% variation in heater resistances. This is normally accomplished by providing output voltage taps on the heater transformer.

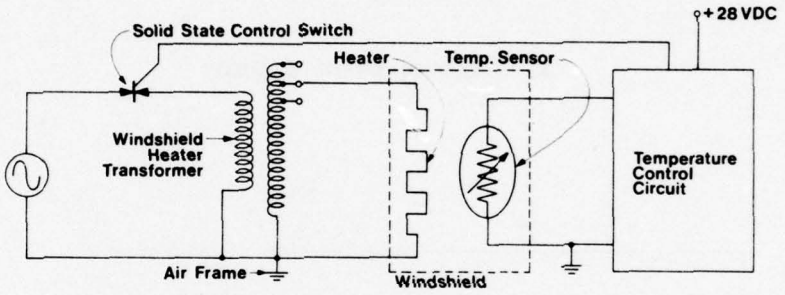
Most transparency de-icing circuits use an active temperature control circuit which operates a relay or solid-state switch to control the power applied to the heater and maintain a pre-determined windshield temperature. The temperature sensing element for the controller is usually a thermistor, or thermocouple wire, imbedded in, or physically attached to, the transparency. Some of the simpler heater circuits may use a thermal switch connected in series with the heater for coarse temperature control. These control circuits are normally powered from the 28VDC source.

Figures 24 and 25 show some simplified windshield heater circuits. These are included here to show some of the typical variations encountered, and to illustrate the fact that in some circuits one end of the heater element and/or temperature sensor may be referenced through some impedance to the airframe.

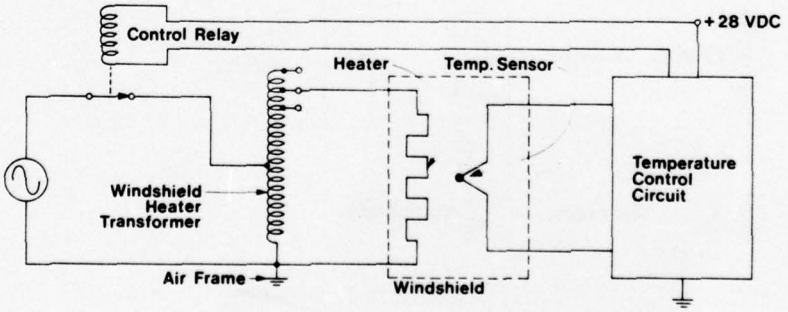
Despite the physical differences, in all cases these heater circuits can be reduced to the "Thevenin" equivalent series circuit as shown in Figure 26. The load impedance (heater resistance) is represented by Z_L. Points "a" and "b" are the heater connection terminals, and Z_{ab} represents the equivalent total impedance looking back from points a and b toward the source. In each case Z_L is resistive. Z_{ab} in the DC heater circuits is also resistive. Z_{ab} in the AC heater circuits is almost totally inductive, consisting of inductive networks of the AC generator, power transformers, and windshield heater transformer. From the various circuits studied it has been found that the heater resistance (Z_L) may range from as low as 6 ohms to as high as 365 ohms. The complexity of the wiring, the impedance networks, and the lack of data on the network components have prevented the establishment of a typical impedance range for Z_{ab} at this time. However, if we assume a typical source impedance of one tenth of the expected load impedance, a reasonable assumption, we could expect Z_{ab} to range from a few tenths of an ohm to 10 ohms. It is suggested that the actual range of Z_{ab} could be established fairly easily by making, and recording, a few



a. Two Heat Ranges with Thermistor Sensing

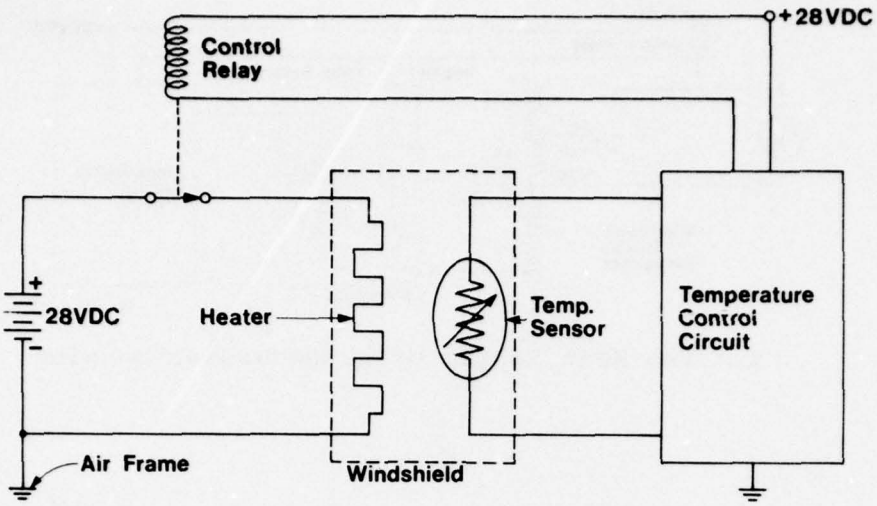


b. Single Heat Range with Thermistor Sensing

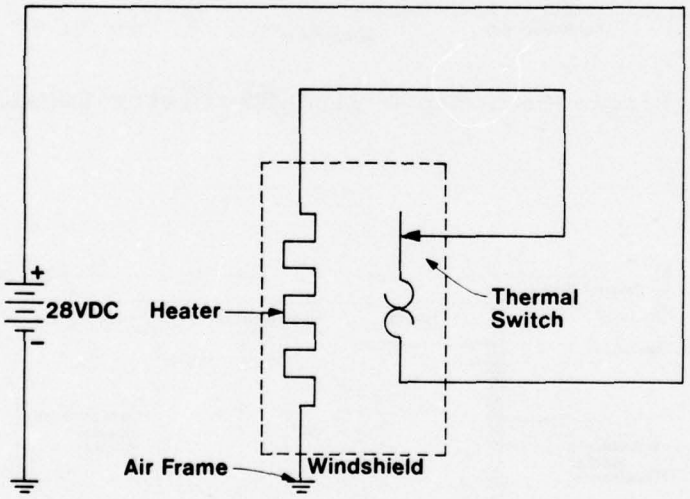


c. Single Heat Range with Thermocouple Sensing

Figure 24. Typical AC Windshield Heater Circuits

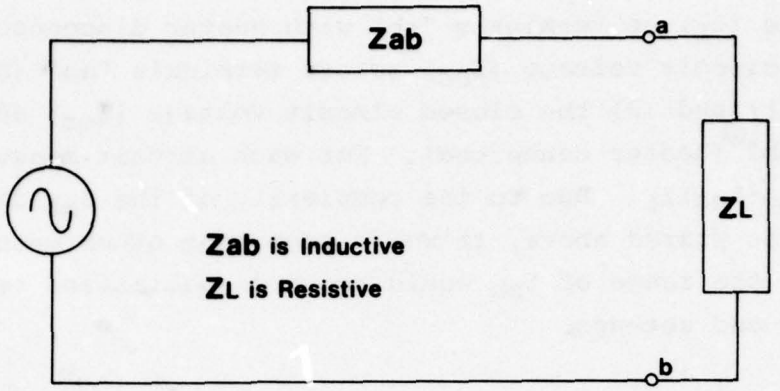


a. Thermistor Sensor

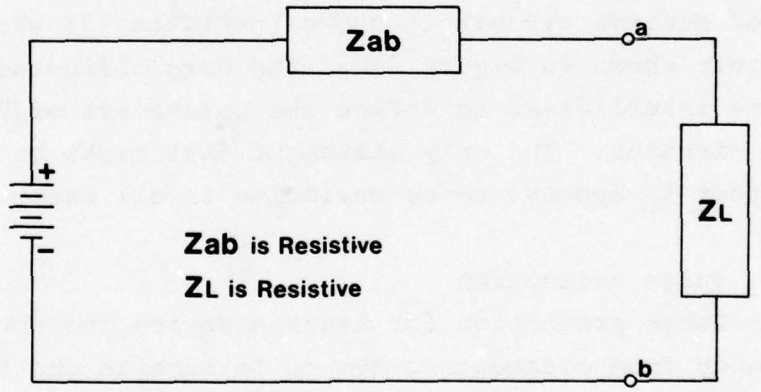


b. Thermal Switch

Figure 25. Typical DC Windshield Heater Circuits



a. Equivalent AC Heater Circuit



b. Equivalent DC Heater Circuit

Figure 26. Equivalent Windshield Heater Circuits

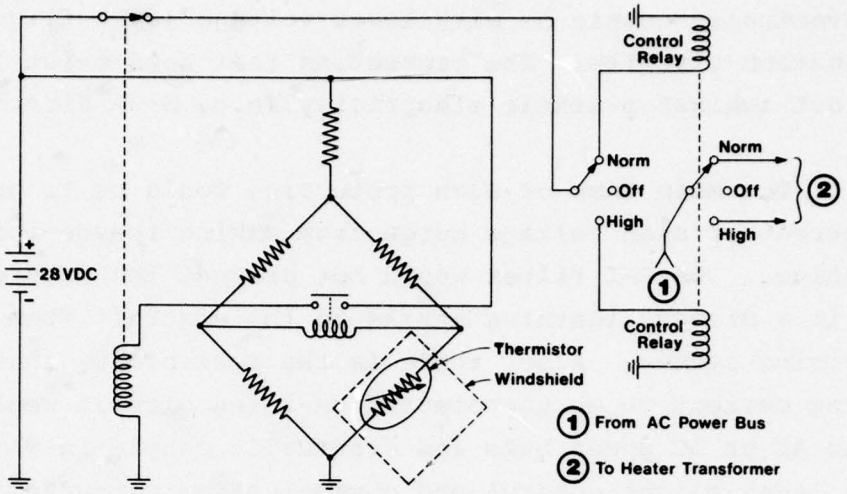
relatively simple measurements in a variety of aircraft transparency circuits. These measurements would consist of (1) the heater resistance (Z_L) at terminals "ab" with heater disconnected; (2) the open circuit voltage (E_{oc}) across terminals "ab" (heater disconnected); and (3) the closed circuit voltage (E_{cc}) across terminals "ab" (heater connected). For each circuit measured then, $Z_{ab} = (E_{oc}-E_{cc})Z_L$. Due to the complexity of the Z_{ab} impedance networks as stated above, it would seem that other means of determining the range of Z_{ab} would require specialized test and equipment and set-ups.

Since the temperature sensor elements are in direct contact with the aircraft transparency, it is also desirable to provide protection for these elements and their control circuitry. In most control circuits the temperature sensor forms one leg of a resistance bridge. An amplifier or micropositioner connected across the bridge detects any imbalance and operates a relay or solid-state switch to control the power applied to the windshield. One such simplified control circuit is shown in Figure 27a with its equivalent circuit shown in Figure 27b. The data collected and studied to date is insufficient to define the parameters of Z_L and Z_{ab} in these circuits. The only statement that might be made at this time is that Z_L appears to be resistive in all cases.

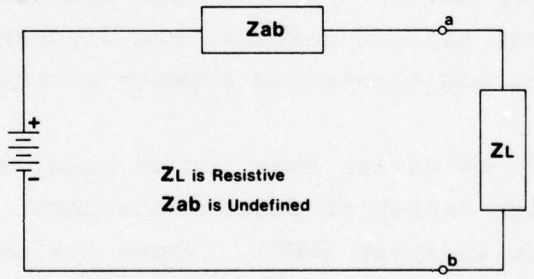
B. Surge Protection

Surge protection for transparencies prevents damage to a transparency from overheating due to failure in the temperature sensing system or in the power controller. If the sensing system leads become open- or short-circuited, protection is provided in the controller by shutting off the output power. Some de-icing systems have radio frequency interference (RFI) filters in conjunction with solid-state switching. These filters reduce transient spikes or surges on the interconnecting wiring.

At the present time, there is no protection against lightning or EMP type surges on transparency systems. The main



a. Typical Transparency Heater Control Circuit



b. Equivalent Circuit of Typical Transparency Heater Control Circuit

Figure 27. Simplified and Equivalent Windshield Heater Control Circuit

task of such protection would be to prevent a high current or high voltage surge from entering onto the AC or DC power buss which would eventually couple in with lower voltage level flight control communication circuits. The protection that does exist is intended to protect against p-static electricity (e.g. S-3A aircraft).

The main task of such protection would be to prevent a high current or high voltage surge from making the de-icing system inoperative. The RFI filter would not prevent the high energy contained in a direct lightning strike to the aircraft from damaging the de-icing system. Also, there is the possibility that the lightning current on an unprotected de-icing circuit would enter onto the AC or DC power buss and eventually couple in with lower voltage level flight control and communication circuits.

Protection does exist that can be added to transparency de-icing systems that would reduce the threat of circuit and secondary circuit damage due to high energy surges. The idea is to shunt or divert the surge from the circuit that is to be protected. There are various transient suppressors that can be added to circuits to accomplish this. These devices include selenium thyrectors, zener diodes, silicon carbide, gas discharge tubes, R-C networks, neon bulbs, and electronic crowbar circuits.

One type of device that can be used on power circuits and can handle the high energy of direct attachment lightning currents is the metal oxide varistor (MOV). These devices are voltage-dependent, symmetrical resistors which perform in a manner similar to back-to-back zener diodes in circuit protective functions. When exposed to high energy voltage transients, the varistor changes from a very high standby value to a very low conducting value, thus clamping the transient voltage to a safe level. (Reference 58).

A typical installation of surge protection devices in a circuit such as the de-icing circuit is shown in Figure 28. The devices are placed line-to-line and line-to-ground, or in the case of an aircraft, line-to-airframe. This arrangement reduces high

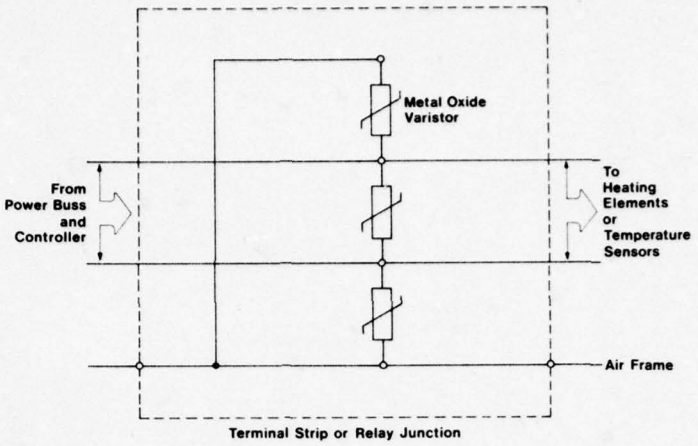


Figure 28. Installation of Lightning Protective Devices in Aircraft Transparency Circuits

transient voltages line-to-line and shunts any transient currents to the airframe. The location where the protective devices should be placed in the circuit depends on the aircraft. Preferable locations are at the terminal strip or relay junction box immediately before the heating elements and temperature sensing devices in the transparency. This location may not be feasible in some current aircraft due to space limitations but could be planned for in future designs.

SECTION V
DATA MATRIX

The data matrix compiled during the program is broken down into groups of data sheets in categories of glazing, interlayer, coating and edge construction materials. The edge construction materials are further subdivided into mechanical support and mounting, seal and gasket, sealant, and adhesive materials. Within each group or subgroup, the data sheets are in alphabetical order by material.

The data summary sheet format is a compromise of a number of possible methods of presentation. As discussed in Section II.D., the electrical properties vary in most cases as a function of frequency, temperature and exposure to humidity. The multidimensional nature of the electrical properties precluded simple presentation of the available data so that material comparisons can be made directly. However, since the intent of the literature survey was not to perform these comparisons but to identify the amount and type of data available, the format in Figure 29 was chosen.

The data summary sheet has rows that summarize each of the electrical characteristics for which data was searched. For each characteristic there are columns for temperature, frequency, and relative humidity variations. The temperature, frequency, and relative humidity columns are each broken down into two rows. For temperature the top row has blocks for the MIL-STD-810C (Reference 59) non-operating temperature extremes (-55° and +75°C) and ambient (23°C). If data was found at these temperatures the block was checked. The bottom row is used to present the actual temperature range of data found. The sources of data are referenced in the "Data" blocks. In the frequency column, the top row has blocks for the three frequencies for which data is normally found in the literature. As before, the bottom row presents the range for which actual data was found. Again, for relative humidity the top row

MATERIAL CHARACTERISTICS DATA SUMMARY

CATEGORY_____ MATERIAL_____

	TEMPERATURE Degrees Celsius				FREQUENCY Hertz				RELATIVE HUMIDITY Percent			
DIELECTRIC CONSTANT	-55	23	+75	Data	60	10^3	10^6	Data	0	50	100	Data
SURFACE RESISTIVITY	-55	23	+75	Data	60	10^3	10^6	Data	0	50	100	Data
VOLUME RESISTIVITY	-55	23	+75	Data	60	10^3	10^6	Data	0	50	100	Data
DIELECTRIC STRENGTH	-55	23	+75	Data	60	10^3	10^6	Data	0	50	100	Data
DISSIPATION FACTOR	-55	23	+75	Data	60	10^3	10^6	Data	0	50	100	Data
ARC RESISTANCE	-55	23	+75	Data	60	10^3	10^6	Data	0	50	100	Data
FLASHOVER STRENGTH	-55	23	+75	Data	60	10^3	10^6	Data	0	50	100	Data

Figure 29. Sample Data Matrix Data Summary Sheet

has blocks for those values of relative humidity usually cited and the bottom row is used to present the actual range of data found.

In several cases data from several sources was used in the preparation of the data. However, there was no attempt at reconciling differences or making value judgments on the data found. Thus if one source of data listed a range of values different from another, a range encompassing both sources is presented.

In evaluating the contents of the summary sheets, the reader must bear in mind the contents of Section II of the report which defines each of the electrical parameters listed and how each may be affected by temperature, frequency, humidity or exposure. Table 2 summarizes the contents of the Data Matrix as contained in Appendix C. As is evident in the table, the materials have been reduced to as generic a term as possible. Data for specific products of individual manufacturers is not separately identified because in many cases the data is not available, sometimes due to their proprietary nature. Also, some of the data that is available is for a specific configuration of the material and would not be compatible with data obtained by the standard test methods.

Originally, it was intended to include an additional appendix which would present the actual data found. However, this would have resulted in a handbook-type report which was beyond the scope of the program.

Subsequent sections of this report address the problems of extrapolating data to fill the many gaps in evidence, and of performing measurements to fill the gaps. In general, the only parameter that can be extrapolated with any confidence is dielectric strength as a function of material thickness. Even then, extrapolations of data from film thicknesses should not be extrapolated to sheet thicknesses and vice-versa.

It is not recommended that measurements be made strictly for the sake of completing the data sheets since there are some options available that, at least from the atmospheric hazard viewpoint, do not require such a monumentous undertaking.

From the vulnerability viewpoint the number of tests necessary (and consequently the test set-up, test specimen preparation and data reduction required) can be significantly reduced by using impulse tests with simulated LEMP and NEMP inputs. Such inputs will encompass all the frequencies of interest with a minimum number of tests.

The materials present are those found to be currently in use on aircraft transparencies and those that might be used in the near future. The basic criteria for glazing materials used for the latter category was they be optically transparent. Other criteria that are important are the continuous heat resistance, resistance to aircraft fluids and atmospheric pollutants, exposure resistance, and, of course, mechanical properties. A temperature value can be selected that corresponds to an equilibrium temperature that would result from convective aerodynamic heating (and radiation into space) at the maximum dynamic soak conditions. The aircraft fluids to which all the materials must be resistant are primarily aviation fuel, hydraulic oil, lubricating oil, grease and water. The atmospheric pollutants are those from aircraft and automotive engine combustion products and from industrial processes. The mechanical properties are those related to aerodynamic loading, structural loading, and bird and ballistic impact.

TABLE 2

SUMMARY OF DATA MATRIX (APPENDIX C) CONTENTS

Category	Material	Page
GLAZING	Acrylic	107
	Acrylonitrile Butadiene Styrene (ABS)	108
	Glass	109
	Polyarylsulfone	110
	Polycarbonate (Film)	111
	Polycarbonate (Sheet)	112
	Polyester	113
	Polymethylpentene	114
	Polysulfone	115
	Polyterephthalate	116
	Polyurethane	117
INTERLAYER BASES	Acrylic (See Glazing Materials)	
	Ethylene Terpolymer	119
	Polyester (See Glazing Materials)	
	Polyurethane (See Glazing Materials)	
	Polyvinyl Butyral (PVB)	120
	Silicone	121
COATINGS	Abcite	123
	Glass Resin	124
	Gold	125
	Inconel	126
	Indium Oxide	127
	ITO	128
	Silicone	129
	Stannus (Tin) Oxide	130
EDGE CONSTRUCTION:		
Mechanical Support and Mounting	Fiberglass Reinforced Epoxy Resin	133
	Nylon	134
	Orlon	135
	Phenolic (Type FBE)	136
Seals and Gaskets	Cork Neoprene Tape	138
	Nylon Cord	139
	Silicone Tape	140
	Synthetic Rubber (Excluding Polyurethane)	141
	Teflon Tape	142
	Vinyl Tape	143
Sealants	Polyamide Resin Base	145
	Polysulfide Base (THIKOL)	146
	Silicone Rubber (RTV)	147
	Zinc Chromate Putty Compound with Asbestos Filler	148
Adhesives	Acrylic Resin Base	150
	Polysulfide Base	151
	Silicone Resin Base	152

SECTION VI
ANALYSIS

As evidenced in the preceding section there are a considerable number of gaps in the published data for electrical properties of transparency materials. However, before suggesting that efforts be expended to obtain the missing data, analyses were performed to determine which electrical parameters were relevant in evaluating the vulnerability of aircraft transparencies to atmospheric electricity and NEMP.

Based on classical methods of electromagnetic theory, an analytical model is available for treating multi-layered systems. The method is described in Appendix A. It was applied to a simple transparency and found to give results that agreed with test data from Reference 29. The method permits a calculation of electric field intensity across a conductive layer, current induced in the layer and the localized temperature rise resulting from the induced current. The electrical parameters of interest were found to be the dielectric constant and electrical conductivity (or resistivity) of the material. Thus it may be concluded that, at least for this application, only these two electrical properties must be known. However, these properties must be known for all materials in the transparency. This includes protective coatings, conductive coatings, reflective coatings, interlayer materials, adhesives, and glazing materials. Also, to enable vulnerability analysis over the entire non-operational and operational ranges, against atmospheric electricity and NEMP threats, the behavior of these two electrical properties must be known as a function of frequency, temperature and humidity (exposure).

When computerized and validated, the method can be used to analyze transparency designs in the atmospheric electricity and NEMP environments. Thus, given a design, the transparency system performance and its susceptibility can be evaluated as a function of number of layers, thicknesses and material electrical properties.

Knowing the variation of conductivity and dielectric constant as a function of frequency, temperature and humidity (exposure), the transparency design can be evaluated over its entire environmental non-operating and operating ranges.

However, availability of an analytical model does not eliminate the requirement to perform tests on aircraft transparencies. Its primary use should be to eliminate the basically trial and error method of transparency design for atmospheric electricity hazards. The method does not consider manufacturing processes, nor their variation, and should not be used in lieu of qualification and quality control testing. Until a specification becomes available for the electrical characteristics of transparencies, these requirements should be included in the Prime Item Specification(s). Qualification testing should be performed on the first production article to determine compliance with puncture, flashover, and related requirements of the procurement specification. The testing should be performed under the most severe operational conditions (environmental and thermal and mechanical loading) for the aircraft on which the transparency will be used. Quality control testing performed on production articles should include, as a minimum, the bulk resistance of conductive coatings and interlayers and thermographs (with current applied) of the conductive layers as an indication of uniformity.

Comparison of various materials indicates that neither dielectric constant nor resistivity (or conductivity) can be extrapolated from one material to another nor can their variations with temperature, frequency, and exposure. Therefore, for vulnerability assessments, this information must be known over the ranges of interest for all materials in the transparency.

Appendix A briefly describes the analytical method and some calculations that demonstrate its validity when compared to available test data. In Appendix B the method is applied, using some simplifying assumptions to two transparency configurations to compare the effects of two conductive layers versus one conductive layer. For proper application, the model must be computerized and verified using specimens under controlled test conditions.

SECTION VII
LIGHTNING ACCIDENT/INCIDENT DATA

Tables 3 and 4 summarize the lightning accident/incident experience of the Air Force and Navy, respectively. The total number reflects those incidents reported that involved atmospheric electricity. The transparency number includes physiological as well as physical effects.

Between 1968 and 1977 there were a total of 779 lightning accidents/incidents involving USAF aircraft (Reference 60). About 4% of these involved the aircraft transparencies. For USAF aircraft, fighters experienced about 50% of the transparency incidents. There is a gradual increase with time in the number of incidents involving the transparencies.

In contrast to the USAF experience, between 1967 and 1976 (Reference 61), there were 90 lightning accidents/incidents involving Navy aircraft, and 65 of these involved the aircraft transparencies (72%). Of the 90 incidents 72 (80%) were on anti-submarine aircraft, namely the S-3 (58%) and P-3 (22%). For the anti-submarine aircraft 40% of the P-3 and 94% of the S-3 incidents involved the aircraft transparencies. A large number of the incidents include experiences of electrical shock and flashblindness by flight crews. It is interesting to note that the S-3 windshields are heated, use polyvinyl butyral (PVB) interlayers and have gold anti-fogging conductive coatings. Because of the high cost of replacement of damaged windshields the S-3 windshields have undergone several design changes.

The differences between USAF and USN incident statistics are a function of several factors. Among these factors are the sizes of the fleets, the types of missions flown, and the geographical areas involved. The differences are most probably not due to aircraft or the flight crews.

TABLE 3

SUMMARY OF USAF LIGHTNING ACCIDENTS/INCIDENTS
AND TRANSPARENCY RELATED INCIDENTS

AIRCRAFT		1968	1969	1970	1971	1972	1973	1974	1975	1976	1977	TOTALS
Fighters	Total	28	15	24	19	18	32	21	30	24	11	222
	Transp.	1	-	1	-	1	3	2	3	2	1	14
	%	3.57	0	4.17	0	5.56	9.38	9.52	10.0	8.33	9.09	6.31
Cargo	Total	24	34	29	69	38	56	50	40	25	26	391
	Transp.	-	1	-	1	1	2	2	1	-	-	8
	%	0	2.94	0	1.45	2.63	3.57	4.00	2.50	0	0	2.05
Trainers	Total	8	31	7	6	13	10	6	5	6	1	75
	Transp.	1	-	-	-	1	1	1	1	-	-	5
	%	12.5	0	0	0	7.69	10.0	16.67	20.0	0	0	6.67
Helicopters	Total	-	1	-	-	-	-	-	-	-	1	2
	Transp.	-	-	-	-	-	-	-	-	-	1	1
	%	0	0	0	0	0	0	0	0	0	100.0	50.0
Bombers	Total	7	18	8	4	9	8	8	9	8	10	89
	Transp.	-	-	-	1	-	-	1	-	-	1	3
	%	0	0	0	25.0	0	0	12.5	0	0	10.0	3.37
Totals	Total	67	81	68	98	78	106	85	84	63	49	779
	Transp.	2	1	1	2	3	6	6	5	2	3	31
	%	2.99	1.23	1.47	2.04	3.85	5.66	7.06	5.95	3.17	6.12	3.98

TABLE 4

SUMMARY OF NAVY LIGHTNING ACCIDENTS/INCIDENTS
AND TRANSPARENCY RELATED INCIDENTS

		1967	1968	1969	1970	1971	1972	1973	1974	1975	1976	TOTAL
Attack (Fighter Bomber)	Total	0	0	1	1	0	1	1	2	2	2	10
	Transp.	0	0	0	1	0	0	1	0	1	0	3
	%	0	0	0	100.0	0	0	100.0	0	50.0	0	30.0
Anti-Sub	Total	1	1	0	2	3	1	5	3	23	34	73
	Transp.	0	0	0	0	0	0	4	2	20	31	57
	%	0	0	0	0	0	0	80.0	66.67	86.96	91.18	78.08
Misc.	Total	0	0	1	1	1	1	1	1	1	0	7
	Transp.	0	0	1	1	0	1	0	1	1	0	5
	%	0	0	100.0	100.0	0	100.0	0	100.0	100.0	0	71.43
Totals	Total	1	1	2	4	4	3	7	6	26	36	90
	Transp.	0	0	1	2	0	1	5	3	22	31	65
	%	0	0	50.0	50.0	0	33.33	71.43	50.0	84.62	86.11	72.22

SECTION VIII
CONCLUSIONS AND RECOMMENDATIONS

A. Conclusions

The following conclusions were derived as a result of the investigations conducted in this program.

1. The electrical properties of transparency materials vary as a function of frequency, temperature, and exposure, sometimes substantially.

2. For transparency materials there is only a limited amount of data available on the electrical properties over the frequency, temperature, and exposure conditions of interest. This is particularly true for the edge construction materials (e.g. abrasion resistant).

3. Generally, the test methods are available to obtain the needed data. They need only be applied over the frequency, temperature, and exposure conditions of interest.

4. A standard test method, such as defined in Reference 6, has not been adopted for flashover strength measurements.

5. At the present time there is no effective protection being provided against LEMP and NEMP surges in anti-icing and control circuits of most aircraft.

6. An analytical method is available to permit evaluation of the atmospheric electricity and NEMP hazards to aircraft transparency systems. The method requires definition of transparency configuration, layer thicknesses, electrical conductivity (or resistivity) and dielectric constant of each material and the type of electromagnetic threat. With these inputs, the electric field response, induced current and temperature rise at the coating-bus interface

can be realistically estimated and the protection requirements defined. However, analysis of the design cannot be a substitute for qualification and quality control testing since such methods do not account for production processes and their variations.

7. Based on nuclear weapon effects methods, the flashblindness hazard from bright sources can be analyzed. However, the luminous output of lightning flashes needs to be defined so that these methods can be applied to the lightning threat.

8. Blast and acoustical noise measurements are needed to assess this hazard to crew members.

9. The physiological effects of flashblindness, shock, and related factors needs to be assessed in combination.

B. Recommendations

1. It is recommended that electrical properties of transparency materials be defined using available standard methods at the frequency, temperature, and exposure ranges of interest. As a minimum data should be obtained at the extreme and ambient temperature and exposure conditions and at the dominant frequencies of LEMP and NEMP. As an alternative to frequency measurements the characteristics should be measured using simulated LEMP and NEMP impulses.

2. To analyze the hazard to electrical circuits in aircraft transparencies the analytical model presented should be coded to facilitate computations and validated using tests on actual canopy systems. The model could be further developed to function as a design tool by addition of routines for optimizing on selected parameters and the ability "peek" at intermediate steps for evaluation.

3. The flashover strength method of Reference 6 needs to be adopted as a standard that will permit comparison between different materials without the influence of geometry effects.

4. The physiological effects of the atmospheric electricity and NEMP environments should be further analyzed, particularly the combined effects of flashblindness, and acoustic and electrical shock, in order to "quantize" the hazard.

5. The amount of disclosure on aircraft transparencies needs to be increased to permit proper evaluation. At the present time some construction materials are left up to the discretion of suppliers without any specification control. This is particularly true in the area of edge construction materials. Also, the manufacturers of "proprietary" products or materials should disclose the generic nature of the materials and their known engineering properties. Done properly, this should not result in disclosure of proprietary processes and compositions.

6. Qualification testing should include verification tests to insure compliance with the procurement specification requirements for conductivity, and flashover and puncture resistance. Quality control tests should include bulk conductivity and thermographs (with current applied) of the conductive layers.

APPENDIX A

ANALYSIS OF AN AIRCRAFT TRANSPARENCY IN AN ELECTROMAGNETIC ENVIRONMENT

W. S. McCormick, Ph.D.

1. INTRODUCTION

A modern aircraft transparency, particularly a windshield, is comprised of several layers of different optically transparent materials, some of which are electrically conductive and are part of electrical heating circuits. In an atmospheric electricity and EMP environment these conductive layers may have currents induced in them that can damage the material as a function of current magnitude or temperature rise or both. Besides the replacement of an expensive windshield, secondary hazards can result, some possibly catastrophic. It is of interest to quantify these induced currents and their heating effect.

A general analysis for the electromagnetic response of a plane stratified medium consisting of any number of parallel homogeneous layers was performed by Wait in Reference 62. Figure A-1 illustrates the general problem of a plane wave with a time factor $\exp(j\omega t)$ incident on such a medium at an incident angle θ.

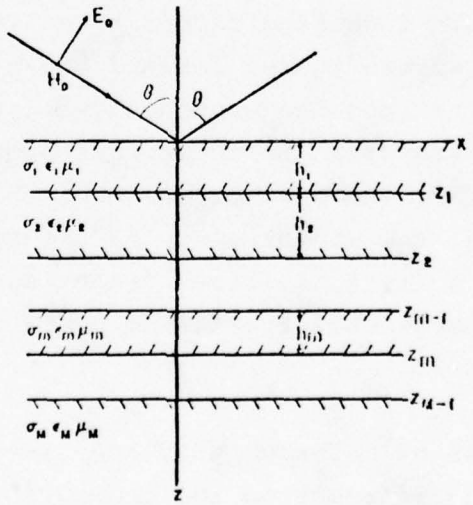


Figure A-1. Stratified Medium Consisting of M Homogeneous Layers (Taken from Reference 62)

In this analysis we consider three different cases of electromagnetic excitation of an aircraft windshield, two of which are treated as special cases of the general theory of electromagnetic waves in stratified media as documented in Reference 62. The three cases considered are:

a. Swept-stroke lightning
b. Precipitation static (p-static) discharge
c. Remote electromagnetic pulse (EMP) excitation

The analytical model is verified by application to a simple transparency consisting of a single conductive film deposited on an acrylic substrate. This example was chosen because experiments on such a configuration were performed by Twomey (Reference 29) and the results could be compared. Application of the model to more complex cases involving multiple conductive layers, as are used in some aircraft, requires availability of a computer and better definition of the electrical properties of aircraft transparency materials than is currently available. However, it is emphasized that Wait's analyses are applicable to multilayered aircraft windshields.

2. SWEPT-STROKE LIGHTNING

a. General Solution

Swept-stroke lightning refers to a lightning strike that attaches to an aircraft area forward of the canopy and is subsequently "swept" across the windshield because of the forward motion of the aircraft. Excluding arc attachment to, and dielectric puncture of, the dielectric, when the lightning current channel lies close to the windshield, the situation can be realistically modelled by an infinite-line current source positioned a distance h from a homogeneous stratified media of infinite extent as shown in Figure A-2.

From equation 48 of Reference 62, the electric field (E-field), E_o, above and adjacent to the media, for a time varying current excitation($I_e^{j\omega t}$) is given by:

$$E_o = \frac{-j\,\mu_o\,\omega\,I_e^{j\omega t}}{4\pi} \int_{-\infty}^{\infty} u_o^{-1} \left[e^{-u_o(z+h)} + R_\perp(\lambda) e^{u_o(z+h)} \right] e^{-j\lambda x}\, d\lambda, \qquad \text{(A-1)}$$

for $Z < 0$

where

$j = \sqrt{-1}$

μ_o = permeability of free space = $4\pi \times 10^{-7}$ H/m

ω = angular frequency = $2\pi f$

f = frequency, in Hertz

I = current, in amperes

e = base of Naperian logarithms 2.718 . . .

$u_o = \sqrt{\lambda^2 + \gamma_o^2}$

γ_o = propagation constant in free space

$\lambda = -j\,\gamma_o \sin\theta$

θ = incidence angle of plane wave (with respect to normal to surface

z = distance along z-axis from source, in meters

h = thickness of layer, in meters

$R_\perp(\lambda)$ = reflection coefficient term for incident plane wave

x = distance along x-axis in meters

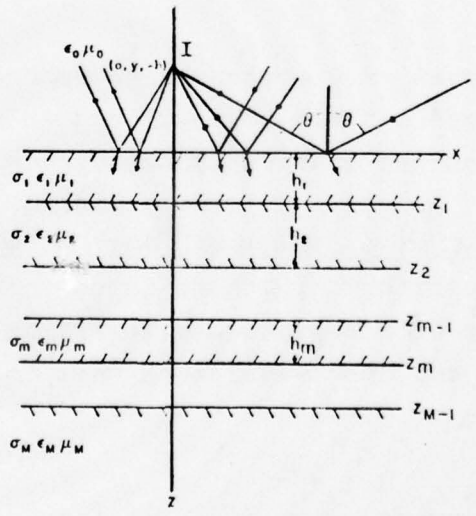


Figure A-2. Line Source Over a Layered Half-Space (Taken from Reference 62)

The reflection coefficient therm $R_{\perp}(\lambda)$ accounts for the presence of the stratified media at z=0. The integral representation for E_o has a clear physical meaning. When the symbol λ is identified with $\frac{2\pi \sin \theta}{\text{wave length}}$, it is clear that expression A-1 is an inverse Fourier transform of the sum of the angle spectrum of an incident wave and a reflected, $R_{\perp}(\lambda)$, wave. Quantitatively, the reflection term has the following expression,

$$R_{\perp}(\lambda) = \frac{N_o(\lambda) - Y_1(\lambda)}{N_o(\lambda) + Y_1(\lambda)} \tag{A-2}$$

where:
$$Y_m = \frac{Y_{m+1}(\lambda) + N_m(\lambda) \tan h\, u_m h_m}{N_m(\lambda) + Y_{m+1}(\lambda) \tan h\, u_m h_m} \cdot N_m(\lambda)$$

with
$$N_m = \frac{u_m}{j\mu_m w} = \frac{\sqrt{\lambda_m^2 + \gamma_o^2}}{j\mu_m w} \tag{A-3}$$

for: $m = 1, 2, \ldots, M-1$

and $Y_m(\lambda) = N_m(\lambda)$

With the above model, a computer-based approach should be able to predict the induced E-field vector field in the conductive coating and thus represent the coating by its Thevenin equivalent circuit.

b. Application to McDonnell Douglas (Reference 29) Test

For the case where there is only one very thin conductive layer on top of a homogeneous layer, expressons (A-1) through (A-3) reduce for the long wavelength case to the transfer function for Z<0 of

$$E_o = \frac{-j\, \mu_o\, \omega\, I_e^{j\omega t}}{2\pi} [\ln(r_1/r_2) + T_o(\beta)] \tag{A-4}$$

where: $r_1^2 = (z+h)^2 + x^2$

$r_2^2 = (z-h)^2 + x^2$

$$T_o(\beta) = \int_0^\infty \frac{e^{-\lambda\beta} \cos \lambda x}{\lambda + j q} d\lambda \qquad \text{(A-5)}$$

$\beta = h - z$

$q = \frac{\sigma_1 \mu_o \omega h_1}{2}$

σ_1 = conductivity of conductive layer, in mhos/meter

h_1 = thickness of gold conductive layer

Since the line current is very close to the conductive layer during a swept-stroke over the windshield, we can assume the nominally induced E-field will occur at x=0 (underneath the swept-stroke) which, according to Reference 62, reduces equation A-4) (at the bottom interface of the layer) to:

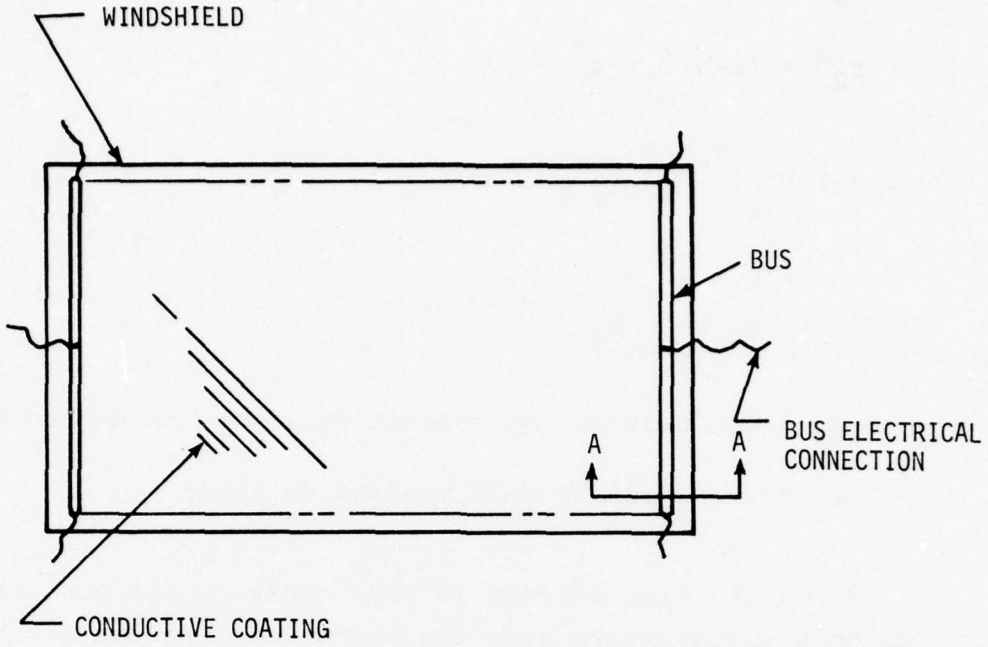
$$E_2 = \frac{j \mu_o \omega I_e^{j|z+h|q}}{2\pi} Ei(-j|z+h|q) \qquad \text{(A-6)}$$

where $Ei(-j|z+h|q)$ is the exponential integral for imaginary argument where:

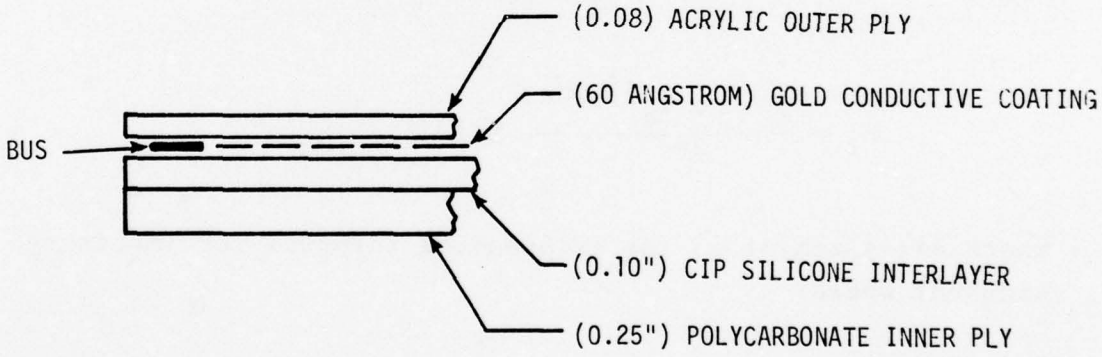
$$Ei(-jg) = \int_g^\infty \frac{\cos t}{t} dt + j\left[\frac{\pi}{2} - \int_0^g \frac{\sin t}{t} dt\right] \qquad \text{(A-7)}$$

where: $g = |z+h|q$

The tests conducted in Reference 29 were performed using a test specimen having the configuration shown in Figure A-3. To analyze this particular configuration at the conductive layer using the model described above we define the following:



a. Top View



b. Cross-sectional View

Figure A-3. Reference 29 Test Specimen Configuration

$\mu_o = 4\pi \times 10^{-7}$ H/m

σ_1 = film conductivity of conductive material

h_1 = thickness of conductive coating = 60 Angstroms

For conductive film materials the conductivity is less than that of the bulk material. The relationship between film conductivity and bulk conductivity, from Reference 17, is:

$$\sigma = \frac{3t\,\sigma_o}{4p_o}\left[\ln\left(\frac{p_o}{t}\right) + 0.4228\right] \quad \text{for } t << p_o \qquad \text{(A-8)}$$

where: σ = film conductivity

t = thickness of film = h_1

σ_o = bulk conductivity = $4.1\text{x}10^5$ mho/meter for gold

p_o = mean free path of material = 570 Angstroms for gold

Therefore (from Eq. A-8):

$$\sigma_1 = 8.66\text{x}10^4 \text{ mho/meter}$$

For the configuration of Figure A-3 under the test condition of Reference 29,

$$|z+h|q \approx \frac{|z|\,\sigma_1\,\mu_o\,h_1\,w}{2} \qquad \text{(A-9)}$$

$$\approx 3.26\text{x}10^{-10}|z|\omega \quad \text{where } z = \text{thickness of outer layer}$$

$$\approx 6.63\text{x}10^{-13}\omega$$

which is <<1 over the LEMP/NEMP excitation bandwidth of interest.

For a small value of the argument, Ei(-jg) can be approximated by:

$$Ei(-jg) \approx \ln(1.78g) + j\,\frac{\pi}{2} \qquad \text{(A-10)}$$

so that E_2 can be expressed as:

$$E_2 = \frac{j\,\omega\,\mu_o\,I_e\,e^{j|z+h|q}}{2\pi}\left[\ln(1.78|z+h|q) + j\,\frac{\pi}{2}\right] \qquad \text{(A-11)}$$

which for the Figure A-3 dimensions reduces to:

$$E_2 \approx \frac{j\,\omega\,\mu_o\,I_e\,e^{j|z+h|q}}{2\pi}\left\{\ln[3.65\text{x}10^{-3}|z+h|f(\text{MHz})] + j\,\frac{\pi}{2}\right\} \qquad \text{(A-12)}$$

Since expression (A-12) is a transfer function, the magnitude of the E_2 field response may be approximated by its absolute value. Hence,

$$|E_2| \approx \frac{\mu_o}{2\pi}\left\{\frac{d}{dt}\,[I(t)]\right\}\ln[3.65\text{x}10^{-3}|z+h|f(\text{MHz})] \qquad \text{(A-13)}$$

In the experiment of Reference 29, $|z| \approx$ the thickness of the outer layer = 0.08 inch, $h \approx 0.56$ inch and $f \leq 0.5$ MHz, so that:

$$|E_2| \quad \frac{\mu_o}{2\pi}\left\{\frac{d}{dt}\,[I(t)]\right\}\ln[5.95\text{x}10^{-5}\,f(\text{MHz})]$$

Letting f = f max (upper bound) = 0.5 MHz

and $$\frac{d\,I(t)}{dt} \approx \frac{I_{peak}}{T_{rise}} \approx \frac{8000}{2\text{x}10^{-6}} \approx 4\text{x}10^{9}\ \text{A/sec} \qquad \text{(A-15)}$$

where I_{peak} and T_{rise} are taken from Figure 19a in Reference 29.

(A-14) becomes:

$$|E_2| \approx \frac{4\pi x10^{-7}(4x10^{9})(10.4)}{2\pi} \approx 8.3 \text{ KV/m} \qquad \text{(A-16)}$$

for a voltage drop across the 1.17 meter conductive coating:

$$V \text{ drop} \approx 9.7 \text{ KV} \qquad \text{(A-17)}$$

Since the induced current density at any point in the conductive coating, J_{Ind}, equals:

$$J_{Ind} \approx \sigma_1 E_{Ind} \qquad \text{(A-18)}$$

it follows that the current density will be maximum underneath the current strike and will decrease in magnitude as x increases from zero. Consequently, the induced current density will not be uniform across the sheet and as a result, the bulk DC conductive sheet resistance of 20 ohms will not apply. A precise prediction of the total induced current must await a computer solution of equation (A-4). Using the bulk resistance of 20Ω, an upper bound can, however, be estimated for the induced current as

$$I_{Induced}^{\text{Upper bound}} \approx \frac{V_{Induced}}{R_{DC}} \approx \frac{9.7x10^{3}}{20} \approx 485 \qquad \text{(A-19)}$$

which is about 12 times the measured value which seems reasonable given the above discussion on current density nonuniformity.

c. Estimation of Temperature Rise at the Conductive Coating-Bus Interface

The upper bound induced current computed in the preceding discussion may be used to predict the temperature rise at the conductive coating-bus interface based on the following assumptions:

(1) A silver impregnated adhesive is used with a conductivity of 4.7×10^6, a specific heat (C_v) of 1.26 Joules/gram/°C and a density of 1.8 grams per cm^3. (handbook approximations)

(2) The primary current path is underneath the strike itself and has a width ($X \approx 2|z+h|$) of 0.02 meters, a height equal to the layer thickness of 7×10^{-9} m, and a length, l, in the direction of current flow equal to 0.002 meters.

(3) There is no significant heat loss from the current "corridor" during the 2-microsecond flash.

The power dissipated per unit volume can be written directly as

$$W = \frac{J^2}{\sigma} = \frac{I^2}{A^2\sigma} \text{ watts/m}^3 \qquad \text{(A-20)}$$

where A = cross-sectional area = 1.4×10^{-10} m^2
I = induced current measured at around 40A

to give

$$W \approx \frac{2500}{1.96\text{x}10^{-20}\text{x}4.7\text{x}10^{6}} \approx 1.74\text{x}10^{16} \text{ watts/m}^3 \qquad \text{(A-21)}$$

or a total heat power into volume of

$$P = WV = \frac{I^2}{A\sigma} d \approx 4860 \text{ watts} \qquad \text{(A-22)}$$

where d is the assumed 2 mm length.

Over an assumed lightning waveform time constant of 41 μsec (Figure 19(c) of Reference 29), a total heat dissipation ΔH of 0.317 Joules occurs. For a specific heat of 1.26, the 0.317 Joule heat dissipation results in a temperature rise, ΔT, equal to

$$\Delta T = \frac{\Delta H}{C_v \text{ V x density}} \approx 31{,}400°C \qquad \text{(A-23)}$$

from 50°F to over 56,000°F which could account for the observed charring of interface during the Reference 29 tests.

3. STATIC ELECTRICITY DISCHARGE

The second major electromagnetic excitation (excluding electromagnetic noise) is the static electricity discharge at the air-windshield interface and the subsequent current pulse. The actual air breakdown is a highly nonlinear plasma phenomena that is difficult if not impossible to analyze. Fortunately, however, the current pulse can be characterized experimentally and the resulting stress on the conductive coating can be predicted using linear techniques. From basic electromagnetics, the normal electric field intensity component for an infinite sheet, E_n, equals

$$E_n = \frac{P_n}{\varepsilon_o} \qquad \text{(A-24)}$$

where: P_n = charge density at breakdown
ε_o = permittivity of free space = 8.854×10^{-12} F/m

At air breakdown, $E_n = 3 \times 10^6$ v/m (function of humidity and temperature), and P_n can be calculated as

$$P_n \approx \varepsilon_o (E_n)_{\text{Breakdown}} \approx 2.66 \times 10^{-5} \text{ Coulomb/m}^2 \qquad \text{(A-25)}$$

The total static charge dissipated during the discharge can be expressed as:

$$Q_s \approx P_n A \approx 27 \times 10^{-6} \text{ Coulombs} \qquad \text{(A-26)}$$

where the surface area of the windshield equals 1 m^2. From recorded induced current waveforms, the rise time, ΔT, of the static discharge is about one microsecond so that the peak current can be estimated as

$$I_p \approx \frac{Q_s}{\Delta T} \approx \frac{27 \times 10^{-6}}{10^{-6}} \approx 27 \text{ Amp} \qquad \text{(A-27)}$$

As can be observed from Figure A-4, the path of the surface discharge assumes an "oak-tree" nature. This rather unusual structure is a consequence of the plasma physics of the discharge and must be observed experimentally in a flash photo of the discharge. One interesting property of the discharge structure is that all branches combine to a main branch or stem at the interface. It follows that the infinite current filament model of the previous section can be applied and that the conductive coating current and interface adhesive temperature wire can be sealed directly from the linearity of the electromagnetic and thermal interaction. Accordingly, both the peak current of 485A and

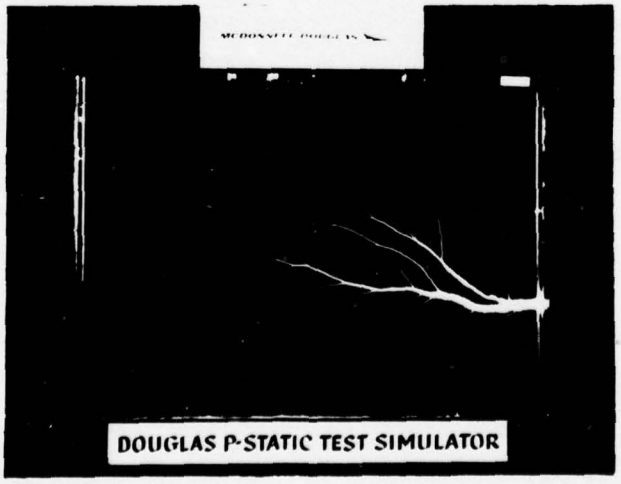


Figure A-4. Douglas P-Static Test Simulator

the maximum temperature rise of 450°F can be scaled by the factor, 27/8000, to give

$$I_{\substack{\text{Upper bound} \\ \text{Induced Static}}} \approx (485)\left(\frac{27}{8000}\right) \approx 1.64 \text{ Amp} \qquad \text{(A-28)}$$

and

$$56{,}000\left(\frac{27}{8000}\right) \approx 189°F \qquad \text{(A-29)}$$

both safe values as was verified in the Reference 29 tests.

4. ELECTROMAGNETIC WAVE EXCITATION

Referring to Figure A-1 and Reference 62, the general solution for a multilayered medium is

$$H_{my} = \left[a_m e^{-u_m z} + b_m e^{u_m z} \right] e^{-j\lambda x} \qquad \text{(A-30)}$$

where $u_m^2 = \lambda^2 + \gamma_m^2$ with λ equal to any arbitrary value,

$$\gamma_m^2 = j\,\sigma_m\,\mu_m\,\omega - \varepsilon_m\,\mu_m\,\omega^2$$

and

$$E_{mx} = -(\sigma_m + j\,\omega\,\varepsilon_m)^{-1}\,\frac{\partial H_{my}}{\partial z} \qquad \text{(A-31)}$$

The reflection from the stratified media can be expressed as

$$\frac{b_o}{a_o} = \frac{K_o - Z_1}{K_o + Z_1}$$

$$Z_1 = K_1 \left[\frac{Z_2 + K_1 \tan h\ (u_1\ h_1)}{K_1 + Z_2 \tan h\ (u_1\ h_1)} \right] \qquad \text{(A-32)}$$

$$\vdots$$

$$Z_m = K_m \left[\frac{Z_{m+1} + K_m \tan h\ (u_m\ h_m)}{K_m + Z_{m+1} \tan h\ (u_m\ h_m)} \right]$$

with

$$K_m = \frac{u_m}{\sigma + j\ \omega\ \varepsilon_m} \qquad \text{(A-33)}$$

Although complicated, equations (A-30 through A-32) can be programmed for a windshield of arbitrary complexity.

It is of interest to note that the windshield has a convenient transmission line analogy for the plane excitation case; Figure A-5 illustrates.

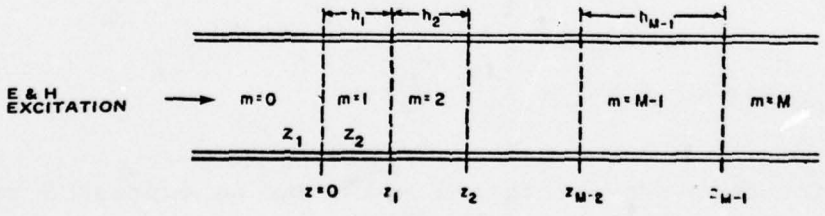


Figure A-5. Transmission Line Analogy for the Stratified Medium of M Layers (Taken from Reference 62)

For the Reference 29 case, the analogy takes the form of three contiguous layers; one of air ($\eta_2 = 377\Omega$), one of acrylic plastic (outer ply, $\eta_1 = 154\Omega$), and the conductive layer itself ($\eta_0 = 20\Omega$). Considering the air-outer surface interface, the transmission coefficient, Γ_t, equals

$$\Gamma_t = \frac{2Z_2}{Z_1 + Z_2} \approx 0.58 \qquad \text{(A-34)}$$

while at the outer-ply, conductive coating interface, the reflection coefficient, Γ_u, equals

$$\Gamma_u = \frac{Z_2 - Z_0}{Z_2 + Z_0} \approx 0.770 \text{ (for coating)} \qquad \text{(A-35)}$$

Since the power dissipated is given by:

$$\text{Power Dissipated} = [\Gamma_t(1 - \Gamma_u)]^2 \times 100 \text{ (percent)} \qquad \text{(A-36)}$$

In our example the incident power density that dissipated in conductive coating is approximately 1.8%, which is quite a reduction.

A final question may be asked pertaining to the effect of the voltage transient on a transparency circuit. Taking a typical AC windshield heater circuit, such as illustrated in Figure 24 b. of this report, and its Thevenin Equivalent, a Thevenin voltage source equal to:

$$V = 9.7 \times 10^3 \left(\frac{27}{8000}\right) \approx 33 \text{ volts peak}$$

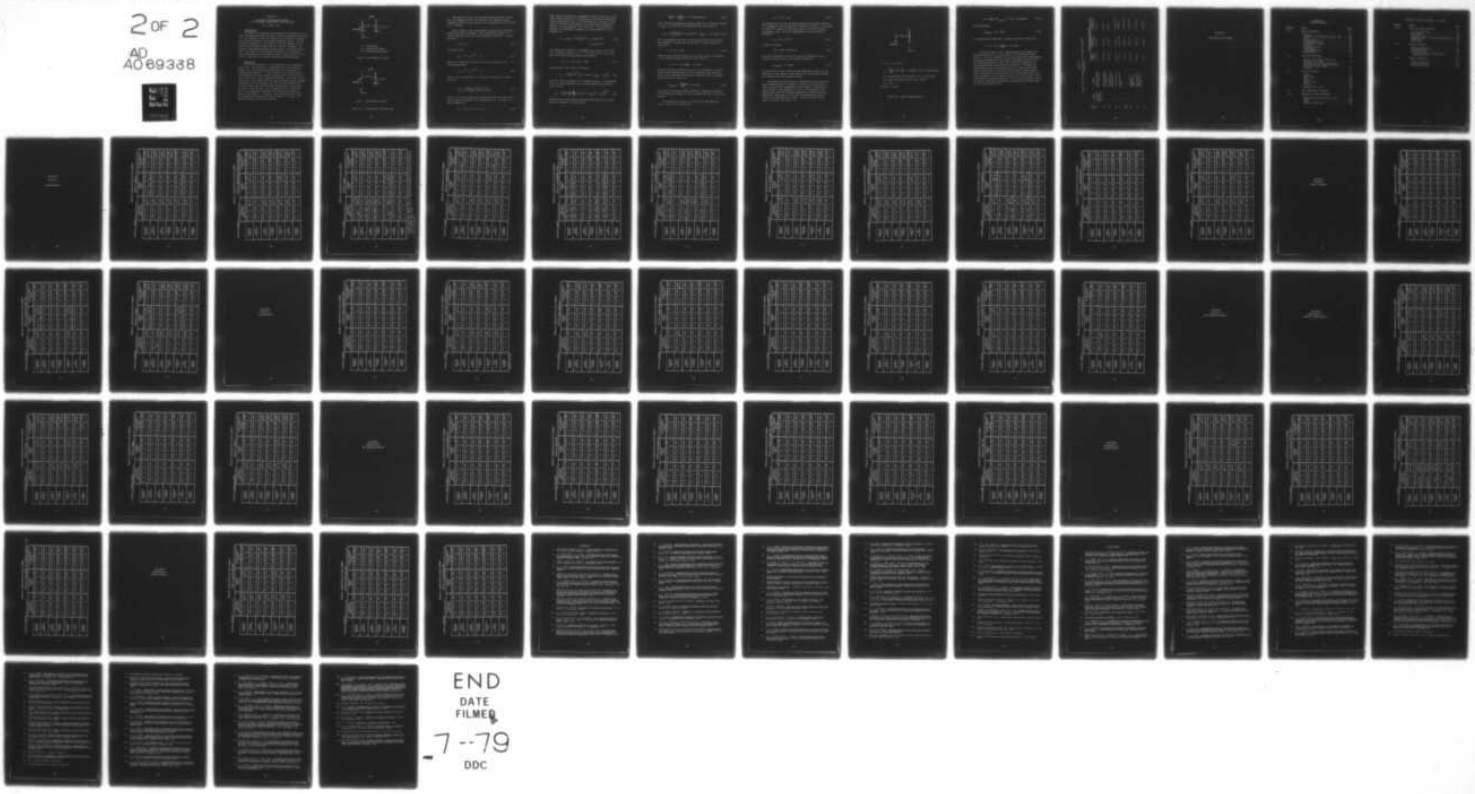
will appear on the circuit.

The Thevenin representation of such a circuit has been developed by McCormick (Reference 63) and validated using the

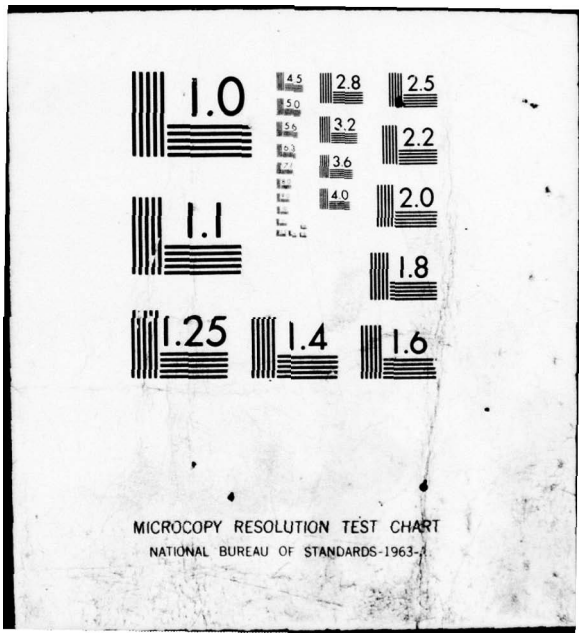
Lightning Transient Analysis (LTA) technique (Reference 64). In this validation, source and load impedances, transformer, and cable lengths representative of an actual aircraft windshield circuit were used. Using open- and short-circuited conditions of the transparency conductive circuit (heating element) voltages of 4 and 0.4 volts were measured, respectively, on the bus side of the transformer. These voltages are in a magnitude range that could cause unprotected aircraft circuits to upset or fail. In fact, upset instances are reported frequently on the bomb bay doors of S-3A aircraft (Reference 61).

AD-A069 338 TECHNOLOGY/SCIENTIFIC SERVICES INC DAYTON OH F/G 1/3
ATMOSPHERIC ELECTRICITY HAZARD (AEH) ASSESSMENT OF AIRCRAFT TRA--ETC(U)
DEC 78 A V SERRANO F33601-78-D-0042
UNCLASSIFIED T/SSI-0140-01 AFFDL-TR-78-164 NL

2 OF 2
AD
A069338



END
DATE
FILMED
7-79
DDC


1.0
1.1
1.25
1.4
1.6
1.8
2.0
2.2
2.5
2.8
3.2
3.6
4.0
4.5
5.0
5.6
MICROCOPY RESOLUTION TEST CHART
NATIONAL BUREAU OF STANDARDS-1963-A

APPENDIX B

APPLICATION OF ANALYTICAL MODEL TO TWO AIRCRAFT TRANSPARENCY CONFIGURATIONS

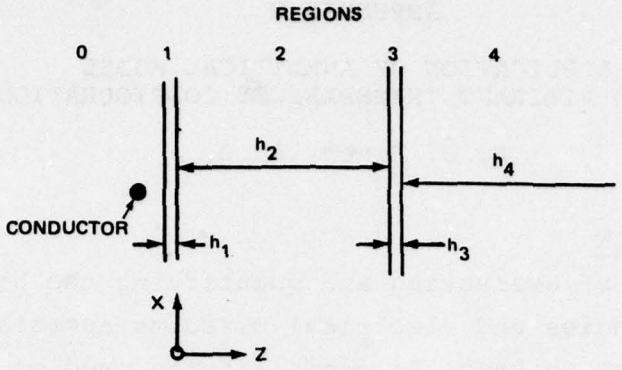
R. B. Finch, Ph.D.

1. INTRODUCTION

As a means of evaluating and quantifying the hazard to aircraft transparencies and electrical circuits associated with them, it is of interest to have the capability to predict or estimate the currents induced in the various conductive layers. As described in Appendix A, this problem, although complex, can be solved using existing models with the aid of a computer. Although a computerized version of the model is currently unavailable, the intent of the following discussion is to suggest a first approximation to estimating current levels within the conductive layers of two aircraft transparency configurations.

2. DISCUSSION

The two configurations to be considered are illustrated in Figure B-1. The first is a transparency with two conductive layers, one on the outside and one under the first layer of nonconductive material. In this case the outer layer would be representative of an anti-static coating while the inner would be an anti-icing layer, electrically heated. The second is the same as the first except that the outer conductive layer has been eliminated. Using equations (50) and (51) from Reference 62 it can be shown that the reflection coefficient is much larger for Case 1 than for Case 2 for the Region 0 and 1 interface. This is not surprising because of the obvious shielding one obtains from Region 1. Because of this shielding the E field and therefore the induced voltage for Region 3 in Case 1 is greatly reduced from that for Case 2.

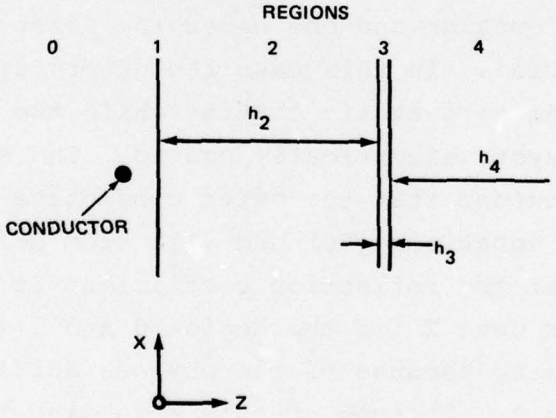


0 = Free space

1,3 = Conductive layers

2,4 = Nonconductive layers

Case 1: Two Conductive Layers



Case 2: One Conductive Layer

Figure B-1. Transparency Cross Sections

Evaluation of Case 1 for the swept-stroke problem is done with the assumption that the conductor (the simulated swept lightning stroke) is very close to the transparency, on the order of 10^{-3} meters.

Upon looking at this multilayered structure the reflection coefficient must be analyzed. When sub-surface layers are highly conducting such that the propagation constant, γ, within the layer:

$$|\gamma_m| >> |\gamma_o| \tag{B-1}$$

it follows that:

$$u_m = (\lambda^2 + \gamma_m^2)^{1/2} \approx \gamma_m \tag{B-2}$$

because the important values of λ are of the order of $|\gamma_o|$. To this approximation:

$$u_e \approx (\lambda^2 + \gamma_e^2)^{1/2} \approx \gamma_e \tag{B-3}$$

where γ_e can be regarded as an effective propagation constant given by:

$$\frac{\gamma_e}{\gamma_1} \approx \left[\frac{(Y_2/N_1) + \tanh u_1 h_1}{1 + (Y_2/N_2) \tanh u_1 h_1} \right]_{\lambda \approx 0} \tag{B-4}$$

where Y_2 is the wave admittance associated with the lower layers and is given by equation (51) of Reference 62. For Case 1 it can be shown that:

$$\gamma_e \approx 2\gamma_1^2 h_1 \approx j^2 \sigma_1 \mu_1 \omega h_1 \tag{B-5}$$

When using this effective propagation constant within the free space region (Region 0) to calculate the reflection coefficient (using equations 50 and 51 from Reference 62) the Case 1 situation is effectively the same as that described in Appendix A, Section 2 b. and equations (A-4) and (A-6). The equivalent problem is illustrated in Figure B-2 using equation (A-9) of Appendix A:

$$g = |Z+h|q \approx \frac{D\ \sigma_1\ \mu_o\ \ h_1\ \omega}{2} = 3.26\text{x}10^{-10} D\ \omega \qquad (B\text{-}6)$$

$$= 2.05\text{x}10^{-9} D\ f$$

with excitation bandwidth of megahertz and with D in the order of a millimeter implies $g << 1$. For small values of the argument the following approximation can be made:

$$E_i(-j\ g) \approx \ln(1.78g) + j\left(\frac{\pi}{2}\right) \qquad (B\text{-}7)$$

Thus equation (B-6) can be written as:

$$E_2 \approx \frac{j\ \omega\ \mu_o\ I\ e^{jg}}{2\pi}\left[\ln(3.65\text{x}10^{-3} D\ f_{MHz}) + j\left(\frac{\pi}{2}\right)\right] \qquad (B\text{-}8)$$

Since the above expression is a transfer function, the magnitude of the E_2 field response may be approximated by its absolute value so that:

$$|Z_2| \approx \frac{\mu_o}{2\pi}\left[\frac{d\ I(t)}{dt}\right]\left\{\left[\ln(3.65\text{x}10^{-3} D\ f_{MHz})\right]^2 + \left(\frac{\pi}{2}\right)^2\right\}^{1/2} \qquad (B\text{-}9)$$

Using the same swept-stroke lightning pulse definition as presented in Appendix A implies that:

$$\frac{d\ I(t)}{dt} \approx \frac{I_{peak}}{T_{rise}} = 4 \times 10^{9} \text{ Amp/second} \qquad \text{(B-10)}$$

With lightning frequencies typically less than 0.5 MHz and letting $f = f_{max} = 0.5$ MHz the field magnitude can be written as

$$|E_2| = \frac{\mu_o}{2\pi}\left[\frac{d\ I(t)}{dt}\right] |\ln(3.65\times10^{-3}\ D\ f_{MHz})| = 10.1 \text{ KV/m} \qquad \text{(B-11)}$$

For a transparency the size of those used in the S-3A aircraft, this implies a voltage drop across the 1.2 meter conductive coating of:

$$V = 12.7\ K \text{ volts} \qquad \text{(B-12)}$$

Using the same Thevenin analogy and scaling factors of Appendix A, the induced voltage would be on the order of:

$$V = 12.7 \times 10^{3}\ \left(\frac{27}{8000}\right) \approx 43 \text{ volts}$$

Using the surface resistance as before of 20Ω/square, an upper bound on the induced current can be predicted when realizing that the S-3A aircraft transparency effective width is approximately 30% of the length as

$$I_{Induced} < \frac{V_{Induced}}{R_{dc}} = 190 \text{ amps} \qquad \text{(B-13)}$$

This value is less than those predicted in Appendix A because of the different values for D and conductivity used in this discussion.

The evaluation of Case 2 is done in the same manner as Case 1. First it is found that:

$$\gamma_e \approx j \sigma_3 \omega \mu_2 h_3 \qquad \text{(B-14)}$$

given again that we have the same problem as described in Section b. of Appendix A and illustrated in Figure B-2 with D = .102 inches (2.59×10^{-3}m) (similar to the outer layer of the S-3A aircraft transparency plus .001 meter displacement of the conductor). Therefore:

$$g = 2.05 \times 10^{-9} D f \qquad \text{(B-15)}$$

as before, giving:

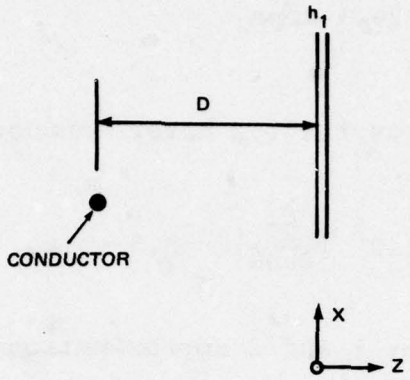
$$|E_2| \approx 9840 \text{ volts/meter} \qquad \text{(B-16)}$$

Using the dimensions of the S-3A aircraft transparency this implies an upper bound on the induced current as

$$I_{Induced} < 177 \text{ amps} \qquad \text{(B-17)}$$

The variation of this value with that computed in Case 1 is due primarily to the change in the value of D, the distance between the conductor and the conductive layer.

The comparison field strength magnitude and resulting estimated induced current in Region 3 of Case 1 can now be calculated utilizing the transmission ratio defined in Reference 19. Using Figure 3 from Reference 19 for $R_s = 30\Omega$/square it was approximated that the expected transmitted Z-field for the one conductive layer case is 6.09 times the transmitted E-field for the two conductive layer case. Using this fact, the E-field in Region 3 for Case 1 is:



$$\mu_o = 4\pi \times 10^{-7} \text{ H/m}$$

$$\sigma_1 = \frac{3h_1 \sigma_o}{4p_o} \left[\ln \frac{p_o}{h_1} + 0.4228 \right] = 8.66 \times 10^4 \text{ mho/meter}$$

σ_o = conductivity of bulk gold = 4.1×10^5 mho/cm

p_o = mean free path of bulk gold = 570 Å

h_1 = 60 Å

$|Z+h|$ = D = .001 m

Figure B-2. Case 1 Approximation

$$|E| = \frac{1}{6.09} |E_2|_{\text{Case 2}} = 1.62 \text{ K volts/meter} \qquad \text{(B-18)}$$

or approximately

$$I_{\text{Induced}} < 29.1 \text{ amps} \qquad \text{(B-19)}$$

The voltage drop across the 1.2 meter conductive coating of:

$$V = 1.62 \times 10^3 \left(\frac{27}{8000}\right) \approx 5.5 \text{ volts}$$

In both the Cases 1 and 2 approximations the induced voltages estimated are at the bus side of the windshield heater circuit. It is of interest to note that some actual measurements have been performed on S-3A aircraft windshield circuits using the Lightning Simulation Test (LST) technique (Reference 65). These measurements are presented in Table B-1. Although the measurements do not correspond exactly in terms of excitation level and location, it can be seen that peak voltages ranged from a minimum of 35 millivolts, with a 200 amp simulated lightning excitation, at the heater controller to 30,000 volts, with a 200,000 amp lightning excitation at the right windshield heater. The latter values were obtained by extrapolating the LST values to the severe threat level.

TABLE B-1

LIGHTNING-INDUCED VOLTAGES MEASURED IN S-3A ELECTRICAL CIRCUITS
(Reference 65)

Test No.	System	Circuit	Lightning-Induced Voltages Measured @ 200A	@ Average Stroke of 30 kA	@ Severe Stroke of 200 kA
113	Windshield Anti-Ice Dwg.1211536	Heater Controller RT-5 (Thermistor)	±0.035 osc.	±5.25 osc.	±35 osc.
114	" "	Heater Controller RT-6 (Thermistor)	±0.035 osc.	±5.25 osc.	±35 osc.
115	" "	One Side of Heater Controller to Gnd. RT-5	±0.625 osc.	±93.8 osc.	±625 osc.
116	" "	Windshield Heater	±10.00 osc.	±1500 osc.	±[1]10,000 osc.
117	" "	Right Windshield Heater	±6.75 osc.	±1012.5 osc.	±[1]6750 osc.
118-117	" "	" "	±30.0 osc.	±[1]4500 osc.	±[1]30,000 osc.
120	" "	One Side of RT Windshield Heater to Grd.	±18.0 osc.	±[1]2700 osc.	±[1]18,000 osc.
121	" "	Right Windshield Heater with Indicator Load	±25 osc.	±[1]3750 osc.	±[1]25,000 osc.
122	" "	" "	±2 osc.	±300 osc.	±[1]2000 osc.

APPENDIX C

DATA MATRIX DATA SHEETS

APPENDIX C
TABLE OF CONTENTS

Section	Title	Page
A-1	GLAZING MATERIALS	106
	Acrylic	107
	Acrylonitrile Butadiene Styrene (ABS)	108
	Glass	109
	Polyarylsulfone	110
	Polycarbonate (Film)	111
	Polycarbonate (Sheet)	112
	Polyester	113
	Polymethylpentene	114
	Polysulfone	115
	Polyterephthalate	116
	Polyurethane	117
A-2	INTERLAYER MATERIALS	118
	Acrylic (See Glazing Materials)	
	Ethylene Terpolymer	119
	Polyester (See Glazing Materials)	
	Polyurethane (See Glazing Materials)	
	Polyvinyl Butyral (PVB)	120
	Silicone	121
A-3	COATING MATERIALS	122
	Abcite	123
	Glass Resin	124
	Gold	125
	Inconel	126
	Indium Oxide	127
	ITO	128
	Silicone	129
	Stannus (Tin) Oxide	130
A-4	EDGE CONSTRUCTION MATERIALS	131
A-4-1	MECHANICAL SUPPORT MATERIALS	132
	Fiberglass Reinforced Epoxy Resin	133
	Nylon	134
	Orlon	135
	Phenolic (Type FBE)	136

APPENDIX C TABLE OF CONTENTS - Concluded

Section	Title	Page
A-4-2	SEAL AND GASKET MATERIALS	137
	Cork Neoprene Tape	138
	Nylon Cord	139
	Silicone Tape	140
	Synthetic Rubber (Excluding Polyurethane)	141
	Teflon Tape	142
	Vinyl Tape	143
A-4-3	SEALANT MATERIALS	144
	Polyamide Resin Base	145
	Polysulfide Base	146
	Silicone Rubber	147
	Zinc Chromate Putty Compound with Asbestos Filler	148
A-4-4	ADHESIVE MATERIALS	149
	Acrylic Resin Base	150
	Polysulfide Base	151
	Silicone Resin Base	152

DATA MATRIX

SECTION A-1

GLAZING MATERIALS

MATERIAL CHARACTERISTICS DATA SUMMARY

CATEGORY GLAZING MATERIAL ACRYLIC

	TEMPERATURE Degrees Celsius				FREQUENCY Hertz				RELATIVE HUMIDITY Percent			
DIELECTRIC CONSTANT	-55	23	+75	Data	60	10^3	10^6	Data	0	50	100	Data
		x		Ref 22	x	x	x			x		Ref 22
					60 Hz - 1 GHz			Ref 24				
SURFACE RESISTIVITY	-55	23	+75	Data	60	10^3	10^6	Data	0	50	100	Data
		x		Ref 22						x		Ref 22
VOLUME RESISTIVITY	-55	23	+75	Data	60	10^3	10^6	Data	0	50	100	Data
		x		Ref 22						x		Ref 22
DIELECTRIC STRENGTH	-55	23	+75	Data	60	10^3	10^6	Data	0	50	100	Data
		x		Ref 22						X		Ref 22
DISSIPATION FACTOR	-55	23	+75	Data	60	10^3	10^6	Data	0	50	100	Data
		x		Ref 22	x	x	x			x		
					60 Hz - 1 GHz			Ref 24				
ARC RESISTANCE	-55	23	+75	Data	60	10^3	10^6	Data	0	50	100	Data
		x		Ref 22						x		Ref 22
FLASHOVER STRENGTH	-55	23	+75	Data	60	10^3	10^6	Data	0	50	100	Data

MATERIAL CHARACTERISTICS DATA SUMMARY

CATEGORY GLAZING

MATERIAL ACRYLONITRILE BUTADIENE STYRENE (ABS)

	TEMPERATURE Degrees Celsius				FREQUENCY Hertz				RELATIVE HUMIDITY Percent			
	-55	23	+75	Data	60	10^3	10^6	Data	0	50	100	Data
DIELECTRIC CONSTANT		x		Ref 22	x	x	x	Ref 22		x		Ref 22
SURFACE RESISTIVITY	-55	23	+75	Data	60	10^3	10^6	Data	0	50	100	Data
VOLUME RESISTIVITY	-55	23	+75	Data	60	10^3	10^6	Data	0	50	100	Data
		x		Ref 22						x		Ref 22
DIELECTRIC STRENGTH	-55	23	+75	Data	60	10^3	10^6	Data	0	50	100	Data
		x		Ref 22						x		Ref 22
DISSIPATION FACTOR	-55	23	+75	Data	60	10^3	10^6	Data	0	50	100	Data
		x		Ref 22	x	x	x	Ref 22		x		Ref 22
ARC RESISTANCE	-55	23	+75	Data	60	10^3	10^6	Data	0	50	100	Data
		x		Ref 22						x		Ref 22
FLASHOVER STRENGTH	-55	23	+75	Data	60	10^3	10^6	Data	0	50	100	Data

MATERIAL CHARACTERISTICS DATA SUMMARY

CATEGORY GLAZING

MATERIAL GLASS *

	TEMPERATURE Degrees Celsius				FREQUENCY Hertz				RELATIVE HUMIDITY Percent			
DIELECTRIC CONSTANT	-55	23	+75	Data	60	10^3	10^6	Data	0	50	100	Data
		x	x	Ref 23**			x	Ref 23	x			Ref 23
	0 - 520°C			Ref 23								
SURFACE RESISTIVITY	-55	23	+75	Data	60	10^3	10^6	Data	0	50	100	Data
									x	x	x	Ref 23
	120°C - 540°C			Ref 23								
VOLUME RESISTIVITY	-55	23	+75	Data	60	10^3	10^6	Data	0	50	100	Data
		x	x	Ref 23					x			Ref 23
	25°C - 520°C			Ref 23								
DIELECTRIC STRENGTH	-55	23	+75	Data	60	10^3	10^6	Data	0	50	100	Data
		x		Ref 23					x			Ref 23
DISSIPATION FACTOR	-55	23	+75	Data	60	10^3	10^6	Data	0	50	100	Data
		x	x	Ref 23	x	x	x	Ref 23				
	0 - 500°C			Ref 23	60 Hz - 10 GHz			Ref 23				
ARC RESISTANCE	-55	23	+75	Data	60	10^3	10^6	Data	0	50	100	Data
FLASHOVER STRENGTH	-55	23	+75	Data	60	10^3	10^6	Data	0	50	100	Data

* Includes silica glass, soda-lime glass, lead alkali glass, borosilicate glass, aluminosilicate glass and solder glass. NOTE: There are considerable differences in the electrical properties of the different types of glass.

** See also Reference 29.

MATERIAL CHARACTERISTICS DATA SUMMARY

CATEGORY GLAZING MATERIAL POLYARYLSULFONE

	TEMPERATURE Degrees Celsius				FREQUENCY Hertz				RELATIVE HUMIDITY Percent			
DIELECTRIC CONSTANT	-55	23	+75	Data	60	10^3	10^6	Data	0	50	100	Data
		x		Ref 22	x	x	x	Ref 22	x	x		Ref 22
									0 - 95%			B-5
SURFACE RESISTIVITY	-55	23	+75	Data	60	10^3	10^6	Data	0	50	100	Data
VOLUME RESISTIVITY	-55	23	+75	Data	60	10^3	10^6	Data	0	50	100	Data
		x		Ref 22						x		Ref 22
DIELECTRIC STRENGTH	-55	23	+75	Data	60	10^3	10^6	Data	0	50	100	Data
		x		Ref 22						x		Ref 22
DISSIPATION FACTOR	-55	23	+75	Data	60	10^3	10^6	Data	0	50	100	Data
		x		Ref 22	x	x	x	Ref 22		x		Ref 22
									0 - 95%			B-5
ARC RESISTANCE	-55	23	+75	Data	60	10^3	10^6	Data	0	50	100	Data
		x		Ref 22						x		Ref 22
FLASHOVER STRENGTH	-55	23	+75	Data	60	10^3	10^6	Data	0	50	100	Data

MATERIAL CHARACTERISTICS DATA SUMMARY

CATEGORY GLAZING

MATERIAL POLYCARBONATE (FILM)

	TEMPERATURE Degrees Celsius				FREQUENCY Hertz				RELATIVE HUMIDITY Percent			
DIELECTRIC CONSTANT	-55	23	+75	Data	60	10^3	10^6	Data	0	50	100	Data
	x	x	x		x	x	x			x		
	-45°C - 135°C			Ref 66	20 Hz - 500 MHz			Ref 66				
SURFACE RESISTIVITY	-55	23	+75	Data	60	10^3	10^6	Data	0	50	100	Data
VOLUME RESISTIVITY	-55	23	+75	Data	60	10^3	10^6	Data	0	50	100	Data
										x		
DIELECTRIC STRENGTH	-55	23	+75	Data	60	10^3	10^6	Data	0	50	100	Data
		x	x							x		
	-45°C - 135°C			Ref 66								
DISSIPATION FACTOR	-55	23	+75	Data	60	10^3	10^6	Data	0	50	100	Data
		x	x			x	x			x		
	-45°C - 135°C			Ref 66	100 Hz - 500 MHz			Ref 66				
ARC RESISTANCE	-55	23	+75	Data	60	10^3	10^6	Data	0	50	100	Data
FLASHOVER STRENGTH	-55	23	+75	Data	60	10^3	10^6	Data	0	50	100	Data

MATERIAL CHARACTERISTICS DATA SUMMARY

CATEGORY GLAZING MATERIAL POLYCARBONATE (SHEET)

	TEMPERATURE Degrees Celsius				FREQUENCY Hertz				RELATIVE HUMIDITY Percent			
DIELECTRIC CONSTANT	-55	23	+75	Data	60	10^3	10^6	Data	0	50	100	Data
	x	x	x	Ref 22	x	x	x	Ref 22		x		Ref 22
	23°C - 175°C			Ref 66	100 Hz - 100 MHz			Ref 66				
SURFACE RESISTIVITY	-55	23	+75	Data	60	10^3	10^6	Data	0	50	100	Data
VOLUME RESISTIVITY	-55	23	+75	Data	60	10^3	10^6	Data	0	50	100	Data
	x	x	x	Ref 22							x	Ref 22
	23°C - 175°C			Ref 66								
DIELECTRIC STRENGTH	-55	23	+75	Data	60	10^3	10^6	Data	0	50	100	Data
		x	x	Ref 22						x		Ref 22
				Ref 66								
DISSIPATION FACTOR	-55	23	+75	Data	60	10^3	10^6	Data	0	50	100	Data
	x	x	x		x	x	x			x		Ref 22
	23°C - 175°C			Ref 66	100 Hz - 100 MHz			Ref 66				
ARC RESISTANCE	-55	23	+75	Data	60	10^3	10^6	Data	0	50	100	Data
		x		Ref 22						x		Ref 22
FLASHOVER STRENGTH	-55	23	+75	Data	60	10^3	10^6	Data	0	50	100	Data

MATERIAL CHARACTERISTICS DATA SUMMARY

CATEGORY INTERLAYER MATERIAL POLYESTER

	TEMPERATURE Degrees Celsius				FREQUENCY Hertz				RELATIVE HUMIDITY Percent			
	-55	23	+75	Data	60	10^3	10^6	Data	0	50	100	Data
DIELECTRIC CONSTANT		x		Ref 24	x		x	Ref 24		x		Ref 24
SURFACE RESISTIVITY	-55	23	+75	Data	60	10^3	10^6	Data	0	50	100	Data
VOLUME RESISTIVITY	-55	23	+75	Data	60	10^3	10^6	Data	0	50	100	Data
		x		Ref 24						x		Ref 24
DIELECTRIC STRENGTH	-55	23	+75	Data	60	10^3	10^6	Data	0	50	100	Data
		x		Ref 24						x		Ref 24
DISSIPATION FACTOR	-55	23	+75	Data	60	10^3	10^6	Data	0	50	100	Data
		x		Ref 24	x		x	Ref 24		x		Ref 24
ARC RESISTANCE	-55	23	+75	Data	60	10^3	10^6	Data	0	50	100	Data
		x		Ref 24						x		Ref 24
FLASHOVER STRENGTH	-55	23	+75	Data	60	10^3	10^6	Data	0	50	100	Data

MATERIAL CHARACTERISTICS DATA SUMMARY

CATEGORY GLAZING MATERIAL POLYMETHYLPENTENE

	TEMPERATURE Degrees Celsius				FREQUENCY Hertz				RELATIVE HUMIDITY Percent			
	-55	23	+75	Data	60	10^3	10^6	Data	0	50	100	Data
DIELECTRIC CONSTANT		x		Ref 22	x	x	x	Ref 22		x		Ref 22
SURFACE RESISTIVITY	-55	23	+75	Data	60	10^3	10^6	Data	0	50	100	Data
		x		Ref 22						x		Ref 22
VOLUME RESISTIVITY	-55	23	+75	Data	60	10^3	10^6	Data	0	50	100	Data
		x		Ref 22						x		Ref 22
DIELECTRIC STRENGTH	-55	23	+75	Data	60	10^3	10^6	Data	0	50	100	Data
		x		Ref 22						x		Ref 22
DISSIPATION FACTOR	-55	23	+75	Data	60	10^3	10^6	Data	0	50	100	Data
		x		Ref 22	x	x	x	Ref 22		x		Ref 22
ARC RESISTANCE	-55	23	+75	Data	60	10^3	10^6	Data	0	50	100	Data
		x		Ref 22								
FLASHOVER STRENGTH	-55	23	+75	Data	60	10^3	10^6	Data	0	50	100	Data

MATERIAL CHARACTERISTICS DATA SUMMARY

CATEGORY GLAZING

MATERIAL POLYSULFONE

	TEMPERATURE Degrees Celsius				FREQUENCY Hertz				RELATIVE HUMIDITY Percent			
DIELECTRIC CONSTANT	-55	23	+75	Data	60	10^3	10^6	Data	0	50	100	Data
		x		Ref 22	x	x	x	Ref 22		x		Ref 22
					60 Hz to 50 MHz			Ref 67,68				
SURFACE RESISTIVITY	-55	23	+75	Data	60	10^3	10^6	Data	0	50	100	Data
										x		Ref 22
VOLUME RESISTIVITY	-55	23	+75	Data	60	10^3	10^6	Data	0	50	100	Data
		x	x	Ref 22						x		Ref 22
	20°C - 190°C			Ref 67,68								
DIELECTRIC STRENGTH	-55	23	+75	Data	60	10^3	10^6	Data	0	50	100	Data
		x		Ref 22						x		Ref 22
DISSIPATION FACTOR	-55	23	+75	Data	60	10^3	10^6	Data	0	50	100	Data
		x	x	Ref 22	x	x	x	Ref 22		x		Ref 22
	15°c - 175°c			Ref 67,68	60 Hz - 50 MHz			Ref 67,68				
ARC RESISTANCE	-55	23	+75	Data	60	10^3	10^6	Data	0	50	100	Data
		x		Ref 22						x		Ref 22
FLASHOVER STRENGTH	-55	23	+75	Data	60	10^3	10^6	Data	0	50	100	Data

MATERIAL CHARACTERISTICS DATA SUMMARY

CATEGORY GLAZING MATERIAL POLYTEREPHTHALATE

	TEMPERATURE Degrees Celsius				FREQUENCY Hertz				RELATIVE HUMIDITY Percent			
DIELECTRIC CONSTANT	-55	23	+75	Data	60	10^3	10^6	Data	0	50	100	Data
SURFACE RESISTIVITY	-55	23	+75	Data	60	10^3	10^6	Data	0	50	100	Data
VOLUME RESISTIVITY	-55	23	+75	Data	60	10^3	10^6	Data	0	50	100	Data
DIELECTRIC STRENGTH	-55	23	+75	Data	60	10^3	10^6	Data	0	50	100	Data
DISSIPATION FACTOR	-55	23	+75	Data	60	10^3	10^6	Data	0	50	100	Data
ARC RESISTANCE	-55	23	+75	Data	60	10^3	10^6	Data	0	50	100	Data
FLASHOVER STRENGTH	-55	23	+75	Data	60	10^3	10^6	Data	0	50	100	Data

MATERIAL CHARACTERISTICS DATA SUMMARY

CATEGORY GLAZING MATERIAL POLYURETHANE

	TEMPERATURE Degrees Celsius				FREQUENCY Hertz				RELATIVE HUMIDITY Percent			
	-55	23	+75	Data	60	10^3	10^6	Data	0	50	100	Data
DIELECTRIC CONSTANT		x		Ref 22	x	x	x	Ref 22		x		Ref 22
SURFACE RESISTIVITY	-55	23	+75	Data	60	10^3	10^6	Data	0	50	100	Data
		x										
VOLUME RESISTIVITY	-55	23	+75	Data	60	10^3	10^6	Data	0	50	100	Data
		x		Ref 22						x		Ref 22
DIELECTRIC STRENGTH	-55	23	+75	Data	60	10^3	10^6	Data	0	50	100	Data
		x		Ref 22						x		Ref 22
DISSIPATION FACTOR	-55	23	+75	Data	60	10^3	10^6	Data	0	50	100	Data
		x		Ref 22	x	x	x	Ref 22		x		Ref 22
ARC RESISTANCE	-55	23	+75	Data	60	10^3	10^6	Data	0	50	100	Data
		x		Ref 22						x		Ref 22
FLASHOVER STRENGTH	-55	23	+75	Data	60	10^3	10^6	Data	0	50	100	Data

DATA MATRIX

SECTION A-2

INTERLAYER MATERIALS

MATERIAL CHARACTERISTICS DATA SUMMARY

CATEGORY INTERLAYER MATERIAL ETHYLENE TERPOLYMER

	TEMPERATURE Degrees Celsius				FREQUENCY Hertz				RELATIVE HUMIDITY Percent			
DIELECTRIC CONSTANT	-55	23	+75	Data	60	10^3	10^6	Data	0	50	100	Data
SURFACE RESISTIVITY	-55	23	+75	Data	60	10^3	10^6	Data	0	50	100	Data
VOLUME RESISTIVITY	-55	23	+75	Data	60	10^3	10^6	Data	0	50	100	Data
DIELECTRIC STRENGTH	-55	23	+75	Data	60	10^3	10^6	Data	0	50	100	Data
DISSIPATION FACTOR	-55	23	+75	Data	60	10^3	10^6	Data	0	50	100	Data
ARC RESISTANCE	-55	23	+75	Data	60	10^3	10^6	Data	0	50	100	Data
FLASHOVER STRENGTH	-55	23	+75	Data	60	10^3	10^6	Data	0	50	100	Data

MATERIAL CHARACTERISTICS DATA SUMMARY

CATEGORY INTERLAYER

MATERIAL POLYVINYL BUTYRAL (PVB)

	TEMPERATURE Degrees Celsius				FREQUENCY Hertz				RELATIVE HUMIDITY Percent			
	-55	23	+75	Data	60	10^3	10^6	Data	0	50	100	Data
DIELECTRIC CONSTANT		x		Ref 69	x	x		Ref 69				
					50 Hz - 10 KHz			Ref 69				
SURFACE RESISTIVITY	-55	23	+75	Data	60	10^3	10^6	Data	0	50	100	Data
VOLUME RESISTIVITY	-55	23	+75	Data	60	10^3	10^6	Data	0	50	100	Data
DIELECTRIC STRENGTH	-55	23	+75	Data	60	10^3	10^6	Data	0	50	100	Data
DISSIPATION FACTOR	-55	23	+75	Data	60	10^3	10^6	Data	0	50	100	Data
		x		Ref 69	x	x		Ref 69				
					50 Hz - 10 KHz			Ref 69				
ARC RESISTANCE	-55	23	+75	Data	60	10^3	10^6	Data	0	50	100	Data
FLASHOVER STRENGTH	-55	23	+75	Data	60	10^3	10^6	Data	0	50	100	Data

MATERIAL CHARACTERISTICS DATA SUMMARY

CATEGORY INTERLAYER MATERIAL SILICONE

	TEMPERATURE Degrees Celsius				FREQUENCY Hertz				RELATIVE HUMIDITY Percent			
	-55	23	+75	Data	60	10^3	10^6	Data	0	50	100	Data
DIELECTRIC CONSTANT		x		Ref 22		x	x	Ref 22		x		Ref 22
					100 Hz & 10 KHz			Ref 24				
SURFACE RESISTIVITY	-55	23	+75	Data	60	10^3	10^6	Data	0	50	100	Data
	200°C			Ref 24								
VOLUME RESISTIVITY	-55	23	+75	Data	60	10^3	10^6	Data	0	50	100	Data
		x		Ref 22						x		Ref 22
DIELECTRIC STRENGTH	-55	23	+75	Data	60	10^3	10^6	Data	0	50	100	Data
		x		Ref 22						x		Ref 22
DISSIPATION FACTOR	-55	23	+75	Data	60	10^3	10^6	Data	0	50	100	Data
		x		Ref 22		x	x	Ref 22		x		Ref 22
					100 Hz & 10 KHz			Ref 24				
ARC RESISTANCE	-55	23	+75	Data	60	10^3	10^6	Data	0	50	100	Data
		x		Ref 22						x		Ref 22
FLASHOVER STRENGTH	-55	23	+75	Data	60	10^3	10^6	Data	0	50	100	Data

DATA MATRIX

SECTION A-3

COATING MATERIALS

MATERIAL CHARACTERISTICS DATA SUMMARY

CATEGORY COATING

MATERIAL ABCITE (ABRASION RESISTANT)

	TEMPERATURE Degrees Celsius				FREQUENCY Hertz				RELATIVE HUMIDITY Percent			
	-55	23	+75	Data	60	10^3	10^6	Data	0	50	100	Data
DIELECTRIC CONSTANT												
SURFACE RESISTIVITY	-55	23	+75	Data	60	10^3	10^6	Data	0	50	100	Data
VOLUME RESISTIVITY	-55	23	+75	Data	60	10^3	10^6	Data	0	50	100	Data
DIELECTRIC STRENGTH	-55	23	+75	Data	60	10^3	10^6	Data	0	50	100	Data
DISSIPATION FACTOR	-55	23	+75	Data	60	10^3	10^6	Data	0	50	100	Data
ARC RESISTANCE	-55	23	+75	Data	60	10^3	10^6	Data	0	50	100	Data
FLASHOVER STRENGTH	-55	23	+75	Data	60	10^3	10^6	Data	0	50	100	Data

MATERIAL CHARACTERISTICS DATA SUMMARY

CATEGORY COATING

MATERIAL GLASS RESIN* (ABRASION RESISTANT)

	TEMPERATURE Degrees Celsius				FREQUENCY Hertz				RELATIVE HUMIDITY Percent			
	-55	23	+75	Data	60	10^3	10^6	Data	0	50	100	Data
DIELECTRIC CONSTANT		x		Ref 70	x		x	Ref 70				
SURFACE RESISTIVITY	-55	23	+75	Data	60	10^3	10^6	Data	0	50	100	Data
VOLUME RESISTIVITY	-55	23	+75	Data	60	10^3	10^6	Data	0	50	100	Data
		x	x	Ref 70					x			Ref 70
DIELECTRIC STRENGTH	-55	23	+75	Data	60	10^3	10^6	Data	0	50	100	Data
		x		Ref 70						x		B-10
DISSIPATION FACTOR	-55	23	+75	Data	60	10^3	10^6	Data	0	50	100	Data
		x		Ref 70	x		x	Ref 70				
ARC RESISTANCE	-55	23	+75	Data	60	10^3	10^6	Data	0	50	100	Data
		x		Ref 70								
FLASHOVER STRENGTH	-55	23	+75	Data	60	10^3	10^6	Data	0	50	100	Data

*THERMOSET SILICONE

MATERIAL CHARACTERISTICS DATA SUMMARY

CATEGORY COATING

MATERIAL GOLD (CONDUCTIVE)

	TEMPERATURE Degrees Celsius				FREQUENCY Hertz				RELATIVE HUMIDITY Percent			
	-55	23	+75	Data	60	10^3	10^6	Data	0	50	100	Data
DIELECTRIC CONSTANT												
SURFACE RESISTIVITY	-55	23	+75	Data	60	10^3	10^6	Data	0	50	100	Data
		x		Ref 17					x			Ref 17
VOLUME RESISTIVITY	-55	23	+75	Data	60	10^3	10^6	Data	0	50	100	Data
		x		Ref 19								
DIELECTRIC STRENGTH	-55	23	+75	Data	60	10^3	10^6	Data	0	50	100	Data
DISSIPATION FACTOR	-55	23	+75	Data	60	10^3	10^6	Data	0	50	100	Data
ARC RESISTANCE	-55	23	+75	Data	60	10^3	10^6	Data	0	50	100	Data
FLASHOVER STRENGTH	-55	23	+75	Data	60	10^3	10^6	Data	0	50	100	Data

MATERIAL CHARACTERISTICS DATA SUMMARY

CATEGORY COATING MATERIAL INCONEL (ANTI-STATIC)

	TEMPERATURE Degrees Celsius				FREQUENCY Hertz				RELATIVE HUMIDITY Percent			
DIELECTRIC CONSTANT	-55	23	+75	Data	60	10^3	10^6	Data	0	50	100	Data
SURFACE RESISTIVITY	-55	23 x	+75	Data Ref 71	60	10^3	10^6	Data	0 x	50	100	Data Ref 71
VOLUME RESISTIVITY	-55	23	+75	Data	60	10^3	10^6	Data	0	50	100	Data
DIELECTRIC STRENGTH	-55	23	+75	Data	60	10^3	10^6	Data	0	50	100	Data
DISSIPATION FACTOR	-55	23	+75	Data	60	10^3	10^6	Data	0	50	100	Data
ARC RESISTANCE	-55	23	+75	Data	60	10^3	10^6	Data	0	50	100	Data
FLASHOVER STRENGTH	-55	23	+75	Data	60	10^3	10^6	Data	0	50	100	Data

MATERIAL CHARACTERISTICS DATA SUMMARY

CATEGORY COATING

MATERIAL INDIUM OXIDE (CONDUCTIVE)

	TEMPERATURE Degrees Celsius				FREQUENCY Hertz				RELATIVE HUMIDITY Percent			
	-55	23	+75	Data	60	10^3	10^6	Data	0	50	100	Data
DIELECTRIC CONSTANT												
SURFACE RESISTIVITY	-55	23	+75	Data	60	10^3	10^6	Data	0	50	100	Data
VOLUME RESISTIVITY	-55	23	+75	Data	60	10^3	10^6	Data	0	50	100	Data
DIELECTRIC STRENGTH	-55	23	+75	Data	60	10^3	10^6	Data	0	50	100	Data
DISSIPATION FACTOR	-55	23	+75	Data	60	10^3	10^6	Data	0	50	100	Data
ARC RESISTANCE	-55	23	+75	Data	60	10^3	10^6	Data	0	50	100	Data
FLASHOVER STRENGTH	-55	23	+75	Data	60	10^3	10^6	Data	0	50	100	Data

MATERIAL CHARACTERISTICS DATA SUMMARY

CATEGORY COATING

MATERIAL ITO (CONDUCTIVE)

	TEMPERATURE Degrees Celsius				FREQUENCY Hertz				RELATIVE HUMIDITY Percent			
	-55	23	+75	Data	60	10^3	10^6	Data	0	50	100	Data
DIELECTRIC CONSTANT												
SURFACE RESISTIVITY	-55	23	+75	Data	60	10^3	10^6	Data	0	50	100	Data
		x		Ref 71								
VOLUME RESISTIVITY	-55	23	+75	Data	60	10^3	10^6	Data	0	50	100	Data
DIELECTRIC STRENGTH	-55	23	+75	Data	60	10^3	10^6	Data	0	50	100	Data
DISSIPATION FACTOR	-55	23	+75	Data	60	10^3	10^6	Data	0	50	100	Data
ARC RESISTANCE	-55	23	+75	Data	60	10^3	10^6	Data	0	50	100	Data
FLASHOVER STRENGTH	-55	23	+75	Data	60	10^3	10^6	Data	0	50	100	Data

MATERIAL CHARACTERISTICS DATA SUMMARY

CATEGORY COATING

MATERIAL SILICONE T-650 (ANTI-STATIC)

	TEMPERATURE Degrees Celsius				FREQUENCY Hertz				RELATIVE HUMIDITY Percent			
	-55	23	+75	Data	60	10^3	10^6	Data	0	50	100	Data
DIELECTRIC CONSTANT		x		Ref 71	x	x	x	Ref 71				
SURFACE RESISTIVITY	-55	23	+75	Data	60	10^3	10^6	Data	0	50	100	Data
VOLUME RESISTIVITY	-55	23	+75	Data	60	10^3	10^6	Data	0	50	100	Data
DIELECTRIC STRENGTH	-55	23	+75	Data	60	10^3	10^6	Data	0	50	100	Data
DISSIPATION FACTOR	-55	23	+75	Data	60	10^3	10^6	Data	0	50	100	Data
ARC RESISTANCE	-55	23	+75	Data	60	10^3	10^6	Data	0	50	100	Data
FLASHOVER STRENGTH	-55	23	+75	Data	60	10^3	10^6	Data	0	50	100	Data

MATERIAL CHARACTERISTICS DATA SUMMARY

CATEGORY COATING

MATERIAL TIN OXIDE (CONDUCTIVE)

	TEMPERATURE Degrees Celsius				FREQUENCY Hertz				RELATIVE HUMIDITY Percent			
	-55	23	+75	Data	60	10^3	10^6	Data	0	50	100	Data
DIELECTRIC CONSTANT												
SURFACE RESISTIVITY	-55	23	+75	Data	60	10^3	10^6	Data	0	50	100	Data
		x		Ref 71								
VOLUME RESISTIVITY	-55	23	+75	Data	60	10^3	10^6	Data	0	50	100	Data
DIELECTRIC STRENGTH	-55	23	+75	Data	60	10^3	10^6	Data	0	50	100	Data
DISSIPATION FACTOR	-55	23	+75	Data	60	10^3	10^6	Data	0	50	100	Data
ARC RESISTANCE	-55	23	+75	Data	60	10^3	10^6	Data	0	50	100	Data
FLASHOVER STRENGTH	-55	23	+75	Data	60	10^3	10^6	Data	0	50	100	Data

DATA MATRIX

SECTION A-4

EDGE CONSTRUCTION MATERIALS

DATA MATRIX

SUBSECTION A-4-1

MECHANICAL SUPPORT MATERIALS

MATERIAL CHARACTERISTICS DATA SUMMARY

CATEGORY MECHANICAL SUPPORT

MATERIAL FIBERGLASS REINFORCED EPOXY RESIN

	TEMPERATURE Degrees Celsius				FREQUENCY Hertz				RELATIVE HUMIDITY Percent			
	-55	23	+75	Data	60	10^3	10^6	Data	0	50	100	Data
DIELECTRIC CONSTANT		x		Ref 22	x	x	x	Ref 22		x		Ref 22
SURFACE RESISTIVITY	-55	23	+75	Data	60	10^3	10^6	Data	0	50	100	Data
VOLUME RESISTIVITY	-55	23	+75	Data	60	10^3	10^6	Data	0	50	100	Data
		x		Ref 22						x		Ref 22
DIELECTRIC STRENGTH	-55	23	+75	Data	60	10^3	10^6	Data	0	50	100	Data
		x		Ref 22						x		Ref 22
DISSIPATION FACTOR	-55	23	+75	Data	60	10^3	10^6	Data	0	50	100	Data
		x		Ref 22	x	x	x	Ref 22		x		Ref 22
ARC RESISTANCE	-55	23	+75	Data	60	10^3	10^6	Data	0	50	100	Data
		x		Ref 22						x		Ref 22
FLASHOVER STRENGTH	-55	23	+75	Data	60	10^3	10^6	Data	0	50	100	Data

MATERIAL CHARACTERISTICS DATA SUMMARY

CATEGORY MECHANICAL SUPPORT MATERIAL NYLON

	TEMPERATURE Degrees Celsius				FREQUENCY Hertz				RELATIVE HUMIDITY Percent			
	-55	23	+75	Data	60	10^3	10^6	Data	0	50	100	Data
DIELECTRIC CONSTANT		x		Ref 22	x	x	x	Ref 22		x		Ref 22
SURFACE RESISTIVITY	-55	23	+75	Data	60	10^3	10^6	Data	0	50	100	Data
VOLUME RESISTIVITY	-55	23	+75	Data	60	10^3	10^6	Data	0	50	100	Data
		x		Ref 22						x		Ref 22
DIELECTRIC STRENGTH	-55	23	+75	Data	60	10^3	10^6	Data	0	50	100	Data
		x		Ref 22						x		Ref 22
DISSIPATION FACTOR	-55	23	+75	Data	60	10^3	10^6	Data	0	50	100	Data
		x		Ref 22	x	x	x	Ref 22		x		Ref 22
ARC RESISTANCE	-55	23	+75	Data	60	10^3	10^6	Data	0	50	100	Data
		x		Ref 22						x		Ref 22
FLASHOVER STRENGTH	-55	23	+75	Data	60	10^3	10^6	Data	0	50	100	Data

MATERIAL CHARACTERISTICS DATA SUMMARY

CATEGORY MECHANICAL SUPPORT MATERIAL ORLON

	TEMPERATURE Degrees Celsius				FREQUENCY Hertz				RELATIVE HUMIDITY Percent			
DIELECTRIC CONSTANT	-55	23	+75	Data	60	10^3	10^6	Data	0	50	100	Data
SURFACE RESISTIVITY	-55	23	+75	Data	60	10^3	10^6	Data	0	50	100	Data
VOLUME RESISTIVITY	-55	23	+75	Data	60	10^3	10^6	Data	0	50	100	Data
DIELECTRIC STRENGTH	-55	23	+75	Data	60	10^3	10^6	Data	0	50	100	Data
DISSIPATION FACTOR	-55	23	+75	Data	60	10^3	10^6	Data	0	50	100	Data
ARC RESISTANCE	-55	23	+75	Data	60	10^3	10^6	Data	0	50	100	Data
FLASHOVER STRENGTH	-55	23	+75	Data	60	10^3	10^6	Data	0	50	100	Data

MATERIAL CHARACTERISTICS DATA SUMMARY

CATEGORY MECHANICAL SUPPORT MATERIAL PHENOLIC

	TEMPERATURE Degrees Celsius				FREQUENCY Hertz				RELATIVE HUMIDITY Percent			
	-55	23	+75	Data	60	10^3	10^6	Data	0	50	100	Data
DIELECTRIC CONSTANT		x		Ref 22								
SURFACE RESISTIVITY	-55	23	+75	Data	60	10^3	10^6	Data	0	50	100	Data
VOLUME RESISTIVITY	-55	23	+75	Data	60	10^3	10^6	Data	0	50	100	Data
		x		Ref 22						x		Ref 22
DIELECTRIC STRENGTH	-55	23	+75	Data	60	10^3	10^6	Data	0	50	100	Data
		x		Ref 22						x		Ref 22
DISSIPATION FACTOR	-55	23	+75	Data	60	10^3	10^6	Data	0	50	100	Data
		x		Ref 22	x	x	x	Ref 22		x		Ref 22
ARC RESISTANCE	-55	23	+75	Data	60	10^3	10^6	Data	0	50	100	Data
		x		Ref 22						x		Ref 22
FLASHOVER STRENGTH	-55	23	+75	Data	60	10^3	10^6	Data	0	50	100	Data

DATA MATRIX

SUBSECTION A-4-2

SEAL AND GASKET MATERIALS

MATERIAL CHARACTERISTICS DATA SUMMARY

CATEGORY SEALS AND GASKETS

MATERIAL CORK NEOPRENE TAPE

	TEMPERATURE Degrees Celsius				FREQUENCY Hertz				RELATIVE HUMIDITY Percent			
DIELECTRIC CONSTANT	-55	23	+75	Data	60	10^3	10^6	Data	0	50	100	Data
SURFACE RESISTIVITY	-55	23	+75	Data	60	10^3	10^6	Data	0	50	100	Data
VOLUME RESISTIVITY	-55	23	+75	Data	60	10^3	10^6	Data	0	50	100	Data
DIELECTRIC STRENGTH	-55	23	+75	Data	60	10^3	10^6	Data	0	50	100	Data
DISSIPATION FACTOR	-55	23	+75	Data	60	10^3	10^6	Data	0	50	100	Data
ARC RESISTANCE	-55	23	+75	Data	60	10^3	10^6	Data	0	50	100	Data
FLASHOVER STRENGTH	-55	23	+75	Data	60	10^3	10^6	Data	0	50	100	Data

MATERIAL CHARACTERISTICS DATA SUMMARY

CATEGORY SEALS AND GASKETS MATERIAL NYLON CORD

	TEMPERATURE Degrees Celsius				FREQUENCY Hertz				RELATIVE HUMIDITY Percent			
DIELECTRIC CONSTANT	-55	23	+75	Data	60	10^3	10^6	Data	0	50	100	Data
SURFACE RESISTIVITY	-55	23	+75	Data	60	10^3	10^6	Data	0	50	100	Data
VOLUME RESISTIVITY	-55	23	+75	Data	60	10^3	10^6	Data	0	50	100	Data
DIELECTRIC STRENGTH	-55	23	+75	Data	60	10^3	10^6	Data	0	50	100	Data
DISSIPATION FACTOR	-55	23	+75	Data	60	10^3	10^6	Data	0	50	100	Data
ARC RESISTANCE	-55	23	+75	Data	60	10^3	10^6	Data	0	50	100	Data
FLASHOVER STRENGTH	-55	23	+75	Data	60	10^3	10^6	Data	0	50	100	Data

MATERIAL CHARACTERISTICS DATA SUMMARY

CATEGORY SEALS AND GASKETS MATERIAL SILICONE TAPE

	TEMPERATURE Degrees Celsius				FREQUENCY Hertz				RELATIVE HUMIDITY Percent			
DIELECTRIC CONSTANT	-55	23	+75	Data	60	10^3	10^6	Data	0	50	100	Data
SURFACE RESISTIVITY	-55	23	+75	Data	60	10^3	10^6	Data	0	50	100	Data
VOLUME RESISTIVITY	-55	23	+75	Data	60	10^3	10^6	Data	0	50	100	Data
DIELECTRIC STRENGTH	-55	23	+75	Data	60	10^3	10^6	Data	0	50	100	Data
DISSIPATION FACTOR	-55	23	+75	Data	60	10^3	10^6	Data	0	50	100	Data
ARC RESISTANCE	-55	23	+75	Data	60	10^3	10^6	Data	0	50	100	Data
FLASHOVER STRENGTH	-55	23	+75	Data	60	10^3	10^6	Data	0	50	100	Data

MATERIAL CHARACTERISTICS DATA SUMMARY

CATEGORY SEALS AND GASKETS

MATERIAL SYNTHETIC RUBBER (EXCL. POLYURETHANE)

	TEMPERATURE Degrees Celsius				FREQUENCY Hertz				RELATIVE HUMIDITY Percent			
DIELECTRIC CONSTANT	-55	23	+75	Data	60	10^3	10^6	Data	0	50	100	Data
SURFACE RESISTIVITY	-55	23	+75	Data	60	10^3	10^6	Data	0	50	100	Data
VOLUME RESISTIVITY	-55	23	+75	Data	60	10^3	10^6	Data	0	50	100	Data
DIELECTRIC STRENGTH	-55	23	+75	Data	60	10^3	10^6	Data	0	50	100	Data
DISSIPATION FACTOR	-55	23	+75	Data	60	10^3	10^6	Data	0	50	100	Data
ARC RESISTANCE	-55	23	+75	Data	60	10^3	10^6	Data	0	50	100	Data
FLASHOVER STRENGTH	-55	23	+75	Data	60	10^3	10^6	Data	0	50	100	Data

MATERIAL CHARACTERISTICS DATA SUMMARY

CATEGORY SEALS AND GASKETS

MATERIAL TEFLON TAPE

	TEMPERATURE Degrees Celsius				FREQUENCY Hertz				RELATIVE HUMIDITY Percent			
	-55	23	+75	Data	60	10^3	10^6	Data	0	50	100	Data
DIELECTRIC CONSTANT												
SURFACE RESISTIVITY												
VOLUME RESISTIVITY												
DIELECTRIC STRENGTH												
DISSIPATION FACTOR												
ARC RESISTANCE												
FLASHOVER STRENGTH												

MATERIAL CHARACTERISTICS DATA SUMMARY

CATEGORY SEALS AND GASKETS

MATERIAL VINYL TAPE

	TEMPERATURE Degrees Celsius				FREQUENCY Hertz				RELATIVE HUMIDITY Percent			
DIELECTRIC CONSTANT	-55	23	+75	Data	60	10^3	10^6	Data	0	50	100	Data
SURFACE RESISTIVITY	-55	23	+75	Data	60	10^3	10^6	Data	0	50	100	Data
VOLUME RESISTIVITY	-55	23	+75	Data	60	10^3	10^6	Data	0	50	100	Data
DIELECTRIC STRENGTH	-55	23	+75	Data	60	10^3	10^6	Data	0	50	100	Data
DISSIPATION FACTOR	-55	23	+75	Data	60	10^3	10^6	Data	0	50	100	Data
ARC RESISTANCE	-55	23	+75	Data	60	10^3	10^6	Data	0	50	100	Data
FLASHOVER STRENGTH	-55	23	+75	Data	60	10^3	10^6	Data	0	50	100	Data

DATA MATRIX

SUBSECTION A-4-3

SEALANT MATERIALS

MATERIAL CHARACTERISTICS DATA SUMMARY

CATEGORY SEALANTS

MATERIAL POLYAMIDE RESIN BASE

	TEMPERATURE Degrees Celsius				FREQUENCY Hertz				RELATIVE HUMIDITY Percent			
	-55	23	+75	Data	60	10^3	10^6	Data	0	50	100	Data
DIELECTRIC CONSTANT		x		Ref 22	x		x	Ref 22		x		Ref 22
								Ref 74				
SURFACE RESISTIVITY	-55	23	+75	Data	60	10^3	10^6	Data	0	50	100	Data
		x		Ref 74								
VOLUME RESISTIVITY	-55	23	+75	Data	60	10^3	10^6	Data	0	50	100	Data
		x		Ref 74						x		Ref 74
DIELECTRIC STRENGTH	-55	23	+75	Data	60	10^3	10^6	Data	0	50	100	Data
		x		Ref 74						x		Ref 74
DISSIPATION FACTOR	-55	23	+75	Data	60	10^3	10^6	Data	0	50	100	Data
		x		Ref 22	x		x	Ref 22		x		Ref 22
								Ref 74				
ARC RESISTANCE	-55	23	+75	Data	60	10^3	10^6	Data	0	50	100	Data
		x		Ref 74						x		Ref 74
FLASHOVER STRENGTH	-55	23	+75	Data	60	10^3	10^6	Data	0	50	100	Data

MATERIAL CHARACTERISTICS DATA SUMMARY

CATEGORY SEALANTS

MATERIAL POLYSULFIDE BASE (THIKOL)

	TEMPERATURE Degrees Celsius				FREQUENCY Hertz				RELATIVE HUMIDITY Percent			
DIELECTRIC CONSTANT	-55	23	+75	Data	60	10^3	10^6	Data	0	50	100	Data
SURFACE RESISTIVITY	-55	23	+75	Data	60	10^3	10^6	Data	0	50	100	Data
VOLUME RESISTIVITY	-55	23	+75	Data	60	10^3	10^6	Data	0	50	100	Data
DIELECTRIC STRENGTH	-55	23	+75	Data	60	10^3	10^6	Data	0	50	100	Data
DISSIPATION FACTOR	-55	23	+75	Data	60	10^3	10^6	Data	0	50	100	Data
ARC RESISTANCE	-55	23	+75	Data	60	10^3	10^6	Data	0	50	100	Data
FLASHOVER STRENGTH	-55	23	+75	Data	60	10^3	10^6	Data	0	50	100	Data

MATERIAL CHARACTERISTICS DATA SUMMARY

CATEGORY SEALANTS MATERIAL SILICONE RUBBER

	TEMPERATURE Degrees Celsius				FREQUENCY Hertz				RELATIVE HUMIDITY Percent			
	-55	23	+75	Data	60	10^3	10^6	Data	0	50	100	Data
DIELECTRIC CONSTANT		x		Ref 73	x	x	x	Ref 73		x		Ref 73
SURFACE RESISTIVITY	-55	23	+75	Data	60	10^3	10^6	Data	0	50	100	Data
		x		Ref 72								
	350 & 450°F			Ref 72								
VOLUME RESISTIVITY	-55	23	+75	Data	60	10^3	10^6	Data	0	50	100	Data
		x		Ref 73								
	350 & 450°F			Ref 72								
DIELECTRIC STRENGTH	-55	23	+75	Data	60	10^3	10^6	Data	0	50	100	Data
		x		Ref 72						x		Ref 72
	450°F			Ref 72								
DISSIPATION FACTOR	-55	23	+75	Data	60	10^3	10^6	Data	0	50	100	Data
		x		Ref 73	x	x	x	Ref 73		x		Ref 73
ARC RESISTANCE	-55	23	+75	Data	60	10^3	10^6	Data	0	50	100	Data
		x		Ref 72						x		Ref 72
	450°F			Ref 72								
FLASHOVER STRENGTH	-55	23	+75	Data	60	10^3	10^6	Data	0	50	100	Data

MATERIAL CHARACTERISTICS DATA SUMMARY

CATEGORY SEALANTS MATERIAL ZINC CHROMATE PUTTY COMPOUND W/ASBESTOS FILLERS

	TEMPERATURE Degrees Celsius				FREQUENCY Hertz				RELATIVE HUMIDITY Percent			
DIELECTRIC CONSTANT	-55	23	+75	Data	60	10^3	10^6	Data	0	50	100	Data
SURFACE RESISTIVITY	-55	23	+75	Data	60	10^3	10^6	Data	0	50	100	Data
VOLUME RESISTIVITY	-55	23	+75	Data	60	10^3	10^6	Data	0	50	100	Data
DIELECTRIC STRENGTH	-55	23	+75	Data	60	10^3	10^6	Data	0	50	100	Data
DISSIPATION FACTOR	-55	23	+75	Data	60	10^3	10^6	Data	0	50	100	Data
ARC RESISTANCE	-55	23	+75	Data	60	10^3	10^6	Data	0	50	100	Data
FLASHOVER STRENGTH	-55	23	+75	Data	60	10^3	10^6	Data	0	50	100	Data

DATA MATRIX

SUBSECTION A-4-4

ADHESIVE MATERIALS

MATERIAL CHARACTERISTICS DATA SUMMARY

CATEGORY ADHESIVES

MATERIAL ACRYLIC RESIN BASE

	TEMPERATURE Degrees Celsius				FREQUENCY Hertz				RELATIVE HUMIDITY Percent			
DIELECTRIC CONSTANT	-55	23	+75	Data	60	10^3	10^6	Data	0	50	100	Data
		x		Ref 74	x		x	Ref 74				
SURFACE RESISTIVITY	-55	23	+75	Data	60	10^3	10^6	Data	0	50	100	Data
		x		Ref 74								
VOLUME RESISTIVITY	-55	23	+75	Data	60	10^3	10^6	Data	0	50	100	Data
		x		Ref 74								
DIELECTRIC STRENGTH	-55	23	+75	Data	60	10^3	10^6	Data	0	50	100	Data
		x		Ref 74								
DISSIPATION FACTOR	-55	23	+75	Data	60	10^3	10^6	Data	0	50	100	Data
		x		Ref 74	x		x	Ref 74				
ARC RESISTANCE	-55	23	+75	Data	60	10^3	10^6	Data	0	50	100	Data
		x		Ref 74								
FLASHOVER STRENGTH	-55	23	+75	Data	60	10^3	10^6	Data	0	50	100	Data

MATERIAL CHARACTERISTICS DATA SUMMARY

CATEGORY ADHESIVES MATERIAL POLYSULFIDE BASE

	TEMPERATURE Degrees Celsius				FREQUENCY Hertz				RELATIVE HUMIDITY Percent			
DIELECTRIC CONSTANT	-55	23	+75	Data	60	10^3	10^6	Data	0	50	100	Data
SURFACE RESISTIVITY	-55	23	+75	Data	60	10^3	10^6	Data	0	50	100	Data
VOLUME RESISTIVITY	-55	23	+75	Data	60	10^3	10^6	Data	0	50	100	Data
DIELECTRIC STRENGTH	-55	23	+75	Data	60	10^3	10^6	Data	0	50	100	Data
DISSIPATION FACTOR	-55	23	+75	Data	60	10^3	10^6	Data	0	50	100	Data
ARC RESISTANCE	-55	23	+75	Data	60	10^3	10^6	Data	0	50	100	Data
FLASHOVER STRENGTH	-55	23	+75	Data	60	10^3	10^6	Data	0	50	100	Data

MATERIAL CHARACTERISTICS DATA SUMMARY

CATEGORY ADHESIVES

MATERIAL SILICONE RESIN BASE

	TEMPERATURE Degrees Celsius				FREQUENCY Hertz				RELATIVE HUMIDITY Percent			
DIELECTRIC CONSTANT	-55	23	+75	Data	60	10^3	10^6	Data	0	50	100	Data
SURFACE RESISTIVITY	-55	23	+75	Data	60	10^3	10^6	Data	0	50	100	Data
VOLUME RESISTIVITY	-55	23	+75	Data	60	10^3	10^6	Data	0	50	100	Data
DIELECTRIC STRENGTH	-55	23	+75	Data	60	10^3	10^6	Data	0	50	100	Data
DISSIPATION FACTOR	-55	23	+75	Data	60	10^3	10^6	Data	0	50	100	Data
ARC RESISTANCE	-55	23	+75	Data	60	10^3	10^6	Data	0	50	100	Data
FLASHOVER STRENGTH	-55	23	+75	Data	60	10^3	10^6	Data	0	50	100	Data

REFERENCES

1. AFSC Design Handbook DH 1-4, Electromagnetic Compatibility, Air Force Systems Command, January, 1977.

2. N. Cianos and E. T. Pierce, A Ground-Lightning Environment for Engineering Usage, Stanford Research Institute, Technical Report 1, August, 1972 (AD 907 891).

3. Samuel Glasstone (editor), The Effects of Nuclear Weapons, Air Force Pamphlet AFP 136-1-3, February, 1974.

4. K. F. Casey, Electromagnetic Shielding by Advanced Composite Materials, Kansas State University, AFWL-TR-77-201, January, 1978.

5. American Society for Testing and Materials, Standard Test Method for D-C Resistance or Conductance of Insulating Materials, ASTM D-257-76, April, 1976.

6. J. J. Chapman and L. J. Frisco, A Practical Interpretation of Dielectric Measurements Up to 100-MC, The Johns Hopkins University, File Number 0199-PH-57-91 (3400), December, 1958, (AD 212 149).

7. American Society for Testing and Materials, Standard Test Method for Dielectric Breakdown and Dielectric Strength of Electrical Insulating Materials at Commercial Power Frequencies, ASTM D-149-75, July, 1975.

8. American Society for Testing and Materials, Standard Test Method for A-C Loss Characteristics and Dielectric Constant (Permittivity) of Solid Electrical Insulating Materials, ASTM D-150-74, November, 1974.

9. Frederick E. Terman, Electronic and Radio Engineering, Fourth Edition, McGraw-Hill, 1955.

10. E. V. Condon and Hugh Odishaw, Handbook of Physics, Second Edition, McGraw-Hill, 1958.

11. R. T. Zeitler and P. E. Craighead, F-16 Lightning Analysis Report, Report No. 16PR757 (Revision A), General Dynamics Corp., June, 1978.

12. R. Alston, Lightning Test of F-15 Canopy, Report No. MDC A2056, McDonnell Aircraft Co., February, 1973.

13. American Society for Testing and Materials, Standard Test Method for High-Voltage, Low-Current, Dry Arc Resistance of Solid Electrical Insulation, ASTM 495-73, December, 1973.

14. J. A. Vaccari, Thermoplastic Polyesters: Versatile Engineering Materials, Materials Engineering, Reinhold Publishing Co. October, 1974.

15. V. C. Plantz, Feasibility Study of Shielding Technigues, Report No. D6-8597-5, The Boeing Co., April, 1965.

16. B. F. Kay, Design Handbook for Helicopter Enclosures (Draft Report), Sikorsky Aircraft Division of United Technology Corp. Report No. SER-50966, August, 1976.

17. S. Y. Liao, Light Transmission and RF Shielding Effectiveness of a Gold Film on a Glass Substrate, IEEE Transactions on Electromagnetic Compatibility, Vol. EMC-17, No. 4, November, 1975.

18. H. A. Lasitter, Low-Frequency Shielding Effectiveness of Conductive Glass, IEEE Transactions on Electromagnetic Compatibility, Vol. EMC-6, No. 2, July, 1964.

19. E. I. Hawthorne, Electromagnetic Shielding with Transparent Coated Glass, Proceedings of the IRE, Vol. 42, No. 3, March, 1954.

20. C. S. King, Windshield/Canopy Cost and Failure Analysis: Task 1-Data Compilation, UD12I-TR-76-69, University of Dayton, October, 1976.

21. J. H. Carlson, Windshield/Canopy/Support Structure (WCSS) Life Cycle Cost and Failure Analysis, AFFDL-TR-75-115, McDonnell Douglas Corporation, September, 1975.

22. Military Standardization Handbook, Plastics, MIL-HDBK-700A, March, 1975.

23. E. B. Shand, Glass Engineering Handbook (Second Edition), McGraw-Hill Book Co., 1958.

24. C. A. Harper (Editor), Handbook of Plastics and Elastomers, McGraw-Hill Book Co., 1975.

25. R. I. Beck, Standardized Windshield Fabrication Specification (Draft), AFFDL-TR-77-97, November, 1977.

26. National Technical Information Service, Lightning, Surge, and Transient Protection - A Bibliography with Abstracts: 1964 - February 1978, NTIS/PS-78/0187, March, 1978.

27. Smithsonian Science and Information Exchange, Thunderstorms and Lightning: A Bibliography of Research Projects, No. LR-15, July, 1978.

28. R. C. Twomey, Effects of Laboratory Simulated Precipitation Static Electricity and Swept Stroke Lightning on Aircraft Windshield Subsystems, McDonnell Douglas Corp., AFFDL-TR-76-75, July, 1976.

29. R. C. Twomey, Precipitation Static Electricity and Swept-Stroke Lightning Effects on Aircraft Transparency Coatings, McDonnell Douglas Corp., AFFDL-TR-77-141, December, 1977.

30. R. Alston, R. Gorton, G. L. Weinstock, Lightning Protection Techniques for Large Canopies on High Speed Aircraft, McDonnell Douglas Corp., AFAL-TR-72-49, January, 1972.

31. W. T. Boord, Exploratory Development of Antistatic Coatings for Use on Aircraft Transparencies, Honeywell, Inc., July, 1976.

32. Ad Hoc Team Report on Aircraft Vulnerability to Lightning Strike Damage

33. Data from the Airlines' Lightning Strike Reporting Project, Summary Report, General Electric Co., March, 1975.

34. Lightning and Aircraft, Lockheed Field Service Digest, Issue #48, March, 1964.

35. W. H. Cushman, Cumulative Flash Blindness Effects Produced by Multiple High Intensity Flashes, Aerospace Medicine, Vol. 42, p. 763-767, 1971.

36. J. W. Flowers, The Channel of the Spark Discharge, The Physical Review, Vol. 64, No's. 7 and 8, p. 225-235, October 1 and 15, 1943.

37. Military Standard, Aircrew Vision Requirements for Military Aircraft, MIL-STD-850B, November, 1970.

38. Electro-Optics Handbook, Technical Series EOH-11, RCA Corporation, 1974.

39. J. H. Hill and G. T. Chisum, Flashblindness Protection, Aerospace Medicine, Volume 33, p. 958-964, 1962.

40. G. Chisum, Flash Blindness Recovery Following Exposure to Constant Energy Adaptive Flashes, Aerospace Medicine, Volume 44, p. 407-713, 1973.

41. W. H. Cushman, Effect of Flash Field Size on Flash Blindness in Aircraft Cockpit, Aerospace Medicine, Volume 42, p. 630-634, 1971.

42. G. T. Chisum and P. E. Morway, Flash Blindness Following Double Flash Exposures, Aerospace Medicine, Volume 45, p. 1013-1016, 1974.

43. G. Chisum, Intraocular Effects on Flash Blindness, Aerospace Medicine, Volume 39, p. 860-868, 1968.

44. G. T. Chisum, Intraocular Effects on Flash Blindness: II - Parafoveal Recovery, Aerospace Medicine, Volume 42, p. 31-35, 1971.

45. B. Ward and W. H. Bowie, and W. H. Cushman, Flash Blindness Recovery With and Without Protection in Simulated Flight Conditions, Aerospace Medicine, Volume 42, p. 149-152, 1971.

46. R. Noble, J. Lago, and J. Micciche, Investigation of the Safety Aspects of Explosive Light Filter (ELF) Flash Blindness Protection System, NADC-AC-6811, June, 1968.

47. W. Thursby, E. Richey, R. Bartholomew, and R. Ebbers, Evaluation of Photochromic Goggle System for Nuclear Flash Protection, SAM-TR-71-20, January, 1971.

48. Visual Aids and Eye Protection for the Aviator, Aerospace Medical Panel Specialists' Meeting, Copenhagen, Denmark, 5-9 April, 1976.

49. D. Boyer, Glare Recovery of Two-Dimensional Tracking Jack with Respect to Various Colors, DARCOM-ITC-02-08-76-015, April, 1976.

50. R. H. Golde, Lightning, Volume 2-Lightning Protection, Academic Press, New York, 1977.

51. V. L. Mangold, L. C. Walko, K. J. Maxwell, and J. G. Schneider, NASA T-38 Lightning Susceptibility Study, AFFDL-TR-78-xx (to be published), Technology/Scientific Services Inc.

52. How Much Current Is Fatal?, Popular Electronics, p. 31, January, 1972.

53. G. L. Weinstock, Lightning Protection on Advanced Fighter Aircraft, Lightning and Static Electricity Conference, 9-11 December, 1970.

54. R. Aston, R. Gaton, and G. Weinstock, Lightning Protection Techniques for Large Canopies on High Speed Aircraft, Lightning and Static Electricity Conference, December, 1972.

55. D. L. Jones, G. G. Goyer, and M. Ploaster, Shock Wave from a Lightning Discharge, Journal of Geophysical Research, Volume 73, May 15, 1968.

56. Sierracin/Sylmar, Sierracin Aircraft and Helicopter Transparencies - Design Data Sheets

57. Military Standard, Aircraft Electric Power Characteristics, MIL-STD-704B, November, 1975.

58. D. C. Kay (Editor), Transient Voltage Suppression Manual, General Electric Co., 1976.

59. Military Standard, Environmental Test Methods, MIL-STD-810C, March, 1975.

60. United States Air Force Lightning Accident/Incident Reports, 1968-1977.

61. United States Navy Lightning Accident/Incident Reports, 1967-1976.

62. J. R. Wait, Electromagnetic Waves in Stratified Media, Second Edition, Pergamon Press, 1970.

63. W. S. McCormick, Discharge Propagation through Heater Circuit, Technology Incorporated internal memorandum dated 15 December, 1978.

64. W. S. McCormick, K. J. Maxwell, and R. B. Finch, Analytical and Experimental Validation of the Lightning Transient Analysis Technique, Technology Incorporated, AFFDL-TR-78-47, March, 1978.

65. J. A. Plumer and L. C. Walko, S-3A Lightning Effects Analysis and Protection Program, Phase 1 - Lightning Effects Analysis, General Electric, SR-74-082, July, 1974.

66. An Engineering Handbook on Merlon Polycarbonate, Mobay Chemical Co.

67. Phone Conversation with R. Helmrich, Dow Chemical Co., Midland, Michigan, 1 September, 1978.

68. D. R. Dreger, The Polysulfones: Heat Resistant, Superstrong and Ultrastable, Machine Design, Penton IPC, January, 1978.

69. Letter Correspondence from R. W. Ross, Typical Properties of SAFLEX PT and SAFLEX DS, Monsanto Polymer and Petrochemicals Co. Product Literature, 9 August, 1978.

70. Owens-Illinois, Inc., Glass Resins Department, Product Literature.

71. Liberty Mirror Division of Libbey-Owens-Ford (LOF) Co., Product Literature.

72. Minnesota Mining and Mfg. Co. (3M), Product Literature for 3M Sealer Type EC-1667 B/A, July, 1959.

73. General Electric Co., RTV Product Literature.

74. Materials Engineering, Materials Selector 78, Penton/IPC, 1978.

BIBLIOGRAPHY

1. National Technical Information Service, Lightning, Surge, and Transient Protection - A Bibliography with Abstracts: 1964-January 1977, NTIS/PS-77/0099, March 1977.

2. C. S. Sims and Y. Park, Spatial Stochastic Analysis of EMP Transients, Oklahoma State University, CS-74-1, March 1974 (AD/A 000-825).

3. R. Vaselich and J. Dixon, Lightning Protection Documentation, Naval Weapons Laboratory, NWL Administrative Report No. AR-124, June 1973 (AD 763-667).

4. M. M. Newman and J. D. Robb, Electrical Breakdown of Aircraft Windshields, Lightning and Transients Research Institute, Technical Paper No. 8, 1948.

5. G. A. Dalin and J. Flores, The Development of Electrical Conducting Transparent Coatings for Acrylic Plastic Sheet, Balco Research Laboratories, WADC Technical Report 53-378, Part 2, December 1954.

6. F. H. Gillery, A Manufacturer's View-Windshield Related Problems, PPG Industries, Inc., Lightning and Static Electricity Conference, December 1972.

7. E. E. Stickley, J. D. Robb and M. M. Newman, Radio Interference from Aircraft Windshield Charging, Lightning and Transients Research Institute, Technical Paper No. 17, December 1949.

8. Military Standardization Handbook, Plastics for Aerospace Vehicles, Part I - Reinforced Plastics and Part II - Transparent Glazing Materials, MIL-HDBK-17A, January 1971.

9. Machine Design, Materials 1978 Reference Issue, Penton/IPC, Inc., March 1978.

10. Plastics Engineering Handbook, Dayton Plastics 1978.

11. J. H. Lawrence, et al, Windshield Technology Demonstrator Program - Detail Design Options Study - Volume I, McDonnell Douglas Corp. MDC-J6951, AFFDL-TR-77-1, September 1977.

12. R. E. Wittman, Conference on Aerospace Transparent Aircraft Enclosures, Air Force Materials Laboratory, AFML-TR-76-54, April 1976.

13. Smithsonian Science Information Exchange, Inc., Aircraft Windows - A Bibliography of Notices of Research Projects, July 1978.

14. R. C. Twomey, Precipitation Static Electricity and Swept Stroke Lightning and Their Effects on Windshield Subsystems, McDonnell Douglas Corp., Paper, April 1978.

15. P. J. Sharp, Static Electrification of Windscreens and Canopies, Lucas Aerospace Ltd., United Kingdom, Paper, April 1975.

16. R. E. Wittman, A Review of Air Force Experience with Static Electricity Problems on Aircraft Windshields, Air Force Materials Laboratory, Lightning and Static Electricity Conference, December 1972.

17. M. M. Newman, J. D. Robb, and J. R. Stahmann, Windshield Static Electrification Problems - Commercial Aircraft Experience and Protection Parameters, Lightning and Transients Research Institute, Lightning and Static Electricity Conference, December 1972.

18. R. O. Brock, Windshield Related Electrostatic Problems - Electrification Studies on the 747, The Boeing Co., Lightning and Static Electricity Conference, December 1972.

19. Defense Documentation Center, Work Units on Aircraft Transparencies and Lightning Environment, Bibliography and Abstracts, January 1978.

20. Defense Documentation Center, Independent Research and Development Programs on Aircraft Transparencies and Lightning Environment, Bibliography and Abstracts, January 1978.

21. American Society for Testing and Materials, Standard Test Methods for Haze and Luminous Transmittance of Transparent Plastics, ASTM-D-1003-61, 1977.

22. American Society for Testing and Materials, Standard Test Methods for Index of Refraction of Transparent Organic Plastics, ASTM-D-542-50, 1977.

23. AFSC Design Handbook DH-2-2, Crew Station and Passenger Accommodations, Air Force Systems Command, May 1975.

24. J. A. Plummer and F. A. Fisher, Lightning Protection of Aircraft, General Electric Co., NASA Reference Publication 1008, October 1977.

25. J. Phillpott, Recommended Practice for Lightning Simulation and Testing Techniques for Aircraft, Culham Laboratory, United Kingdom Atomic Energy Authority, Report CLM-R 163, 1977.

26. C. A. Harper, Handbook of Wiring, Cabling, and Interconnecting for Electronics, McGraw-Hill Book Co., 1972.

27. Military Standardization Handbook, Adhesives, MIL-HDBK-691A, May 1965.

28. Military Handbook, Adhesives - A Guide to Their Properties and Uses as Described by Federal and Military Specifications, MIL-HDBK-725, May 1972.

29. Military Standardization Handbook, Glass, MIL-HDBK-722, August 1969.

30. H. E. Littell, Improved Windshield and Canopy Protection Development Program, PPG Industries, Inc., AFFDL-TR-74-75, June 1974 (AD/B 013-203).

31. G. Haacke, Exploratory Development of Transparent Conductor Materials, American Cyanamid Co., AFML-TR-75-21, March 1975 (AD/A 008-783).

32. J. L. Martinelli, Evaluation of the 'Sierracote' Electrically Heated Windshield in an L-23D, Report of Test, Project No. AVN 3458, March 1959 (AD/A 029-759).

33. J. M. Lloyd and P. P. Budenstein, Effects of Excess Charge Density on Dielectric Breakdown of Solids, Auburn University, November 1977 (AD/A 048-267).

34. H. L. Bassett and S. H. Bomar, Jr., Dielectric Constant and Loss Tangent Measurement of High-Temperature Electromagnetic Window Materials, Georgia Institute of Technology, AFWL-TR-69-92, December 1969 (AD 864-731).

35. L. E. Cummings, Triboelectric Charging of Aircraft Dielectric Surfaces in the Microwave Frequency Region (1-4GHz), Air Force Avionics Laboratory, AFAL-TR-70-137, October 1970 (AD 879-684).

36. J. C. Anderson, Dielectrics, Reinhold Publishing Co., 1964.

37. Air Force Cambridge Research Laboratory, Handbook of Geophysics and Space Environments, USAF, 1965.

38. R. F. Weilminster, Feasibility of Using Radioisotopes for Elimination or Reduction of Precipitation Static Problems as Related to Aircraft, Air Force Avionics Laboratory, AFAL-TR-69-163, August 1969.

39. Irvin Langmuir, Investigation of Fundamental Phenomena of Precipitation Static, General Electric Co., May 1945.

40. W. C. McDonald, Glass/Plastic Transparent Armor for the UH-1 Helicopter, Goodyear Aerospace Corp., AMMRC-CTR-77-27, October 1977 (AD/A 047-323).

41. B. F. Kay and J. H. McGarvey, A Design Handbook for Helicopter Transparent Enclosures, 33rd Annual National Forum of the American Helicopter Society, May 1977.

42. C. K. Purvis and N. J. Stevens, Charging Characteristics of Materials: Comparison of Experimental Results with Simple Analytical Models, Lewis Research Center, NASA Technical Memorandum TMX-73606, October 1976.

43. PPG Industries, Inc. Product Literature

44. Lightning and Transients Research Institute, Lightning Hazards and Protection for Lockheed F-104 Aircraft, L & T Report No. 447, February 1966.

45. Lightning and Transients Research Institute, FAA-USAF Lightning Hazard Studies of the F-100 Aircraft in Thunderstorm Researches, L & T Report No. 447, Appendix I, February 1966.

46. M. M. Newman and J. D. Robb, Development of Lightning Protection Methods, Final Report, Lightning and Transients Research Institute, L & T Report No. 279, June 1954.

47. M. M. Newman and J. D. Robb, Development of Lightning Protection Methods, Interim Report, L & T Report No. 201, February 1952.

48. Lightning and Transients Research Laboratory, Lightning Protection of Aircraft Insulated Sections and Antenna Systems, L & T Report No. 187, July 1952.

49. E. L. Hill, A Theory of the Shielding of Radio Waves at Low and Medium Frequencies, Lightning and Transients Research Institute, Report No. 188, July 1951.

50. D. A. Miller and J. E. Bridges, Review of Circuit Approach to Calculate Shielding Effectiveness, ITT Research Institute, IEEE Transactions on Electromagnetic Compatability, Volume I, EMC-10, No. 1, March 1968.

51. M. M. Newman, J. D. Robb, J. R. Stahmann, Electromagnetic Hazards Inside Aircraft - I: Penetration through Canopies and Radomes and Associated Protective Techniques, Lightning and Transients Research Institute, AFAL-TR-66-215, September 1966.

52. A. H. Sharbaugh, An Introduction to the Theory and Measurement of Dielectric Constant and Loss, General Electric Co., Report No. 57-RL-1787, September 1957.

53. Corning Glass Works, Product Literature

54. Optical Coating Laboratory, Inc., Product Specifications

55. J. R. Plumer, Development of Spall- and Scratch-Resistant Windshields, Army Materials and Mechanics Research Center, AMMRC TR-74-19, August 1974 (AD/A 002-513).

56. A. S. Zingerman, A Statistical Method for Determining the Piercing Voltage of a Dielectric, ZHURL TEKHNICHESKOI FIZIKI, V18, 1029-43, 1948.

57. The Netherlands Armed Forces Scientific and Technical Documentation and Information Center, A Bibliography on EMP, TDCK 65282, 1968-1974.

58. R. A. Weeks, D. L. Kinser, and J. M. Lee, Charge Trapping and Dielectric Breakdown in Lead Silicate Glasses, CONF 760929-1, Circa 1976.

59. Military Specification, Glass, Monolithic, Aircraft Glazing, MIL-G-25667B, June 1970.

60. Military Specification, Plastic Sheet, Polycarbonate, Transparent, MIL-P-83310(USAF), January 1971.

61. Military Specification, Glass, Laminated, Flat, Bullet-Resistant, MIL-G-5485C, April 1971.

62. Military Specification, Plastic, Sheet Acrylic, Heat-Resistant, MIL-P-5425C, June 1967.

63. Military Specification, Plastic, Sheets and Parts, Modified Acrylic Base, Monolithic, Crack Propagation Resistant, MIL-P-25690A, August 1960.

64. Military Specification, Glass, Laminated, Aircraft Glazing, MIL-G-25871A (ASG) July 1958.

65. Military Standard, Aircrew Station Vision Requirements for Military Aircraft, MIL-STD-880B, November 1970.

66. Military Specification, Windshield Systems, Fixed Wing Aircraft - General Specification for, MIL-W-81752 (AS) April 1970.

67. Military Specification, Window, Non-Icing, Laminated Flat Glass, Electrically Heated, With Controls, MIL-W-18445 (Ships) October 1968.

68. Rohm and Haas Co., Product Literature

69. Textar Plastics, Summary of Transparency Qualification Testing, TSP-7801-31001, January 1978.

70. E. I. DuPont, Product Literature

71. Polaroid Corporation, Product Literature

72. Continental Optical Corporation, Product Literature

73. Materials and Design Engineering, Materials and Processes Manual No. 220, Reinhold Publishing Co., June 1964.

74. Materials and Design Engineering, New Polysulfone Thermoplastics Stands Up at 300°F, Reinhold Publishing Co., May 1965.

75. J. E. Hauck, Glass Parts: How to Select and Specify, Materials and Processes Manual No. 243, Materials Engineering, Reinhold Publishing Co., August 1967.

76. C. R. Schrankel, Glass, Glass-Ceramics: Versatile Materials, Materials Engineering, Reinhold Publishing Co., December 1968.

77. J. A. Vaccari, Safer Aircraft Glasses Up Visibility, Resist Impact, Materials Engineering, Reinhold Publishing Co., August 1969.

78. J. A. Vaccari, Thermoplastic Polyesters: Versatile Engineering Materials, Materials Engineering, Reinhold Publishing Co., October 1974.

79. M. L. Yaffee, New Cockpit Enclosure Materials Sought, Aviation Week and Space Technology, McGraw-Hill, 20 January 1975.

80. G. R. Forger, Plastics and Elastomers Turn on to Electrical Conductivity, Materials Engineering, Reinhold Publishing Co., August 1977.

81. M. E. Rogers, The Importance of Airframe Conductance in Relation to Its Atmospheric Electrical Environment, Royal Aircraft Establishment, Tech Memo Avionics 47, 1970.

82. W. F. Grether, Optical Factors in Aircraft Windshield Design as Related to Pilot Visual Performance, Aerospace Medical Research Laboratory, AMRL-TR-73-57, July 1973.

83. M. N. England, X-20 Window Tests, Air Force Flight Dynamics Laboratory, AFFDL-TR-65-211, January 1966.

84. O. J. Maltenicks, Improved Rain-Repellent Coatings for Aircraft Windshields, Canopies, and Other Non-Metallic Components, Lockheed-Georgia Co., AFML-TR-70-199, Part I August 1970, and Part II August 1972.

85. N. D. Miller, Visual Recovery from High Intensity Flashes, Ohio State University, July 1965 (AD 627-325).

86. W. F. Provines and B. Kislin, Transparencies Used in Military Aviation and Their Effects on Vision, USAF School of Aerospace Medicine, SAM-TR-70-303, April 1970 (AD 731-616).

87. R. V. Gran and P. R. Marshall, Degradation Limits of Plastic Windshields in Service, Federal Aviation Agency, FAA-ADS-57, November 1965 (AD 654-552).

88. M. W. Windsor, W. R. Dawson, and R. S. Moore, Photochromic Eye-Protective Device Based on Triplet Absorption, Annual Research Report, TRW Systems, Report No. 05465-6002-R0002, 1966 (AD 645-342).

89. E. A. Strouse, Development of De-Icing Techniques for Dielectric Windows, Perkin-Elmer Corp., AFML-TR-75-99, August 1975 (AD/A 017-097).

90. L. M. Cook, et al, Development of Design, Test, and Acceptance Criteria for Army Helicopter Transparent Enclosures, PPG Industries, Inc. USAAMRDL-TR-73-65, September 1973 (AD 772-936).

91. R. J. Followill and J. W. Adcock, Comparative Evaluation of Two Types of Electrically Heated Windshields Installed on a CV-2A Airplane, U.S. Army Aviation Test Board, September 1963 (AD/A 031-900).

92. J. R. Plumer and W. C. McDonald, Evaluation of Scratch- and Spall-Resistant Windshields, U.S. Army Aviation Systems Command, AVSCOM Report No. 76-22, December 1976, (AD/A 038-849).

93. C. K. Park and F. F. Holly, The Use of Opaque Louvres and Shields to Reduce Reflections within the Cockpit: A Trigonometrical and Plane Geometry Approach, Army Aeromedical Research Laboratory, USAARL Report No. 76-4, September 1975 (AD/A 017-366).

94. K. H. Wilcox, Environmental Testing of the Improved Engine and Windshield Anti-Ice and Rotor Blade De-Ice Systems Installed in the CH-46A Helicopter, Naval Air Test Center Technical Report No. ST18R-66, March 1966 (AD/A 011-116).

95. Triplex Safety Glass Co. Ltd, The Effect of Storage on the Strength of Annealed and Toughened Clear White Plate Glass, Ministry of Technology Materials Division Report 153 (U.K.), September 1968 (AD 680-648).

96. R. A. Huyett and G. E. Wintermute, Environmental Resistance of Coated and Laminated Polycarbonate Transparencies, Goodyear Aerospace Corporation, AFML-TR-76-24, March 1976 (AD/A 026-412).

97. D. J. Peake and N. J. Della Valle, A Study of Windshield Temperatures in Flight on the RCAF Yukon Aircraft, National Aeronautical Establishment (Canada), NRC No. 9824 (AD 824-531).

98. E. O. Richey, Predicting Eye Safe Separation Distances from Nuclear Detonations, USAF School of Aerospace Medicine, SAM-TR-76-38, December 1976.

99. A. F. Shoemaker, High Performance Aircraft Windshield Development Program, Corning Glass Works, AFML-TR-66-69, June 1966 (AD 812-203).

100. G. M. Korb, R. D. Dayton, and D. Sommerville, Development and Experimental Verification of A Computer Program for Predicting Temperature Distribution and Heat Transfer through Coated and Uncoated, Single or Multi-Glaze Window Systems, Midwest Research Institute, AFFDL-TR-69-28, April 1969 (AD 851-479).

101. W. C. Gelling and W. A. Benner, CH-113, CH-46A, CH-53A Investigations, Ice Protection Systems, Royal Canadian Air Force Central Experimental and Proving Establishment, Report No. 1892, August 1966 (AD 802-952).

102. Emerson & Cuming, Inc., Product Literature

103. R. F. Stengel, Polycarbonate is Key to Lightweight, Birdproof F-111 Windshield, Design News, July 17, 1978.

104. H. Lee and K. Neville, Handbook of Epoxy Resins, McGraw-Hill Book Co., 1967.

105. H. Lee and K. Neville, Handbook of Adhesive Bonding, McGraw-Hill Book Co., 1973.

106. D. F. Aitken, Engineer's Handbook of Adhesives, 1972.

107. H. R. Simonds and J. M. Church, A Concise Guide to Plastics, Second Edition, Reinhold Publishing Corp., 1963.

108. Minnesota Mining and Manufacturing Co., Product Literature

109. Military Specification, Tape and Sheet, Adhesive, Rubber and Cork Composition, MIL-T-6841C, February 1965.

110. Military Specification, Sealing Compound, Temperature-Resistant, Integral Fuel Tanks and Fuel Cell Cavities, High Adhesion, MIL-S-8802D, September 1967.